Dear editor,

We thank both referees for their positive feedback, the constructive comments and valuable hints to further publications connected to our work. We addressed all mentioned comments and changed the manuscript accordingly. We are now pleased to send to you the revised version of the manuscript.

The improvements in the presented manuscript addressing the main points of criticism are summed up as follows:

(i) Missing key publications, for instance, Yamamoto and Springman (2014), Gischig et al. (2011), Ulusay (2015), Yasufuku et al. (2003), Coulomb (1773), Mohr (1900), Schön (2015), Hall and Thorn (2014) were added to the text and included in the discussion.

(ii) We included a comparison between our findings and the direct shear tests by Davies et al. Further, we marked the valid temperature range for the failure criterion (Fig. 8) to stress the fact that the calculated equations for cohesion and friction are only valid for temperatures between -0.5 and -8 °C. Hence, we cannot say anything about the behaviour of cohesion and friction between -0.5 and 0 °C. In the author response we explained in detail why we use linear fits.

(iii) The applied small rock surface roughness is a compromise between both requirements: a good sample-reproducibility in terms of uniform test conditions (without spending too much time and costs) and a simulation of rock surfaces as close as possible to conditions in the field. In future we consider to perform more tests on varying surface roughness, but this is beyond the scope of this first study.

(iv) We added a detailed discussion on the assumption that the influence of the rock type is less important for the shear strength of ice-filled joints. Here, we considered properties like the thermal conductivity, the porosity, the type and strength of the constitutive minerals as well as thermal strain.

(v) We modified our model on the unloading of an underlying frozen rock mass, we added a figure and gave more information on how the approach works.

Best regards,

Philipp Mamot

On behalf of all authors

Dear editor,

We have carefully addressed all mentioned comments and have improved significantly the structure and the language of the manuscript according to the comments. All detailed changes are listed hereafter.

Philipp Mamot and co-authors

Response by the author to comments of Referee 1 and 2

RC = Referee comment

AC = Author comment

C = Changes by the authors

Line 7:

RC1: I assume you mean air temperatures in a general context here. – related to the term "warming"

AC/C: We reworded the sentence more concisely into *"Instability and failure of permafrost-affected rock slopes have significantly increased coincident to rising air temperature related to climate change in the last decades."*

Line 9:

RC1: The referee suggested to delete the term "effects in"

AC/C: Changed as suggested

Lines 12-14:

RC1: The referee…

(1) proposed to write "shearing experiments" instead of "shear experiments"
(2) proposed to present the information on the strain rate earlier in the sentence
(3) deleted the word "relevant"

(4) added the word “of” to “i.e. 4-30 m rock overburden”

(5) exchanged the word “i.e.” by “representing”

(6) added the word “observed” to “typical for recent rock slope failures in alpine permafrost”

AC/C: We adjusted the proposed changes in the revised manuscript as follows:

“For this, we performed 141 shearing experiments with rock-ice-rock "sandwich" samples at constant strain rates (10^{-3} s^{-1}) provoking ice fracturing, under stress conditions ranging from 100 to 800 kPa, representing 4–30 m of rock overburden, and at temperatures from -10 to -0.5 °C, typical for recent observed rock slope failures in alpine permafrost.”

Line 13:

RC2: It is not quite clear how you calculate the strain rates. Normally for shear tests the shear strain is calculated using the sample height divided by the shear deformation. As you are interested in the deformation of the ice, it would make sense to use the thickness of the ice infill (approx. 3mm) as height. From Fig. S3 the rate of shear deformation seems to be approx. 0.01mm/s. I cannot see how you get to a strain rate of 10^-3/s.

AC: The strain rate is important to make sure that ice fracturing rather than creep is the dominant deformation mode, as 10^{-3} s^{-1} is the strain rate threshold for ice fracturing. Thus, the minimum test strain rate is 1.58 * 10^{-3} s^{-1}, which combines the minimum accounted deformation speed (0.005 mm/s) and the maximum ice layer thickness of 4 mm; this is how we get to the strain rate of 10^{-3} s^{-1}. The shear rate is hereby calculated as the shear velocity [mm/s] divided by the height of the ice layer [mm]. As indicated in the manuscript (line 206) the ice layer thickness varied from 2-4 mm. The mean strain rate averaged for all sample runs is $4.8 \pm 1.4 * 10^{-3}$ s^{-1}.

C: Correspondingly, we adjusted the mean strain rate in line 231 in the revised manuscript and added some sentences for explanation:

*“The mean horizontal displacement rate was 0.7 ± 0.1 mm/min, corresponding to a mean strain rate of 4.8 ± 1.4 * 10-3 s-1. The minimum test strain rate was 1.58 * 10-3 s-1, which combines the minimum accounted deformation speed (0.005 mm/s) and the maximum ice layer thickness of 4 mm. The shear rate was hereby calculated as the shear velocity [mm/s] divided by the height of the ice layer [mm]. This strain rate guaranteed the dominant deformation mode to be ice fracturing instead of creep, as 10-3 s-1 is the strain rate threshold for ice fracturing (Arenson and Springman, 2005a; Sanderson, 1988). As the shear and compressive strength of pure and dirty ice increase with the strain rate (Arenson et al., 2007; Sanderson, 1988; Schulson and Duval, 2009; Yasufuku et al., 2003), variations in the shear rate were kept as low as possible (with ± 0.1 mm/min) and had no measureable influence on the shear strength at failure (Fig. S1b).”*

and in line 627:

“…and (iv) with high strain rates ($4.8 \pm 1.4 * 10^{-3}$ s^{-1}) coinciding with the accelerating final failure stage.”

Before section 1 – Introduction

RC1: Davies et al report that the lowest strength of an ice filled joint is reached not at but just below zero degrees. How does this compare to your results?

AC/C: As our tests are not performed at temperatures warmer than -0.5 °C a comparison to the study by Davies et al. (2000) will be difficult (see also below, comment to lines 387). We decided to point to the study by Davies et al. as follows (line 399 in the revised manuscript):

"We did not perform tests at temperatures warmer than -0.5 °C because we assume the ice to melt or be squeezed out of the rock cylinders which leads to shearing along rock-rock contacts. Cohesion will be absent at the melting point and shear strength values will rise. This is shown by the tests of Davies et al. (2001) when comparing shear strengths of ice-concrete samples with concrete-concrete samples."

Line 34:

RC1: The referee exchanged "e.g." by "for example"

AC/C: Adjusted as proposed

Line 35:

RC1: The referee proposed to check

a) Beniston, M., Farinotti, D., Stoffel, M., Andreassen, L. M., Coppola, E., & Eckert, N. (2018). The European mountain cryosphere: A review of its current state , trends , and future challenges. The Cryosphere, 12, 759–794. https://doi.org/10.5194/tc-12-759-2018 and

b) Baer, P., Huggel, C., McArdell, B. W., & Frank, F. (2017). Changing debris flow activity after sudden sediment input: a case study from the Swiss Alps. Geology Today, 33(6), 216–223. https://doi.org/10.1111/gto.12211.

AC/C: We checked and included the suggested references and modified the volume of the rock slope as follows:

"…as for example, the recent 3–4 $* 10^6$ m^3 rock slope failure at Pizzo Cengalo, Graubünden, CH, on 23 August 2017 (Baer et al., 2017; Beniston et al., 2018; pers. comm. with Phillips, 2018)."

The citations are included in the reference list in chapter 11 (lines 638-639 and lines 642-643).

Line 37:

RC2: Rock-ice interlocking would only be expected for rough contact surfaces. The surfaces in your experiments are very smooth, so it is very unlikely that you will be able to see interlocking.

AC: We agree with the fact that our experiments simulate the adhesion of rock-ice interfaces rather than rock-ice interlocking due to the smooth shear surfaces. However, we think it to be important to deliver the full information as the introduction part is somehow a state of the art.

C: In order to consider the referee´s comment, we added a sentence in chapter 4.1, line 450 (revised manuscript), as follows:

"In this study, the bonding of the rock-ice interface is mostly established by adhesion whereas rock-ice interlocking is less important due to the small surface roughness of the rock samples."

Line 41:

RC1: Haeberli did not define the term, maybe use Müller 1947

AC: This might be a misunderstanding. The reference "Harris et al., 1988" refers to the Glossary of Permafrost and Related Ground-Ice Terms, Permafrost Subcommittee, published by Harris et al.

C: Hence, we stuck to the reference "Harris et al., 1988".

Lines 41-42:

RC1: The referee

(1) deleted the term "fulfilled"

(2) wrote: Active layer thaw doesn't make sense. Either you say below the maximum active layer thickness, or, as I prefer, just use maximum thaw depth.

(3) proposed to be consistent with capital A or not – related to the term "Alpine"

AC/C: We adjusted the proposed changes in the revised manuscript to "Permafrost conditions are below the maximum thaw depth which typically ranges between 2–8 m in alpine environments…"

Further, we changed the first letter of "alpine" and adjusted this writing style (small letters) in the remaining manuscript.

Line 44:

RC2: Normally 'discontinuities' is the more general term.

AC: We agree with the referee that "discontinuity" is the more general term than "joints" or "fractures". Obviously the wording "joints and fractures are used as general terms" was wrong and led to a misunderstanding. Actually, we aimed to say that the long term "discontinuity" will be substituted by the much shorter words "fractures" and "joints" within this manuscript.

C: So we modified the sentence as follows (line 43 in the revised manuscript):

"In this manuscript, both, joints and fractures are used to substitute the more general term "rock discontinuities".

Line 47:

RC2: Asked about the relevance of fracture toughness of rock bridges in the respective context

AC: The fracture toughness of rock bridges is one component of four which form the shear resistance along discontinuities in a permafrost-affected rock slope after Krautblatter et al. (2013). We wanted to present all components in terms of completeness and in a next step to show on which components we focus in the presented study. That is why we would like to keep the "fracture toughness of rock bridges" in the list of relevant mechanical parameters.

C: Consequently, we did not cancel this parameter from the list.

Line 75:

RC1: Any impact from stresses caused by thermal expansion of the bedrock as it warms?

AC/C: We added some sentences in section 1 (line 77 in the revised manuscript) to account for this information:

"Warming of permafrost in rock slopes reduces the shear resistance along rock joints in a chronological order by (i) reducing the fracture toughness of cohesive rock bridges, (ii) by lowering friction along rock-rock contacts, (iii) by altering the creep of ice infillings and (iv) finally reducing the fracture toughness of the ice itself and of rock-ice contacts (Krautblatter et al., 2013). Cyclic thermal expansion or contraction in the shallow bedrock occurs due to warming or cooling as a result of daily or seasonal variations in temperature. Variations of high frequency and magnitude can cause thermal gradients in the rock which leads to alterations in the stress field. This can induce thermal fatigue which, over long timescales, reduces the shear resistance along weakened discontinuities (Draebing et al., 2017; Gischig et al., 2011; Hall and Thorn, 2014; Jia et al., 2015; Weber et al., 2017)."

Further, we included a short comment on stresses induced by thermal expansion/contraction and their effect on the shear strength of ice-filled rock joints (section 4.1, line 477 in the revised manuscript):

"(iv) Rock minerals heat up differently and can generate thermal stresses (Gómez-Heras et al., 2006) in the intact rock and along discontinuities causing thermal fatigue and a reduction in the shear resistance (Dräbing et al., 2017). However, we do not expect an impact on the shear strength as repetitive temperature cycles with high magnitude and frequency are required for thermal stress fatigue (Hall and Thorn, 2014). During our tests, temperatures were kept constant."

The new citations are included in the reference list in chapter 11.

Line 90:

RC1: Asked to comment on what is commercial ice.

AC: Commercial ice is artificially produced in the laboratory. Butkovich (1954b) describes it with the following words "…virtually free of air bubbles and the grains were prismatic in shape with dimensions of 5 to 20 mm by 40 to 70 mm." (Hobbs, 1974, page 329)

C: We renamed the description from "commercial" to "artificial" (line 95 in the revised manuscript)

Line 90:

RC2: Asked to explain what commercial ice is.

AC: Commercial ice is artificially produced in the laboratory. Butkovich (1954b) described it with the following words: "…virtually free of air bubbles and the grains were prismatic in shape with dimensions of 5 to 20 mm by 40 to 70 mm." (Hobbs, 1974, page 329)

C: To clarify what we meant, we used "artificial" instead of "commercial" (line 95 in the revised manuscript)

Line 90:

RC1: At what strain rate? – related to the previous sentence

AC: The experiments by Schulson were performed at strain rates of 10^{-3} and 10^{-1} s^{-1}.

C: We added this information to the corresponding sentence in the revised manuscript, line 94: *"…The unconfined compressive strength of polycrystalline ice decreases by 82 % (from approx. 17 to approx. 3 MPa) with increasing temperature from -50 to 0 °C (at strain rates of 10^{-3} and 10^{-1} s^{-1}; Schulson and Duval, 2009)."*

Line 92:

RC1: Explain relevance – related to *"The fracture toughness of polycrystalline ice decreases by 27 %..."*

AC: The fracture toughness describes the resistance of the ice to crack propagation and is important for tensile and compressive failure. As such, we added this parameter to the compressive and the tensile strength.

C: However, as the correlation between temperature and fracture toughness is rather weak with $r^2 = 0.22$ and errors are pretty big (Schulson and Duval, 2009), we deleted the sentence in the revised manuscript, line 96.

Line 119:

RC2: Proposed to exchange the term *"on the laboratory rock sample scale"* with "on rock samples in the laboratory"

AC/C: Changed as proposed (line 116 in the revised manuscript)

Line 119:

RC2: Asked what is meant by "scaling properties of fracturing dynamics"

AC: We meant the scaling properties of fracture dynamics in the domains of size, space and time.

C: Correspondingly, we added the missing information to the text (line 117 in the revised manuscript):

"Scaling properties of fracturing dynamics in the domains of size, space and time have usually been observed during mechanical loading (Alava et al., 2006)."

Line 123:

RC1: Check Yamamoto and Springman CGJ 51(10) 1178-1195. 2014 – related to Eq. (3)

AC/C: We read the publication proposed by the referee and included it in the revised manuscript by adding references and information in...:

line 51: *"..and the ductile temperature- and stress-dependent creep of ice and ice-rich soils (Arenson and Springman, 2005a; Sanderson, 1988; Yamamoto and Springman, 2014) have been investigated in a number of studies,.."*

line 114: *"..AE events can indicate damage increase, i.e. microcrack generation and coalescence, initiation and propagation of fractures or shearing and failure along fractures (Cox and Meredith, 1993; Scholz, 1968). AE technology has been used extensively on rock samples in the laboratory (Lockner, 1993; Nechad et al., 2005; Yamamoto and Springman, 2014)."*

line 591: *"AE is generally well capable to anticipate rock-ice failure as (i) all failures are predated by an AE hit increase, (ii) the hit rate increases well before brittle failure starts and (iii) AE hits peak immediately prior to failure. This AE pattern coincides with observations in triaxial constant strain rate tests on frozen soil (Yamamoto and Springman, 2014). The experiments conducted clearly show that precursors before failure can be observed by the AE technique providing complementary information to the displacement measurements.*

line 596: *"It is interesting to consider that in ice, even secondary and tertiary creep are constituted by the generation and healing rate of microfractures (Paterson, 1994; Sanderson, 1988). The measured pre-failure increase in AE activity is, thus, an indication for damage increase, i.e. microcrack generation and coalescence (Fig. S3) typical for cryospheric damage propagation (Murton et al., 2016; Yamamoto and Springman, 2014)."*

The citation is included in the reference list in chapter 11.

Line 139:

RC1: Assuming horizontal conditions. In steep rock faces the stress conditions are different. However, for the sensitivity study presented it is OK to use these assumptions. – related to the phrase: "*Normal stresses of 100, 200 and 400 kPa (corresponding to rock overburdens of approx. 4, 8 and 15 m) were chosen to reconstruct relevant stress conditions for ice- and rock-ice-fracturing processes in permafrost rock joints…"*

AC: We agree with the referee`s comment that in steep rock faces shear planes are often rather inclined than running horizontally and stress conditions are different. When we increase the inclination of a shear plane at a certain depth, the normal stress acting on it will decrease and downhill forces will increase. Certainly, shear planes with a specific normal stress but higher dips will also exist in greater depths. For example, a shear plane with an inclination of 60 ° and a normal stress of 100 kPa would occur in a depth of 8 m instead of 4 m, when oriented horizontally.

C: To prevent any misunderstanding, we rephrased this paragraph and shifted the paragraph to section 2.3 in the revised manuscript, line 229:

"In steep rock faces shear planes are rather inclined than horizontal. With increasing inclination of shear planes at certain depths, the normal stress acting on them will decrease and downhill forces will increase. Correspondingly, a shear plane with a normal stress of 200 kPa but a dip > 0° will also exist in depths greater than 4 m."

Lines 147-149:

RC1: Not sure if this is correct. The ice to rock interface likely also also affected by the porosity of the rock and the chemistry. Both parameters affect the ice crystal growth, which in turn is responsible for the strength of the interface. – related to the sentence "*We assume that the shear strength of rock-ice interfaces is mostly affected by temperature, normal stress and joint surface roughness while the rock type is less important."*

AC/C: We shifted the respective paragraph to section 4.1 (line 452) because it makes more sense to discuss the topic there.

We agree that the porosity of the rock and the type of constitutive minerals could also affect the shear strength of an ice-filled rock joint. As no publication on this topic has been published yet, our assumption relies on observations during our experiments and on publications on specific and relevant characteristics of the different rock types. Hence, we listed a few arguments supporting the opposite opinion in the revised manuscript:

"So far the failure of ice-filled permafrost rock joints has been studied using concrete as a rock analogue (Davies et al., 2000; Günzel, 2008). For the first time, we use rock to closely reproduce real conditions along rock joints. Synthetic materials possibly deviate from shear strength values representative for rock joints in the field. For instance, ice sliding on granite shows a friction coefficient μ approx. 0.5 higher than ice sliding on glass or metals, all having a similar surface asperity roughness. The higher friction of the granite-ice interfaces is due to a higher effective adhesion (Barnes et al., 1971). We assume that the shear strength of rock-ice interfaces is mostly affected by temperature, normal stress, strain rate and joint surface roughness. However, the applied constant strain rate as well as the standardised preparation of a uniform joint surface roughness prohibit any potential effects on the shear strength. We postulate that the influence of the rock type on the shear strength is less important:

(i) The thermal conductivity of the rock may affect the shear strength by facilitated melting along heat-insulating surfaces causing a decrease in friction (Barnes et al., 1971). The thermal conductivity of rocks varies in a range of 0.3–5.4 W m-1 K-1 (Clauser and Huenges, 1993; Schön, 2015). A metal like brass, with a much higher thermal conductivity of 100 W m-1 K-1, would lead to a warming at the interface 14.5 °C lower than granite (Barnes et

al., 1971). Due to the relatively small range of thermal conductivities for different rock types we do not expect a rock type-dependent effect on the shear strength.

(ii) The porosity of the rock and the type of constitutive minerals may play a role for the growth of ice crystals along the rock-ice interface which in turn affects the shear strength. The strain rate and the compressive strength of ice crystals are significantly higher for those oriented parallel to the applied stress than for those oriented randomly (Hobbs, 1974; Paterson, 1994). However, we assume any potential rock type-dependent orientations of ice crystals to be deleted before shearing starts due to the applied uniaxial compression during initial consolidation.

(iii) The strength of the constitutive minerals of the rock surfaces may control the friction of the rock-ice contact. However, we assume the strength of minerals to play a minor role for the shear strength, because at the rock-ice interface the ice will fail before the rock material and ice strength will control the failure process. In our tests we could not observe particles breaking off the rock surfaces. Elastic moduli of most rock minerals (bulk modulus k: 17–176 GPa; shear modulus μ: 9–95 GPa) are 2–20 times higher than of ice (k: 8.9 GPa; μ: 3.5 GPa) (Schulson and Duval, 2009; Schön, 2015). The small applied roughness of the shear surfaces additionally prevented any relevant impact of differing mineral strengths.

(iv) Rock minerals heat up differently and can generate thermal stresses (Gómez-Heras et al., 2006) in the intact rock and along discontinuities causing thermal fatigue and a reduction in the shear resistance (Dräbing et al., 2017). However, we do not expect an impact on the shear strength as repetitive temperature cycles with high magnitude and frequency are required for thermal stress fatigue (Hall and Thorn, 2014). During our tests, temperatures were kept constant.

Thus, the tests using limestone represent rock-ice fracturing along joints of all rock types. To use rock instead of other materials probably has a greater effect on the shear strength than different rock types. Still, a potential shear strength dependence on different rock types has to be proven in additional experiments."

We added the new references "Schön, 2015" and "Gómez-Heras et al., 2006" to the reference list (section 11).

Lines 147-149:

RC2: I am fully aware that using synthetic materials such as concrete is not ideal, but I can't quite follow your logic here: You state that the friction of ice on granite is different to glass or metals. However, you assume that the rock type is not important, even though different minerals, such as silicates and calcite have different strength, hardness and chemical bonding, which all may affect the rock-ice friction. – with respect to the sentence "*We assume that the shear strength of rock-ice interfaces is mostly affected by temperature, normal stress and joint surface roughness while the rock type is less important.*"

AC/C: We shifted the respective paragraph to section 4.1 (line 452) because it makes more sense to discuss the topic there.

We agree that the strength and type of the constitutive minerals could also affect the shear strength of an ice-filled rock joint. As no publication on this topic has been published yet, our assumption relies on observations during

our experiments and on publications on specific and relevant characteristics of the different rock types. Hence, we listed a few arguments supporting the opposite opinion:

"So far the failure of ice-filled permafrost rock joints has been studied using concrete as a rock analogue (Davies et al., 2000; Günzel, 2008). For the first time, we use rock to closely reproduce real conditions along rock joints. Synthetic materials possibly deviate from shear strength values representative for rock joints in the field. For instance, ice sliding on granite shows a friction coefficient μ approx. 0.5 higher than ice sliding on glass or metals, all having a similar surface asperity roughness. The higher friction of the granite-ice interfaces is due to a higher effective adhesion (Barnes et al., 1971). We assume that the shear strength of rock-ice interfaces is mostly affected by temperature, normal stress, strain rate and joint surface roughness. However, the applied constant strain rate as well as the standardised preparation of a uniform joint surface roughness prohibit any potential effects on the shear strength. We postulate that the influence of the rock type on the shear strength is less important:

(i) The thermal conductivity of the rock may affect the shear strength by facilitated melting along heat-insulating surfaces causing a decrease in friction (Barnes et al., 1971). The thermal conductivity of rocks varies in a range of 0.3–5.4 W m-1 K-1 (Clauser and Huenges, 1993; Schön, 2015). A metal like brass, with a much higher thermal conductivity of 100 W m-1 K-1, would lead to a warming at the interface 14.5 °C lower than granite (Barnes et al., 1971). Due to the relatively small range of thermal conductivities for different rock types we do not expect a rock type-dependent effect on the shear strength.

(ii) The porosity of the rock and the type of constitutive minerals may play a role for the growth of ice crystals along the rock-ice interface which in turn affects the shear strength. The strain rate and the compressive strength of ice crystals are significantly higher for those oriented parallel to the applied stress than for those oriented randomly (Hobbs, 1974; Paterson, 1994). However, we assume any potential rock type-dependent orientations of ice crystals to be deleted before shearing starts due to the applied uniaxial compression during initial consolidation.

(iii) The strength of the constitutive minerals of the rock surfaces may control the friction of the rock-ice contact. However, we assume the strength of minerals to play a minor role for the shear strength, because at the rock-ice interface the ice will fail before the rock material and ice strength will control the failure process. In our tests we could not observe particles breaking off the rock surfaces. Elastic moduli of most rock minerals (bulk modulus k: 17–176 GPa; shear modulus μ: 9–95 GPa) are 2–20 times higher than of ice (k: 8.9 GPa; μ: 3.5 GPa) (Schulson and Duval, 2009; Schön, 2015). The small applied roughness of the shear surfaces additionally prevented any relevant impact of differing mineral strengths.

(iv) Rock minerals heat up differently and can generate thermal stresses (Gómez-Heras et al., 2006) in the intact rock and along discontinuities causing thermal fatigue and a reduction in the shear resistance (Dräbing et al., 2017). However, we do not expect an impact on the shear strength as repetitive temperature cycles with high magnitude and frequency are required for thermal stress fatigue (Hall and Thorn, 2014). During our tests, temperatures were kept constant.

Thus, the tests using limestone represent rock-ice fracturing along joints of all rock types. To use rock instead of other materials probably has a greater effect on the shear strength than different rock types. Still, a potential shear strength dependence on different rock types has to be proven in additional experiments."

We added the new references “Schön, 2015” and “Gómez-Heras et al., 2006” to the reference list (section 11).

Line 149:

RC1: The referee marked the term “*we use limestone as a representation for all rock types”* with red colour.

AC/C: We modified the discussion on the application of the failure criterion to all rock types by adding more arguments supported by experimental observations and prior publications (see above, response to lines 147-149).

Line 150:

RC1: Marked the words “small” in relation to the range in thermal conductivity of rocks” in the initial submission.

AC: We used the wording “small” because in comparison with other materials like metals, for example, the range of thermal conductivity is small.

C: We tried to make our point clearer by adding more information (see above, response to lines 147-149):

”The thermal conductivity of the rock may affect the shear strength by facilitated melting along heat-insulating surfaces causing a decrease in friction (Barnes et al., 1971). The thermal conductivity of rocks varies in a range of 0.3–5.4 W m^{-1} K^{-1} *(Clauser and Huenges, 1993; Schön, 2015). A metal like brass, with a much higher thermal conductivity of 100 W* m^{-1} K^{-1}*, would lead to a warming at the interface 14.5 °C lower than granite (Barnes et al., 1971). Due to the relatively small range of thermal conductivities for different rock types we do not expect a rock type-dependent effect on the shear strength.”*

Line 152:

RC1: Refers to his previous comment on the thermal expansion (line 75) – related to *“As such, we do not expect any effect of the thermal conductivity on the shear strength…”*

AC/C: We added a short discussion on this as follows (see above, response to lines 147-149):

“(iv) Rock minerals heat up differently and can generate thermal stresses (Gómez-Heras et al., 2006) in the intact rock and along discontinuities causing thermal fatigue and a reduction in the shear resistance (Dräbing et al., 2017). However, we do not expect an impact on the shear strength as repetitive temperature cycles with high magnitude and frequency are required for thermal stress fatigue (Hall and Thorn, 2014). During our tests, temperatures were kept constant.”

Line 153:

RC1: Unclear why since it isn’t just the surface roughness that affects the strength of the interface. – related to the phrase *“the standardised preparation of a uniform joint surface roughness for all rock samples in this study prohibits any potential effect of differing rock types.”*

AC/C: We agree with the referee´s opinion that more potential effects of differing rock types do exist. Therefore, we listed several characteristics and discussed them (see above, response to lines 147-149).

Lines 153-155:

RC2: Asked for supporting evidence for our statement: “To use rock instead of other materials probably has a greater effect on the shear strength than different rock types.”

AC/C: We shifted the respective statement to the first part of the paragraph and then listed a few arguments including references to support the statement (see above, response to lines 147-149).

Line 167:

RC1: Added the word “is” and deleted the words “deformation rates” in the sentence “*Since 2007, the rock mass creeps slowly at an average of 3.75 mm/year with more than five times higher deformation rates in July to October in comparison to the remaining months.”*

AC/C: We made two sentences out of one and formulated them in a way easier to understand (line 152 in the revised manuscript):

“Since 2007, the rock mass creeps slowly at an average of 3.75 mm/year. From July to October it moves more than five times faster than in the remaining months.”

Lines 176-184:

RC1: The referee suggested to present the four points as a list instead within the running text.

AC/C: Adjusted as proposed

Line 177:

RC1: It would be helpful to plot the principal stresses for the cross section. – referred to Fig. 1

AC/C: We changed Fig. 1 as proposed and included normal stresses (line 154 in the revised manuscript):

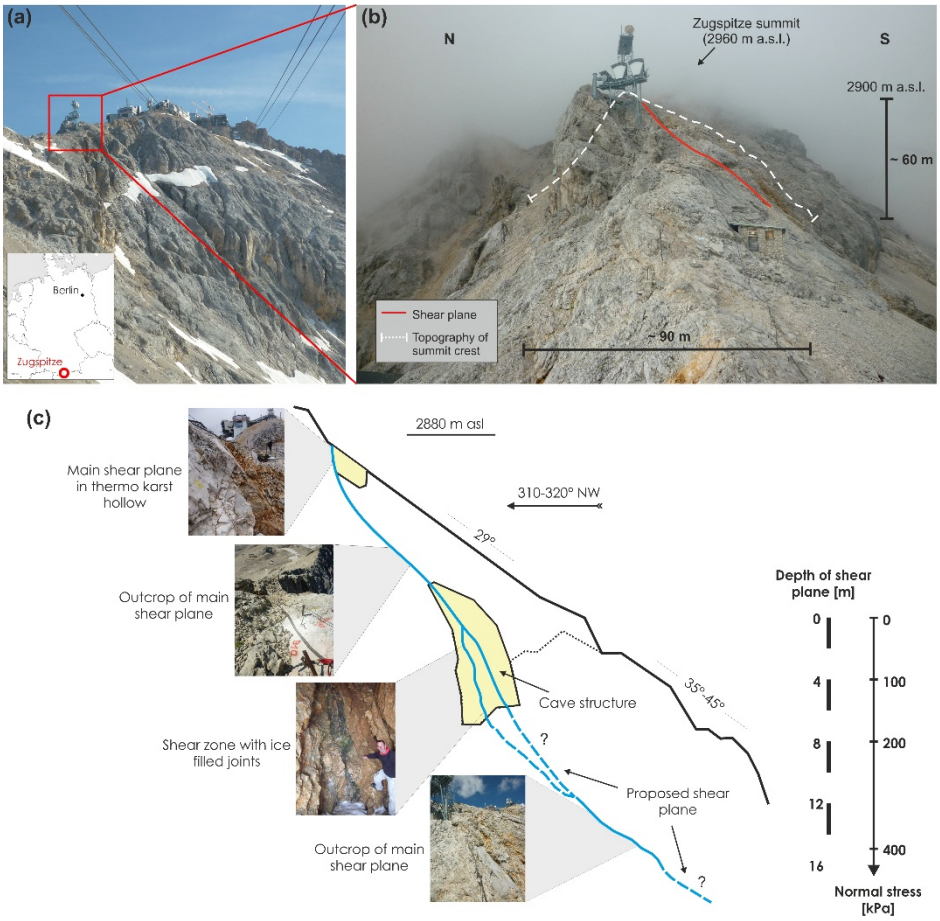

For a better link to the figure, we shifted its reference to another sentence (line 164 in the revised manuscript): *"(i) The depth of the main shear plane is assessed to a maximum of 10–15 m due to field mapping. The corresponding normal stresses on this shear plane (mostly ≤ 400 kPa) lie within the range of the tested stress levels (Fig. 1c)."*

Further, we increased the font and thickness of the lines for a better perceptibility (see Fig. 1).

Line 180:

RC1: Not clear what depths you are referring to. Referred to *"Current borehole temperatures at the peak of the Zugspitze average -1.3 °C within the permafrost core area and approach minima of -6 °C at the margins…"*

AC/C: We added the information of the corresponding depths as follows (line 166 in the revised manuscript):

"(iii) The Zugspitze summit area is located at the lower permafrost extension limit. Current borehole temperatures at the peak of the Zugspitze average -1.3 °C within the permafrost core area (approx. 24 m away from the south face and 21 m away from the north face) and approach minima of -6 °C at the margins (ca. 5 m away from the north face) (Böckli et al., 2011; Gallemann et al., 2017; Krautblatter et al., 2010; Noetzli et al., 2010)."

Line 184:

RC1: Be specific about the period. – referred to *"A climatic warming in the last century and an even stronger temperature increase since the 1990s can be observed at the Zugspitze, i.e. the mean annual air temperature (MAAT) in 1991–2007 was 0.8–1.1 °C warmer than in prior 20th century reference periods…"*

AC/C: We changed the sentence in order to give a more specific information on the reference periods (line 171 in the revised manuscript):

"(iv) A climatic warming in the last century and an even stronger temperature increase since the late 1980s can be observed at the Zugspitze, i.e. the mean annual air temperature (MAAT) in 1991–2007 was 0.8–1.1 °C warmer than in the three prior 30 year reference periods between 1901 and 1990 (Gallemann et al., 2017; Krautblatter et al., 2010)."

Lines 188-198:

RC1: Deleted the second part of the sentence

AC/C: Deleted as suggested

Lines 192-193:

RC1: Deleted the information in brackets

AC/C: Deleted as suggested

Lines 192-193:

RC2: Asked for a reference related to the standardized roughness recommendation by the ISRM

AC/C: We included two references as proposed (line 181 in the revised manuscript):

"Following the ISRM recommendations for standardised tests (Ulusay, 2015) and Coulson (1979, in Cruden and Hu, 1988), the roughness of the specimen's surfaces was produced using abrasive grinding powder.."

Additionally, we added the references to Cruden and Hu (1988) and Ulusay (2015) to the list in section 11.

Line 195:

RC2: This is a very smooth surface; the amplitude and wavelength of natural joints is much larger than 0.185mm. As you state above, the surface roughness does have an effect, such as rock-ice interlocking (which was also mentioned earlier). You may also have to consider localised pressure melting at asperities. – with reference to the used diameter of the abrasive grains of 0.185 mm.

AC: We are in agreement with the referee about the influence of surface roughness on the shear strength and failure behaviour. However, we decided to account for both requirements equally: on the one hand a good sample-reproducibility in terms of uniform test conditions (without spending too much time and costs) and on the other hand a simulation of rock surfaces as close as possible to conditions in the field. In future we consider to perform more tests on varying surface roughness, but this is beyond the scope of this first study.

C: Therefore, we would like to stick to the roughness amplitude of 0.185 mm (line 181 in the revised manuscript).

Lines 196-197:

RC2: I do not agree with this statement. Porosity and chemistry of the rock material are likely to have an effect. – related to the sentence *"The uniform joint surface roughness prohibits any potential effect of differing rock types on the shear strength results."*

AC: We agree with the referee´s comment as joint surface roughness does have an effect on the shear strength but it is independent of the rock type. We also agree with the referee´s opinion that some other characteristics (for example porosity or mineral composition) varying with the rock type may affect the shear strength. To account for this, we listed several characteristics and discussed them (see above, response to lines 147-149).

C: Consequently, we modified the sentence as follows (line 185 in the revised manuscript):

"..The uniform joint surface roughness prohibits any potential effect on the shear strength results.."

Line 198:

RC1: Exchanged the word "basin" with "bath"

AC/C: Changed as suggested

Line 206:

RC1: Exchanged the expression "flowing out" with "draining"

AC/C: Changed as suggested

Lines 209-211:

RC2: The constant-strain results for 'sandwich' samples and concrete-ice samples do differ significantly. The samples with 25mm infill do not show brittle failure. – with respect to the sentence *"In other shear experiments, the shear strength of sandwich samples with a 1 mm thick ice layer did also not differ significantly from the results of concrete-ice specimens representing a 25 mm thick ice infilling (Günzel, 2008)."*

AC: We checked the publication of Günzel (2008) and have to admit that shear strengths of concrete-ice samples and sandwich samples, tested at constant strain, do differ from each other. However, constant stress experiments

show similar shear strength results for both sample types (page 585). These include brittle failure as the dominant deformation type: “Constant-stress experiments with both sample types show that here the predominant type of deformation is breaking the connection between the ice and the concrete.” (page 586) We hope that we did not misunderstand this.

C: Consequently, we would like to stick to the reference to Günzel (2008) and specify the information on the tests as follows (line 197 in the revised manuscript):

“..In other shear tests with constant stress, the shear strength of sandwich samples with a 1 mm thick ice layer did also not differ significantly from the results of concrete-ice specimens representing a 25 mm thick ice infilling (Günzel, 2008)…”

Line 224/Fig. 3:

RC1: Perspective of the ice layer is off. – related to Fig. 3

AC/C: We changed Fig. 3b by shifting the overlain sketch of the specimen rings and the ice layer to the left. In this way the perspective onto the cylinders and the gap with the ice layer is good (see below):

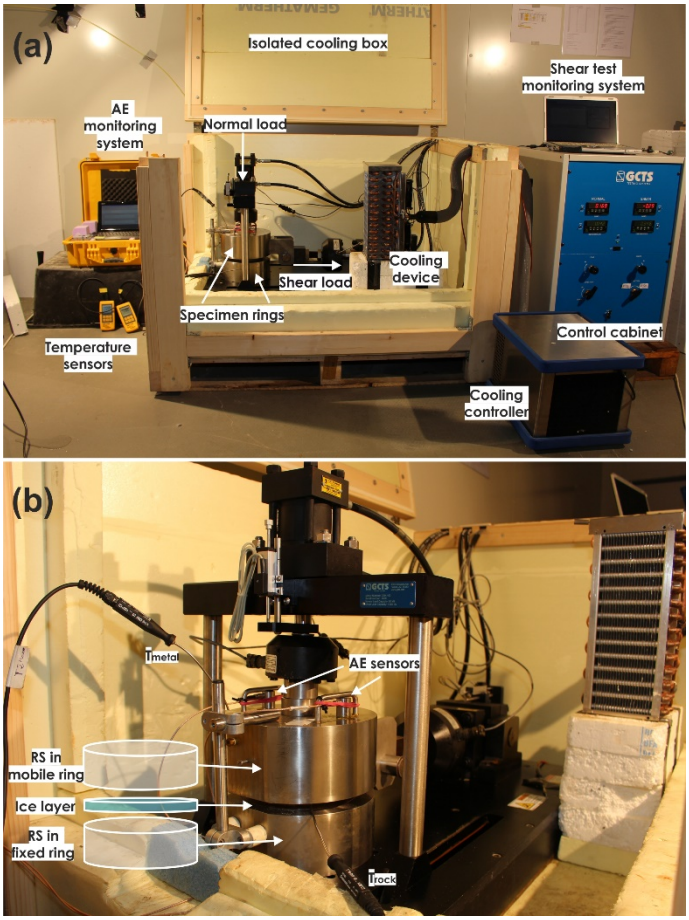

In the caption of Fig. 3 we added two short explanations for abbreviations used in the figure (line 213 in the revised manuscript):

"Experimental setup showing the laboratory shear machine, acoustic emission monitoring system, the cooling device and the cooling box. RS = rock sample. T = Rock temperature sensor."

Line 228:

RC2: Proposed to exchange the word "campaign" with "series"

AC/C: Changed as suggested

Lines 244-245:

RC1: Also check Yasufuku, N., Springman, S. M., Arenson, L. U., & Ramholt, T. (2003). Stress-dilatancy behaviour of frozen sand in direct shear. In M. Phillips, S. M. Springman, & L. U. Arenson (Eds.), Proceedings of the 8th International Conference on Permafrost (pp. 1253–1258). Zurich, Switzerland: A.A. Balkema.

AC/C: We checked the study by Yasufuku et al. (2003) and added the reference to line 236 in the revised manuscript:

"As the shear and compressive strength of pure and dirty ice increase with the strain rate (Arenson et al., 2007; Sanderson, 1988; Schulson and Duval, 2009; Yasufuku et al., 2003), variations in the shear rate were kept as low as possible…"

The citation is included at the end of the reference list in chapter 11.

Line 268:

RC1: Asked for the used version of MATLAB

AC/C: The version of MATLAB was "R2017a (9.2.0.556344)". We added this information to (line 260 in the revised manuscript):

"The linear fitting is estimated by a linear regression model using the LinearModel class of MATLAB (Version R2017a (9.2.0.556344))."

Line 277/Fig. 4:

RC1: "Would be better to show strain and not deformation." – referred to Fig. 4

AC/C: We modified the figure by displaying the deformation of the sample with the shear strain in %, suggested by the referee:

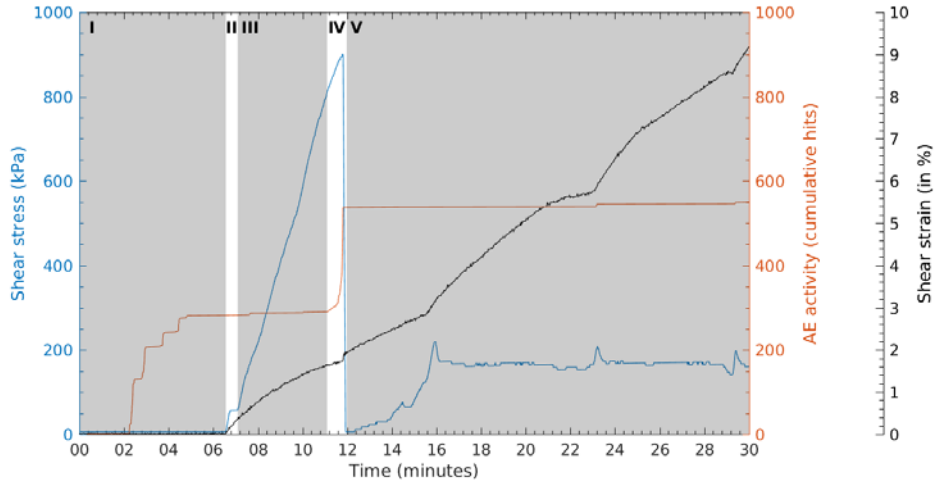

Correspondingly, we slightly modified the first sentence of the caption (line 270 in the revised manuscript):

"Typical curves of shear stress, shear strain and acoustic activity for a shear test at T = -3 °C and σ = 200 kPa."

Line 277/Fig. 4:

RC2: Axis labels for both y-axes are missing. As the blue y-axis goes up to 1.0, it is not clear if the shear stress and deformation is normalised in any way?

AC/C: We addressed this comment and modified Fig. 4 (line 269 in the revised manuscript):

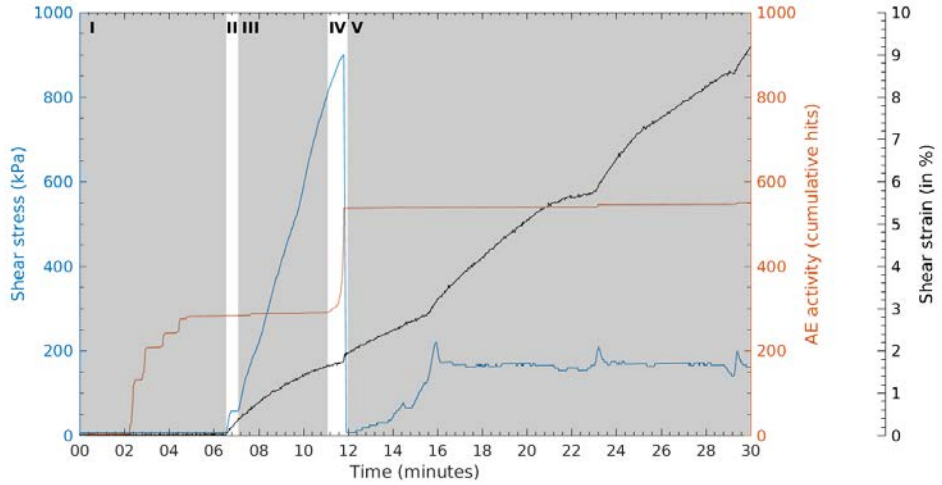

Moreover, we modified the first sentence of the caption (line 270 in the revised manuscript):

"Typical curves of shear stress, shear strain and acoustic activity for a shear test at T = -3 °C and σ = 200 kPa."

In the supplementary material we modified Fig. S3 (line 69) in the same way as Fig. 4.:

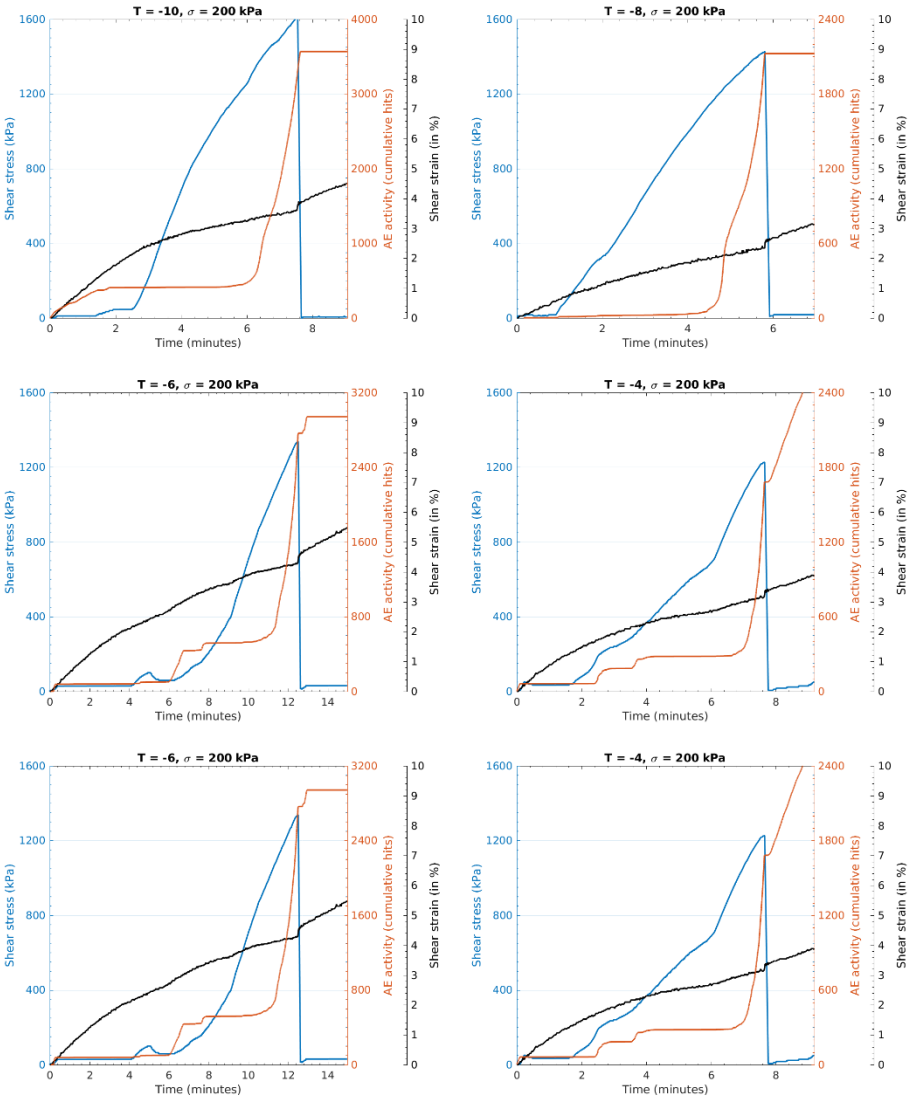

Line 283:

RC2: Proposed to add the word “before” in the phrase *“the experiment starts with a consolidation of approximately five minutes before applying the specified normal load.”*

AC/C: The specified normal load is applied in the first stage of consolidation. That is why we do not want to add the word “before” as it suggests the normal load to be applied after consolidation (line 276 in the revised manuscript).

Line 288:

RC1: Exchanged the expression “deformation” with “failure”

AC/C: Changed as suggested

Line 292:

RC1: Exchanged the expression “an” with “a minor”

AC/C: Changed as suggested

Line 292:

RC1: Really? The AE signals represent ice healing? Or do you refer to the residual strength being ice healing, or the small increases are a indicating that some ice must have healed and are now braking?” – referred to the sentence *“…the post-failure shear stress exhibits several small peaks, which are often accompanied by a minor increase in AE hits and audible cracking (ice healing).”*

AC: When mentioning “ice healing” we primarily referred to the peaks in shear stress which are supposed to represent healed ice that breaks. More than 90 % of the tests with observed post-failure-peaks revealed failures within the ice or a mixture of failures in the ice and along rock-ice contacts. Thus, the peaks of shear stress could also be caused by ice-ice interlocking and subsequent failure when stresses exceed a threshold.

C: We changed the last sentence of the paragraph and added three ones for explanation (line 283 in the revised manuscript):

“In a few experiments (such as in Fig. 4), the post-failure shear stress exhibits several small peaks, which are often accompanied by a minor increase in AE hits, audible cracking and a pronounced rise in shear strain. The peaks in shear stress may refer to healed ice that breaks when stresses exceed a certain threshold. Further, more than 90 % of the samples with observed post-failure-peaks also failed within the ice or both in the ice and along the rock-ice interface. Hence, these peaks may also be caused by ice-ice interlocking leading to the observed decrease in shear strain (Fig. 4). Subsequent failure occurs when the shear stresses overcome the ice strength.”

We also corrected the sentence in line 280 in terms of the description of the shear strain behaviour at failure:

“Correspondingly, the ice infill between the rock cylinders fails and shear deformation reaches one of its maximum values.”

Line 292:

RC2: Asked if ice healing really gives cracks – related to the phrase *“…the post-failure shear stress exhibits several small peaks, which are often accompanied by a minor increase in AE hits and audible cracking (ice healing).”*

AC: Sorry for this misunderstanding by putting “ice healing” in brackets and not adding any comments on this. When mentioning “ice healing” we primarily referred to the peaks in shear stress which are supposed to represent healed ice that breaks. More than 90 % of the tests with observed post-failure-peaks revealed failures within the ice or a mixture of failures in the ice and along rock-ice contacts. Thus, the peaks of shear stress could also be caused by ice-ice interlocking and subsequent failure when stresses exceed a threshold.

C: We changed the last sentence of the paragraph and added three ones for explanation (line 283 in the revised manuscript):

"In a few experiments (such as in Fig. 4), the post-failure shear stress exhibits several small peaks, which are often accompanied by a minor increase in AE hits, audible cracking and a pronounced rise in shear strain. The peaks in shear stress may refer to healed ice that breaks when stresses exceed a certain threshold. Further, more than 90 % of the samples with observed post-failure-peaks also failed within the ice or both in the ice and along the rock-ice interface. Hence, these peaks may also be caused by ice-ice interlocking leading to the observed decrease in shear strain (Fig. 4). Subsequent failure occurs when the shear stresses overcome the ice strength."

We also corrected the sentence in lines 280 in terms of the description of the shear strain behaviour at failure:

"Correspondingly, the ice infill between the rock cylinders fails and shear deformation reaches one of its maximum values."

Line 294/Fig. 5:

RC1: Can you show in a log-log plot? – related to Fig. 5c

AC/C: We plotted Fig. 5c as proposed (see below):

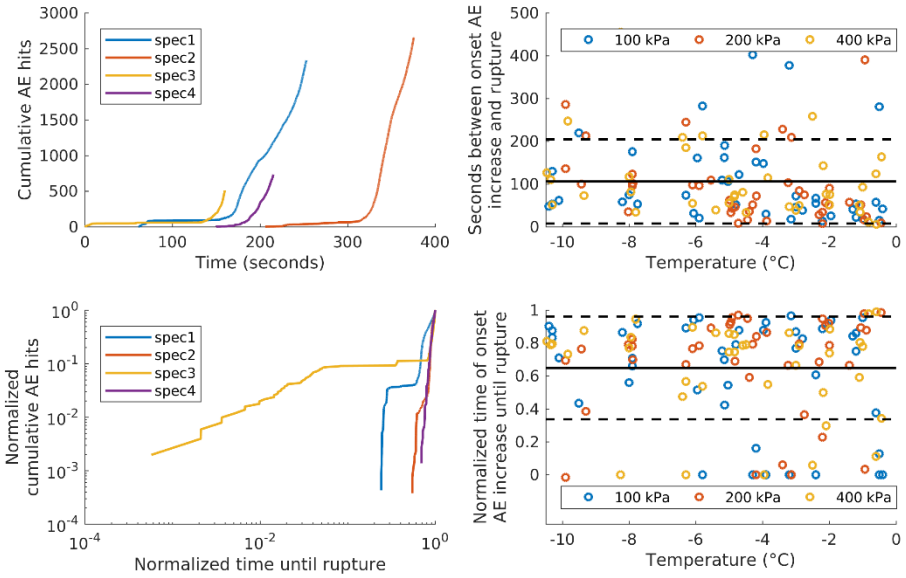

However, we still use the old version of Fig. 5c for the manuscript because in our opinion – with consistent time steps – it shows more clearly that the onset of AE increase starts rather shortly before failure. In this way, the stage of AE hit increase can be compared more easily with the rest of the remaining stages of the test. Further, the percentage of AE hits before the onset of increase (stages 1 and 2) and after it (stage 3 and 4) can be compared in a way that is more understandable.

Nevertheless, we changed the American "normalized" to the British "normalised" in the labels of Fig. 5c and 5d as the whole manuscript is written in British English.

Line 294/Fig. 5a:

RC2: Why does recording start at different times? What is time zero? Start of shear? Please give some explanation. – related to Fig. 5a

AC: In Fig. 5a and Fig. 5c, time zero corresponds to the shear start of the experiments. Curves starting at x > 0 represent tests where the first AE signals were recorded a certain time after shear start.

C: We added the missing explanation to the caption of Fig. 5 (line 291 in the revised manuscript):

"Figure 5: Time series of (a) cumulative AE hits and (c) normalised cumulative AE hits with 400 kPa normal stress and at -4° C. Time zero corresponds to the shear start of the experiments (spec1-4). Curves starting at x > 0 represent tests where first AE signals were recorded a certain time after shear start. The temperature-dependent time between onset of AE increase and rupture is displayed in seconds (b) and normalised (d)…"

Line 300:

RC1: Exchanged the expression "rupture" with "failure"

AC/C: Changed as suggested

Line 327:

RC1: What about stress? – referred to the observations on the relationship between temperature and failure type

AC/C: To include our observations on the relation between normal stress and failure type we changed the title of section 3.2 into *"Observed failure type and its dependence on temperature and normal stress"*.

Then we added a new figure (Fig. S6) to the supplementary material (line 97):

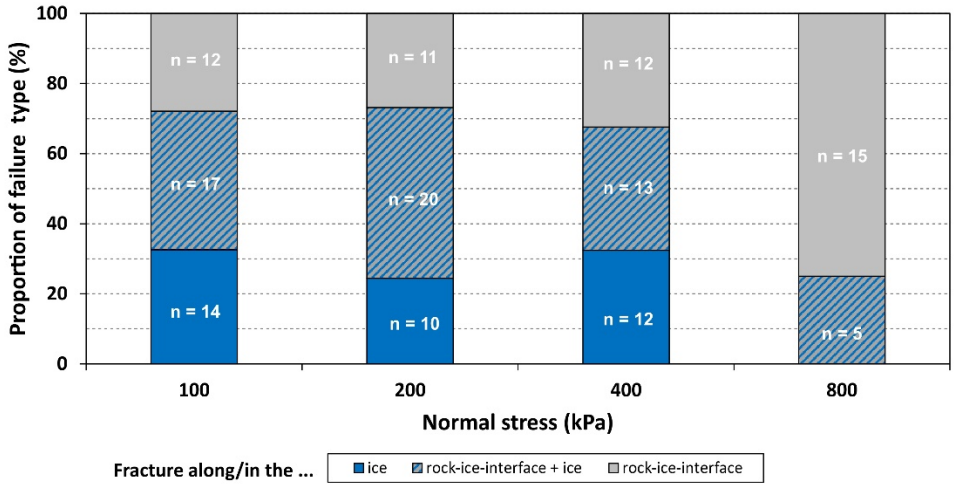

Within the supplement: We added a caption and a few sentences for explanation (line 98 and following):

"*Figure S6: "Proportions and absolute numbers of failure types for normal stresses from 100 to 800 kPa and temperatures from -10 to -0.5 °C."*

A new paragraph (lines 100 and following) was added:

"*A relationship between failure type and normal stress could not be identified for stress levels 100–400 kPa (Fig. S6). However, at normal stresses of 800 kPa fracturing in the ice does not occur at all whereas fracturing of rock-ice contacts dominates with 75 %. This overrepresentation of failures along the rock-ice interface may be caused due to the absence of tests at 800 kPa and temperatures below -5 °C where (at ≤ 400 kPa) much higher proportions of failures within the ice were observed (Fig. 6)."*

Further, the old numbers of the figures in the supplementary material were changed and we included the figure in the "legend" at the first page (line 18):

"(vii) the relationship between failure type and normal stress level (Fig. S6),"

In the main manuscript (line 325): In order to account for the referee`s comment we added the sentence

"A clear relationship between failure type and normal stress could not be identified (Fig. S6)."

Further, the old numbers of the figures in the manuscript were changed (lines 328, 360).

Line 327:

RC2: Asked if stress had an effect on the failure type too

AC/C: To include our observations on the relationship between normal stress and failure type we changed the title of section 3.2 into "*Observed failure type and its dependence on temperature and normal stress*".

Then we added a new figure (Fig. S6) to the supplementary material (line 97):

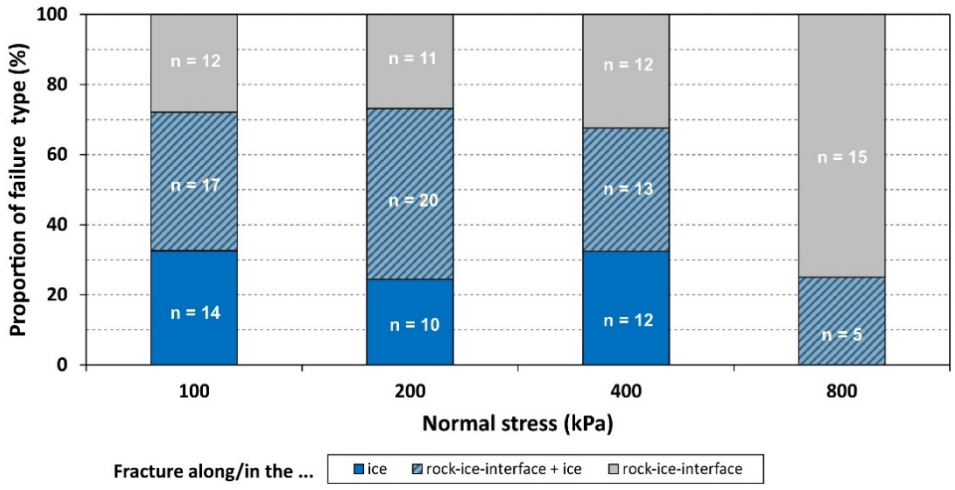

Within the supplement: We added a caption and a few sentences for explanation (line 98 and following):

"*Figure S6: "Proportions and absolute numbers of failure types for normal stresses from 100 to 800 kPa and temperatures from -10 to -0.5 °C."*

A new paragraph (lines 100 and following) was added:

"*A relationship between failure type and normal stress could not be identified for stress levels 100–400 kPa (Fig. S6). However, at normal stresses of 800 kPa fracturing in the ice does not occur at all whereas fracturing of rock-ice contacts dominates with 75 %. This overrepresentation of failures along the rock-ice interface may be caused due to the absence of tests at 800 kPa and temperatures below -5 °C where (at ≤ 400 kPa) much higher proportions of failures within the ice were observed (Fig. 6).*"

Further, the old numbers of the figures in the supplementary material were changed and we included the figure in the "legend" at the first page (line 18):

"(vii) the relationship between failure type and normal stress level (Fig. S6),"

In the main manuscript (line 325): In order to account for the referee`s comment we added the sentence "*A relationship between failure type and normal stress could not be identified (Fig. S6).*"

Further, the old numbers of the figures in the manuscript were changed (lines 328, 360).

Line 345:

RC2: I am not quite sure about that. The y-axes have a very different scale to the x-axes. If you plot the data in graphs with equal scale for both axes you will see that the correlation is very weak. – with respect to Fig. 7 and our description of the results: "*The low values of R^2 are partially an effect of the tests clustering around the four predefined stress levels.*"

AC: We agree with the referee that the clustering of the data points around the three or four predefined normal stress levels does not have an effect on the values of R^2. When adding more data points at other normal stress levels than 100, 200, 400 or 800 kPa and with similar standard deviations, the values of R^2 do not increase.

C: Consequently, we deleted the respective sentence "*The low values of R^2 are partially an effect of the tests clustering around the four predefined stress levels.*" (line 340 in the revised manuscript).

Line 349/Fig. 7:

RC1: Combine a) with b) as illustrated – related to Fig. 7

AC/C: We modified Fig. 7 as suggested (line 341 in the revised manuscript):

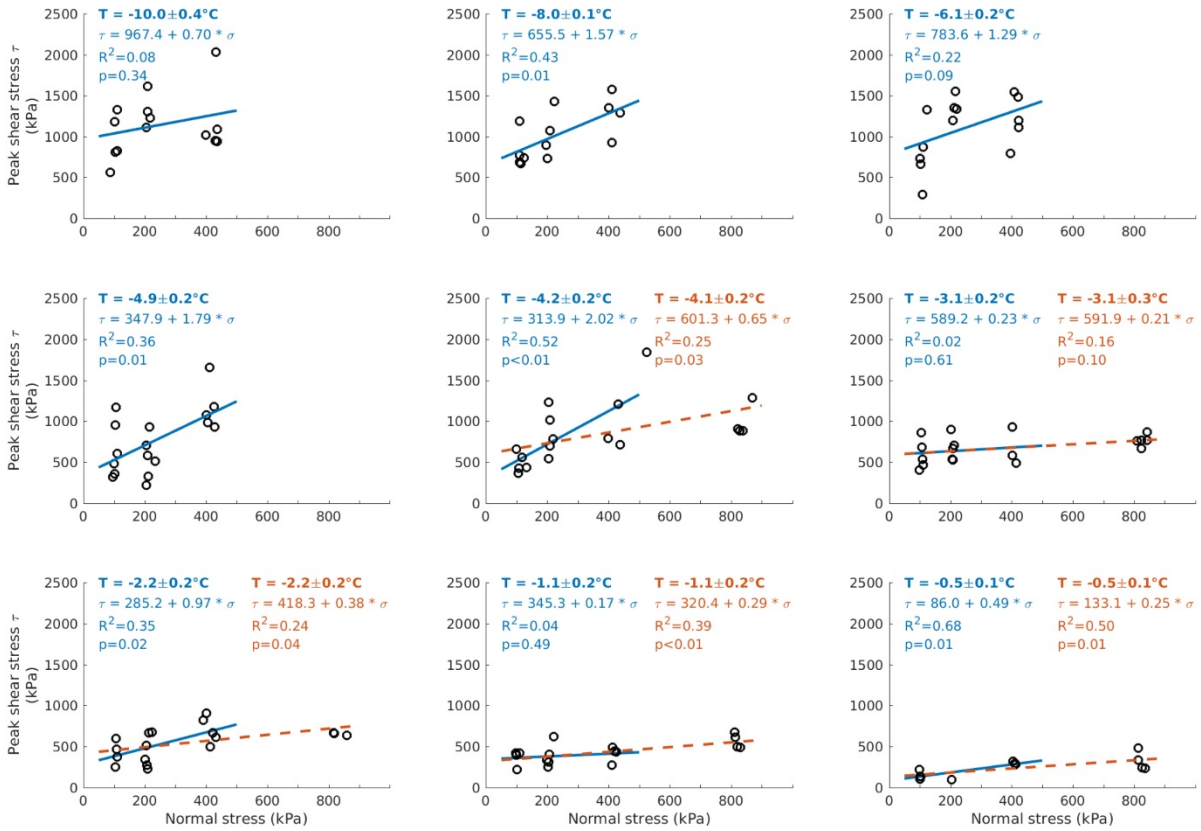

As a consequence, we had to adjust the corresponding caption of Figure 7 as follows (line 342 in the revised manuscript):

"Measured shear stress at failure as a function of normal stress for temperatures between -10 and -0.5 °C. The temperature values are corrected by the means (including standard deviation) of the respective temperature level. Normal stress levels of 100, 200 and 400 kPa were applied for the whole temperature range. 800 kPa was additionally tested between -4 and -0.5 °C. Blue solid lines = calculated regression lines for normal stresses 100-400 kPa. Orange dashed lines = calculated regression lines for 100-800 kPa. Regression lines were used to derive temperature-specific cohesion and friction values. p = Probability of rejecting the null hypothesis (H0) although it is true."

Further, we had to change references to the respective figure from "Fig. 7a" or "Fig. 7b" to "Fig. 7", in lines 338 and 580.

Line 349/Fig. 7:

RC2: Agreed with Arenson´s comment as the first referee who wrote "Combine a) with b) as illustrated" – see Arenson´s comments

AC/C: We modified Fig. 7 as suggested (line 341 in the revised manuscript):

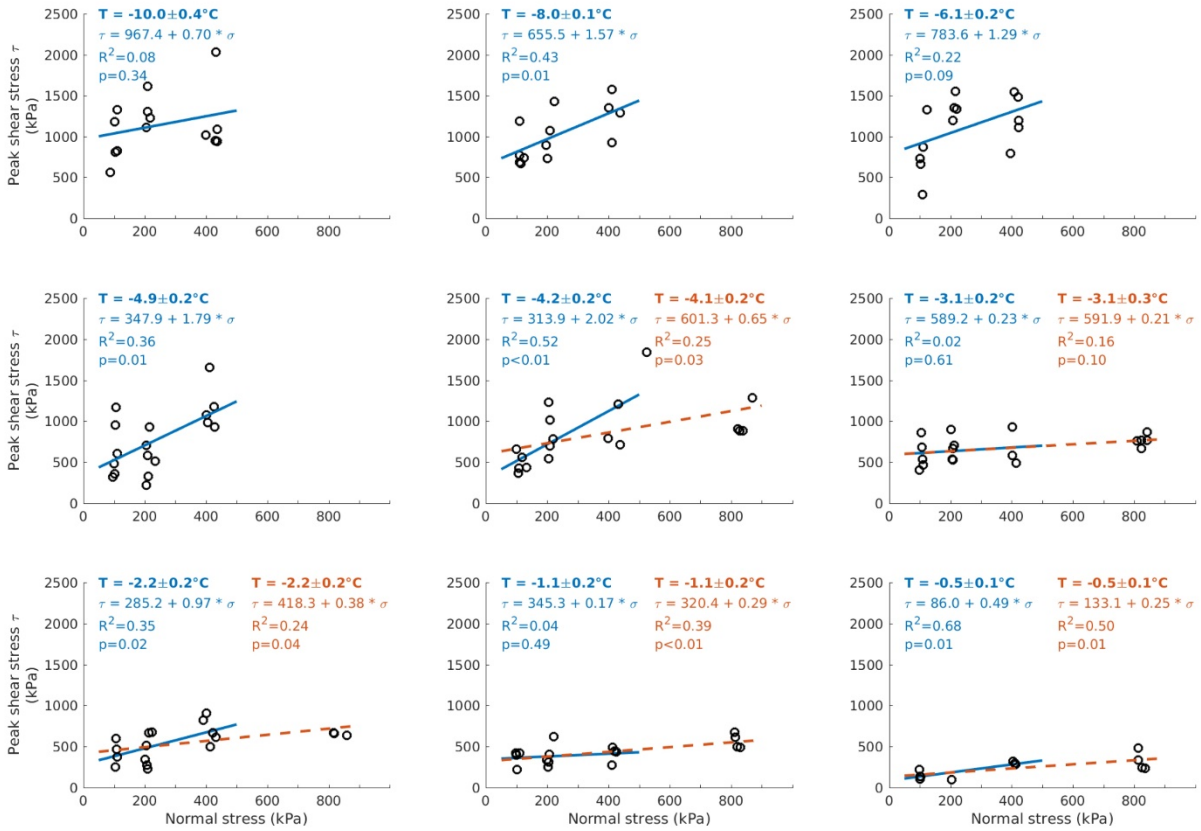

As a consequence, we had to adjust the corresponding caption of Figure 7 as follows (line 342 in the revised manuscript):

"Measured shear stress at failure as a function of normal stress for temperatures between -10 and -0.5 °C. The temperature values are corrected by the means (including standard deviation) of the respective temperature level. Normal stress levels of 100, 200 and 400 kPa were applied for the whole temperature range. 800 kPa was additionally tested between -4 and -0.5 °C. Blue solid lines = calculated regression lines for normal stresses 100-400 kPa. Orange dashed lines = calculated regression lines for 100-800 kPa. Regression lines were used to derive temperature-specific cohesion and friction values. p = Probability of rejecting the null hypothesis (H0) although it is true."

Further, we had to change references to the respective figure from "Fig. 7a" or "Fig. 7b" to "Fig. 7", in lines 338 and 580.

Line 351:

RC2: I don't quite understand how the temperature data are corrected and indeed why they need to be corrected. – related to the Fig. caption *"The temperature values are corrected by the means (including standard deviation) of the respective temperature level."*

AC: We did not want to use the values of the temperature classes as they do not represent the real temperatures of the samples close to the moment of failure. Therefore, we used the measured rock temperatures of all experiments belonging to a specific temperature class and calculated the mean and corresponding standard deviation.

C: We changed the respective sentence in the caption of Fig. 7 for a more detailed and understandable explanation (line 342 in the revised manuscript):

"Figure 7: Measured shear stress at failure as a function of normal stress for temperatures between -10 and -0.5 °C. The temperature values are the means (including standard deviations) of the measured rock sample temperatures (close to the moment of failure) of all experiments belonging to a specific temperature level. Normal stress levels of 100, 200 and 400 kPa were applied for the whole temperature range."

Line 358:

RC1: Suggested to add a reference to the Mohr-Coulomb equation

AC/C: We added three references of Coulomb (1773), Mohr (1900) and Jaeger et al. (2007) to the failure criterion (line 350 in the revised manuscript):

"To develop a shear strength description of ice-filled permafrost rock joints we used the linear and stress-dependent Mohr-Coulomb failure criterion (a combination of Coulomb (1773) and Mohr (1900); a discussion of its limitations is given in Jaeger et al. (2007)).."

Further, we extended the reference list by these three publications in section 11.

Line 360:

RC1: Not sure if you can really apply the concept of effective stresses here as you don't know the pore water pressures. Please stay with total stresses. – referred to the explanation of Eq. (5)

AC/C: We deleted the word "effective" and changed the symbol from effective σ' to normal stress σ (line 356 in the revised manuscript).

Line 360:

RC2: Recommends to use total normal stress and not effective normal stress

AC/C: Changed as recommended (line 356 in the revised manuscript).

Line 376/Fig. 8:

RC1: The referee drew a red exponential curve into Fig. 8a and 8b giving an alternative to the linear curves by the authors. He commented on this with the following words: "For the cohesion I would not have expected a linear, but exponential trend. (b) makes most sense to me. Have you looked at such correlations? At 0 Degrees you shouldn't have a cohesion either".

AC: Considering the temperatures tested in our experiments, we do not know how cohesion and friction behave between -0.5 and 0 °C. As such, the valid upper boundary of temperatures for the calculated parameters and failure criterion is -0.5 °C. Correspondingly, the curves were not calculated/displayed for temperatures warmer than -0.5 °C. If we assume to have no cohesion at the melting point (where we fully agree with the referee), exponential curves are supposed to be very sensitive in the range of -0.5 to 0 °C. That is why we still keep to the linear curves.

C: In order to stress the fact that the equations for cohesion and friction are only valid for temperatures between -0.5 and -8 °C, we added grey areas displaying the valid temperature ranges (see below; line 371 in the revised manuscript):

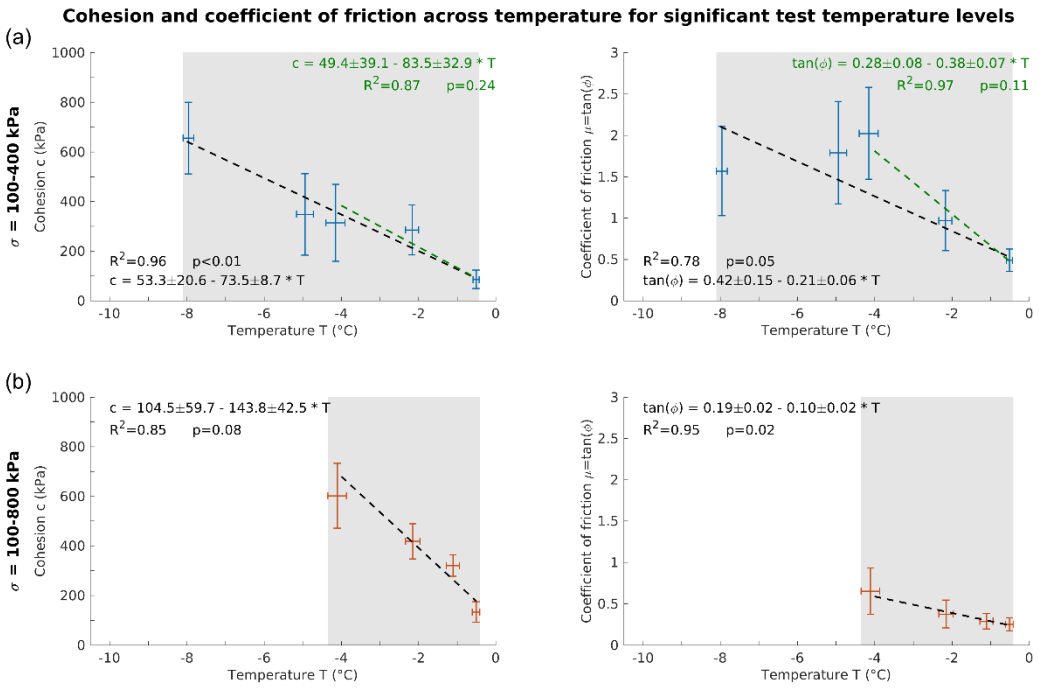

Due to this change in the figure, we had to add further explanation in the caption of Fig. 8 (line 377 in the revised manuscript):

"…The grey areas represent the valid temperature range for the respective parameter."

Line 376/Fig. 8:

RC2: I agree with Arenson's comments on the linear relationships; I assume that zero degrees still has ice content (and water)? Then cohesion should be zero. No ice and rock-rock contact at zero degrees would be an entirely different situation. – referred to Fig. 8

AC/C: Considering the temperatures tested in our experiments, we do not know how cohesion and friction behave between -0.5 and 0 °C. Correspondingly, the curves were not calculated/displayed for temperatures warmer than -0.5 °C. If we assume to have no cohesion at the melting point (where we fully agree with the referee), exponential curves are supposed to be very sensitive in the range of -0.5 to 0 °C. That is why we still keep to the linear curves.

In order to stress the fact that the equations for cohesion and friction are only valid for temperatures between -0.5 and -8 °C, we added grey areas displaying the valid temperature ranges (see below, line 371 in the revised manuscript):

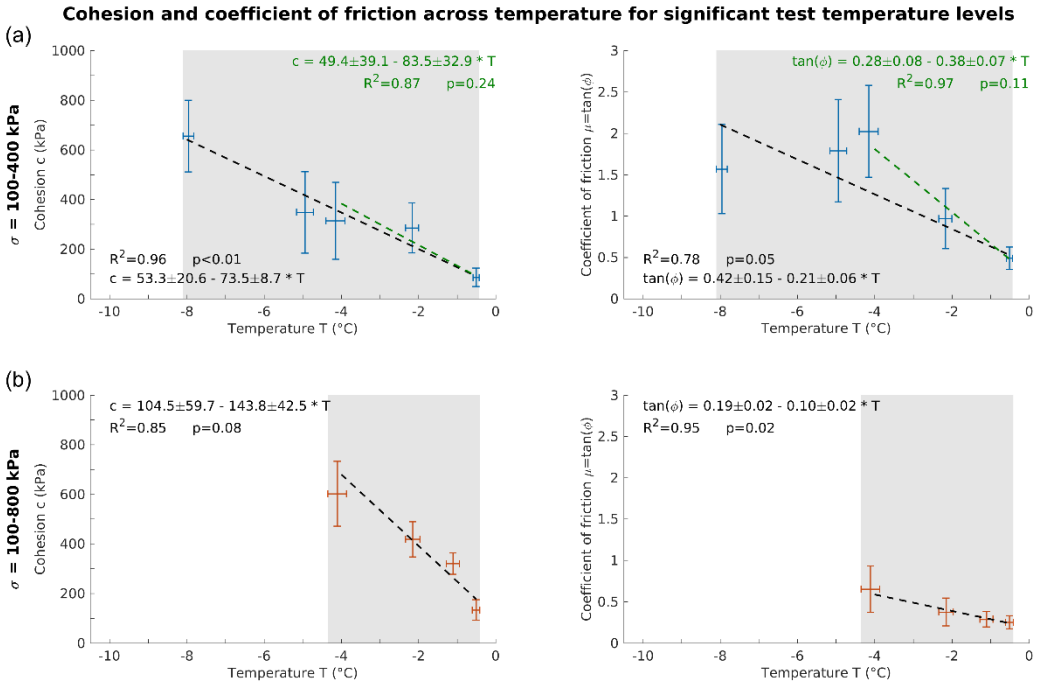

Due to this change in the figure, we had to add further explanation in the caption of Fig. 8 (line 377 in the revised manuscript):

"…*The grey areas represent the valid temperature range for the respective parameter.*"

We agree that no cohesion will be present at 0 °C and when the ice layer has melted. However, as the formula is just valid for temperatures from -8 to -0.5 °C (see sentence below Eq. (6)), cohesion values at a temperature of 0 °C are not supposed to be calculated with the formula. Tests at temperatures warmer than -0.5°C have not been performed as we assume the ice layer to be squeezed out of the rock cylinders leading to shearing along rock-rock contacts. In this case another surface material is involved in the shearing and may lead to different results. This can be observed in Davies et al. (2000, 2001) when comparing ice-concrete samples with concrete-concrete samples.

Hence, we would like to stick to the linear functions and added an explanation to prevent further misunderstandings (line 399 in the revised manuscript)

"We did not perform tests at temperatures warmer than -0.5 °C because we assume the ice to melt or be squeezed out of the rock cylinders which leads to shearing along rock-rock contacts. Cohesion will be absent at the melting point and shear strength values will rise. This is shown by the tests of Davies et al. (2001) where the shear strengths of ice-concrete samples closely approach the concrete-concrete sample line."

Line 387:

RC1: This implies that at 0 degree you have a cohesion of 53.3 kPa. Where does it come from? – with reference to Eq. (6)

AC: We agree that no cohesion will be present at 0 °C and when the ice layer has melted. However, as the formula is just valid for temperatures from -8 to -0.5 °C (see sentence below Eq. (6)), cohesion values at a temperature of 0 °C are not supposed to be calculated with the formula. Tests at temperatures warmer than -0.5°C have not been performed as we assume the ice layer to be squeezed out of the rock cylinders leading to shearing along rock-rock contacts. In this case another surface material is involved in the shearing and may lead to different results. This can be observed in Davies et al. (2000, 2001) when comparing ice-concrete samples with concrete-concrete samples.

C: Hence, we would like to stick to this formula and added an explanation to prevent further misunderstandings (line 399 in the revised manuscript):

"We did not perform tests at temperatures warmer than -0.5 °C because we assume the ice to melt or be squeezed out of the rock cylinders which leads to shearing along rock-rock contacts. Cohesion will be absent at the melting point and shear strength values will rise. This is shown by the tests of Davies et al. (2001) where the shear strengths of ice-concrete samples closely approach the concrete-concrete sample line."

Line 407:

RC1: It would be beneficial to include an error range, consider the large range in your test results. - with reference to Eq. (8)

AC/C: Changed as suggested

Line 431:

RC2: Asked if 23 * 10^3 m^3 is meant referring to the expression "23.000 m^3"

AC/C: We changed the writing style of this rock failure volume and some more (see below) to a uniform writing style used in the whole manuscript:

- Line 69: *."..97 % of them had volumes* $\leq 3 \times 10^4$ m^3 *which correspond to the relevant.."*
- Line 71: *"..94 % of the failures had volumes* $\leq 2.3 \times 10^4$ m^3 *which also refer.."*
- Line 428: *"...dominates rock failure volumes of* $\leq 2.3 \times 10^4$ m^3 *where all ice.."*
- Line 626: *"..Our tests apply to failures of permafrost rock slopes (i) with volumes of* $\leq 2.3 \times 10^4$ m^3*, (ii) with ice.."*

Line 434:

RC2: Suggested to exchange "anyhow" by "however"

AC/C: Changed as suggested

Line 447:

RC2: Pointed to her comment in the abstract (line 13).

AC/C: Referring to our response to line 13 (see above) we would like to let the strain rate of 10^{-3} s^{-1} unchanged.

Line 494:

RC2: This model may be a little too simplified. As you have cohesion in your model the reduction of mass above the sliding plane will increase slope stability. (For pure frictional sliding the slope stability would be independent of the normal stress.) I recommend that you do some model calculations with commercially available software. – with respect to the concept in Fig. 10.

AC: We would like to avoid any model calculations with commercially available software because this is beyond the scope of this paper. However, we agree with the referee that the presented model is too simple.

C: Hence, we modified Fig. 10 (line 518 in the revised manuscript) and added more detailed information about what we originally meant (including a new Fig. 11, line 530 in the revised manuscript):

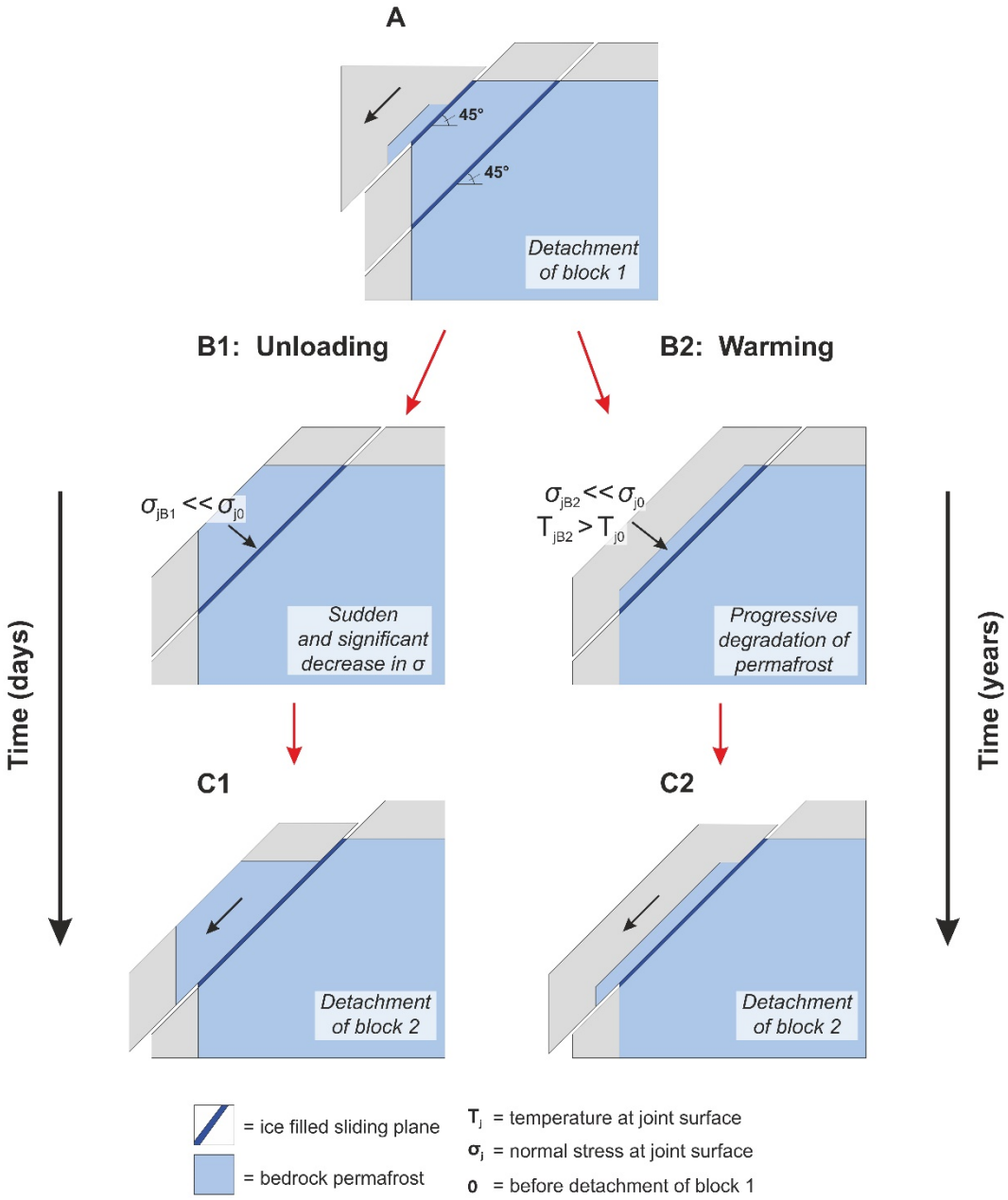

Line 523 in the revised manuscript:

"This study shows that both warming and unloading of ice-filled rock joints, lead to a significant drop in shear resistance, which may cause a self-enforced rock slope failure propagation. The progressive degradation of bedrock permafrost and ice in rock joints may control the cohesion and friction angle of the joints. However, as soon as a first slab has detached from the rock slope (A in Fig. 10), further slabs below can become unstable and finally detach as the shear strength along the ice-filled failure plane is affected by progressive warming (i.e. permafrost degradation, B2 in Fig. 10), but even faster by sudden unloading (B1 in Fig. 10). The latter is represented by a significant drop in normal stress in the Mohr-Coulomb failure criterion (Fig. 11).

Temperature class [°C]	Coefficient of friction [μ]	Cohesion [kPa]	Normal stress-dependent friction at σ_1 =			
			100 kPa	200 kPa	400 kPa	800 kPa
$\|\tau\| = \sigma * (0.42 - 0.21 * T) + (53.3 - 73.5 * T)$						
			Unloading reduces stability of underlying frozen rock mass		Critical stability loss of underlying frozen rock mass	
-10	2.52	788	252	504	1008	2016
-8	2.10	641	210	420	840	1680
-6	1.68	494	168	336	672	1344
-5	1.47	421	147	294	588	1176
-4	1.26	347	126	252	504	1008
-3	1.05	274	105	210	420	840
			Unloading increases stability of underlying frozen rock mass			
-2	0.84	200	84	168	336	672
-1	0.63	127	63	126	252	504
-0.5	0.53	90	53	105	210	420

Figure 11: Three scenarios of rock slope stability after the sudden unloading of an underlying frozen rock mass with 45 ° fractures. Green boxes: Increasing stability of underlying frozen rock mass. Unloading increases shear resistance relative to shear forces in 45 ° fractures. Orange boxes: Reducing stability. Unloading reduces shear resistance (friction) relative to shear stress in 45 ° fractures. Red boxes: Critical stability loss. Friction loss along underlying 45 ° fractures even exceeds ice cohesion.

We consider three scenarios of rock slope stability depending on the reduction in normal stress and its relationship to cohesion along a specific shear plane with an inclination of 45 °. Correspondingly, all changes in shear forces equal the changes in the shear resistance $\Delta\tau = \Delta\sigma$. However, instability may increase when the loss in friction surpasses the loss of applied shear forces: $\Delta\sigma * tan\,\varphi > \Delta\tau$. This may happen in an underlying frozen rock mass upon unloading when μ or $(0.42 - 0.21 * T) > 1$. The cohesion may possibly compensate the decrease in friction when $c > \Delta\sigma * tan\,\varphi$. In this case the shear plane could become more unstable without complete failure. This is valid for temperatures between -10 and -3 °C and normal stresses 100–200 kPa (orange boxes in Fig. 11). When the loss of friction in an underlying frozen rock mass upon unloading is much bigger than the reduction in the shear forces $\Delta\sigma * tan\,\varphi \gg \Delta\tau$ and even exceeds the ice cohesion $c < \Delta\sigma * tan\,\varphi$, then failure along the shear plane is strongly promoted. This is valid for temperatures between -10 and -0.5 °C and normal stresses 400–800 kPa (red boxes in Fig. 11). Rock slope stability in an underlying frozen rock mass upon unloading is only weakly affected if the reduction in friction is smaller than the reduction in the shear force: $\Delta\sigma * tan\,\varphi + c < \Delta\tau$. This is valid for temperatures between -2 and -0.5 °C and normal stresses 100–200 kPa (green boxes in Fig. 11). In summary, the red scenario in Fig. 11 indicates a high likelihood of subsequent failures by unloading the underlying frozen rock mass, the orange scenario exposes a moderate likelihood and the green scenario shows a small likelihood. Unloading may lead to instability or even failure when the shear planes (i) are affected by a high reduction in normal stress exceeding the ice cohesion and/or (ii) are below -2 °C due to a friction coefficient higher than 1."

Lines 503-504:

RC1: The referee deleted the term “thermal” and suggested to change the position of the bracket “(B1 in Fig. 11)”

AC/C: Changed as suggested (line 407 in the revised manuscript).

Lines 509-513:

RC1: Suggested to present the five points as a list and not within the running text.

AC/C: Adjusted as proposed

Lines 521-527:

RC1: Suggested to present the three points as a list and not within the running text.

AC/C: Adjusted as proposed

Lines 529-530:

RC2: Recommended to change the structure of the sentence from *“Due to the fact that at higher stresses significantly exceeding 400 kPa brittle fracturing can be suppressed in favour of creep behavior, we also conducted experiments at 800 kPa.”* into “We also conducted experiments at 800 kPa because at higher stresses significantly exceeding 400 kPa brittle fracturing can be suppressed in favour of creep behavior.”

AC/C: We deleted the sentence because it transports redundant information (line 579 in the revised manuscript).

Line 544:

RC1: What it? The number of signals or the rate? - referred to *“AE is generally well capable to anticipate rock-ice failure as (i) […], (ii) […] and (iii) it peaks immediately prior to failure.”*

AC/C: Changed to *“AE is generally well capable to anticipate rock-ice failure as (i) […], (ii) […] and (iii) AE hits peak immediately prior to failure.”* (line 590 in the revised manuscript)

Line 544:

RC1: Suggested to exchange the term “this manuscript” by “the experiments conducted”

AC/C: Changed as proposed

Line 554:

RC1: Added “ing” to the word “load”

AC/C: changed as proposed

Line 570:

RC1: Be consistent with rock wall vs. rockwall

AC/C: As suggested by the referee, we wrote the term uniformly as “rock wall”

Line 578:

RC1: Please do not simply copy - paste text from the manuscript, but prepare a condensed summary in the first paragraph – related to the conclusion

AC/C: As proposed by the referee we condensed the first two paragraphs of the conclusion as follows (line 617 in the revised manuscript):

“Most of the documented failures in permafrost rock walls are likely triggered by the mechanical destabilisation of warming bedrock, discontinuities with rock bridges as well as joints with or without ice fillings. The latter may evolve into shear planes supporting destabilisation on a larger spatial scale and leading to failure. To anticipate failure in a warming climate, we need to better understand how rock-ice mechanical processes affect rock slope destabilisation with temperatures increasing close to 0 °C.

This paper presents a systematic series of constant strain-rate shear tests on sandwich-like limestone-ice-limestone samples (i) to simulate the brittle failure of ice infillings and rock-ice interfaces along ice-filled shear planes of rockslides, ii) to study its dependence on temperature and normal stress and (iii) to develop a new brittle failure criterion for ice-filled permafrost rock joints. The setup and boundary conditions of our experiments are inspired by a 10^4 m³, ice-supported rockslide at the Zugspitze summit crest. Our tests apply to failures of permafrost rock slopes (i) with volumes of $\leq 2.3 \times 10^4$ m³, (ii) with ice-filled shear planes in a depth of 4–15 m, (iii) with bedrock temperatures between -0.5 °C and -10 °C and (iv) with high strain rates ($4.8 \pm 1.4 * 10^{-3}$ s^{-1}) coinciding with the accelerating final failure stage. Tests at a rock overburden of 30 m and temperatures from -4 to -0.5 °C were performed to study a potential stress-dependent transition from brittle fracture to creep. Of all the previous laboratory studies on the shear strength of ice-filled joints, the data set presented is the most extensive, containing 141 tests at nine temperature and four normal stress levels. For the first time, pre-conditioned rock from a permafrost-affected rock slope was used.”

We also condensed the last two paragraphs of the conclusion as follows (line 646 in the revised manuscript):

“The failure criterion contains a temperature-dependent cohesion and coefficient of friction decreasing by 12 % °C^{-1} and by 10 % °C^{-1} respectively with increasing sub-zero temperatures. The model fits well to the measured calibration means and even to the values excluded from the model development which mostly lie within or close to the calculated error margin. Further, we show that the failure type depends on the temperature and is

also affected by higher normal stresses (i.e. 800 kPa) above -4 °C which can presumably be explained by an enhanced pressure melting effect along the rock-ice interface.

The new failure criterion can be applied in numerical modelling and enables scientists and engineers to anticipate more accurately the destabilisation of degrading permafrost rock slopes, as it reproduces better real shear strength conditions along sliding planes."

Line 597:

RC1: Added an "a" and "failure criterion" to the first part of the sentence "*It is based on a Mohr-Coulomb failure criterion, it refers…"*

AC/C: Changed as proposed (line 644 in the revised manuscript).

A temperature- and stress-controlled failure criterion for ice-filled permafrost rock joints

Philipp Mamot[1], Samuel Weber[2], Tanja Schröder[1], Michael Krautblatter[1]

[1]Chair of Landslide Research, Technical University of Munich, 80333 Munich, Germany
[2]Department of Geography, University of Zurich, 8057 Zurich, Switzerland

Correspondence to: Philipp Mamot (philipp.mamot@tum.de)

Abstract. Instability and failure of permafrost-affected rock slopes have significantly increased coincident to ~~warming~~ rising air temperature related to climate change in the last decades. Most of the observed failures in permafrost-affected rock walls are likely triggered by the mechanical destabilisation of warming bedrock permafrost including ~~effects in~~ ice-filled joints. The failure of ice-filled rock joints has only been observed in a small number of experiments, often using concrete as a rock analogue. Here, we present a systematic study of the brittle shear failure of ice and rock-ice interfaces, simulating the accelerating phase of rock slope failure. For this, we performed 141 shearing experiments with rock-ice-rock "sandwich" samples at constant strain rates (10^{-3} s^{-1}) provoking ice fracturing ~~(10^{-3} s^{-1})~~, under ~~relevant~~ stress conditions ranging from 100 to 800 kPa, representing ~~i.e.~~ 4–30 m of rock overburden, and at temperatures from -10 to -0.5 °C, typical for recent observed rock slope failures in alpine permafrost. To create close to natural but reproducible conditions, limestone sample surfaces were ground to international rock mechanical standard roughness. Acoustic emission (AE) was successfully applied to describe the fracturing behaviour, anticipating rock-ice failure as all failures are predated by an AE hit increase with peaks immediately prior to failure. We demonstrate that both, the warming and unloading (i.e. reduced overburden) of ice-filled rock joints lead to a significant drop in shear resistance. With a temperature increase from -10 °C to -0.5 °C, the shear stress at failure reduces by 64–78 % for normal stresses of 100–400 kPa. At a given temperature, the shear resistance of rock-ice interfaces decreases with decreasing normal stress. This can lead to a self-enforced rock slope failure propagation: as soon as a first slab has detached, further slabs become unstable through progressive thermal propagation and possibly even faster by unloading. Here, we introduce a new Mohr-Coulomb failure criterion for ice-filled rock joints that is valid for joint surfaces which we assume similar for all rock types, and which applies to temperatures from -8 to -0.5 °C and normal stresses from 100 to 400 kPa. It contains a temperature-dependent friction and cohesion which decrease by 12 % ~~/~~°C^{-1} and 10 % ~~/~~°C^{-1} respectively due to warming and it applies to temperature and stress conditions of more than 90 % of the recently documented accelerating failure phases in permafrost rock walls.

1 Introduction

Rock slope failures in high mountain areas potentially endanger human lives, settlements and alpine infrastructure. The impact of the climate-induced degradation of mountain permafrost on rock slope destabilisation has been inferred from numerous studies in the last two decades (Fischer et al., 2006; Gruber et al., 2004; Gruber and Haeberli, 2007; Ravanel and Deline, 2015). Rock slope failures influenced by permafrost degradation are expected to respond to a warming climate by more frequent events (Gobiet et al., 2014; Ravanel and Deline, 2011). The majority of failures in permafrost-affected rock frequently expose ice-filled joints as potential shear and detachment planes (Dramis et al., 1995; Gruber and Haeberli, 2007; Ravanel et al., 2010), as for example~~e.g.,~~ the recent 3~~–4.15~~ $\ast$ 10^6 m³ rock slope failure at Pizzo Cengalo, Graubünden, CH, on 23~~3~~ August 2017 (Baer et al., 2017; Beniston et al., 2018; pers. comm. with Phillips, 2018~~7~~). Fractures and fractured zones in mountain bedrock permafrost usually contain ice to depths of several tens of metres (Deline et al., 2015; Gruber and Haeberli, 2007). Ice fillings can contribute to systematically higher shear strengths due to rock-ice-interlocking and adhesion, and thus increase rock slope stability especially when the ice is at a low temperature. This bonding of ice-filled joints is reduced or even lost as the temperature increases (Davies et al., 2001; Gruber and Haeberli, 2007).

Rock joints that are located within bedrock permafrost (ground that remains permanently frozen for at least two consecutive years; Harris et al., 1988) are referred to as "permafrost rock joints" in this paper. Permafrost conditions are ~~fulfilled~~ below the maximum ~~active layer~~ thaw depth which typically ranges between 2–8 m in ~~Alpine~~ alpine environments (Böckli et al., 2011; Delaloye et al., 2016) and apply to ice-filled rock fractures, rock pores and microfractures (Gruber and Haeberli, 2007). In this manuscript, both, joints and fractures are used to substitute the more~~as~~ general term~~s for~~ "rock discontinuities".

To anticipate failure in a warming climate, we need to improve the understanding of how rock-ice mechanical components control rock slope destabilisation and failure between -10 and 0 °C. Generally, warming of permafrost in rock slopes affects the shear stress along sliding planes in terms of (i) ~~the~~ fracture toughness of rock bridges, (ii) ~~the~~ friction of rock-rock contacts, (iii) ~~the~~ ductile creep behaviour of ice and (iv) ~~the~~ brittle failure of ice infillings (Krautblatter et al., 2013). Whereas the mechanics of frozen rock (~~Dwivedi et al., 2000;~~ Glamheden and Lindblom, 2002; Kodama et al., 2013; ~~Krautblatter et al., 2013;~~ Mellor, 1973), the mechanics of frozen rock joints without fillings (Dwivedi et al., 2000; Krautblatter et al., 2013) and the ductile temperature- and stress-dependent creep of ice and ice-rich soils (Arenson and Springman, 2005a; Sanderson, 1988; Yamamoto and Springman, 2014) have been investigated in a number of studies, the brittle failure of ice infillings is still poorly understood. We hypothesise that the brittle failure of ice infillings (i.e. either along rock-ice interfaces or inside the ice) is a common final failure mechanism, which is documented by numerous exposed ice-filled joint surfaces subsequent to failure. It is mechanically dependent on fast deformations (i.e. strain rates) and, thus, is likely to control the final failure of many recent events. This study aims at developing the first comprehensive temperature- and stress-dependent brittle failure criterion for ice-filled joints based on shear tests~~141 mechanical tests~~ on rock-ice-rock samples.

Fracturing of ice and rock-ice-contacts mainly occur~~s~~ below a rock overburden $\leq$ 20 m and become~~s~~ less important at greater depths, where rock mechanical components take over at greater stresses (Krautblatter et al., 2013). Here, higher confinement suppresses brittle failure and may favour creep deformation of ice (Renshaw and Schulson, 2001; Sanderson, 1988). Shear tests on concrete-ice and concrete-ice-concrete "sandwich" samples under constant stress show that fracturing along rock-ice

interfaces is the dominant failure process that occurs at a simulated rock overburden of 5–25 m, i.e. 135–630 kPa ~~(Günzel, 2008; Krautblatter et al., 2013)~~. Constant strain experiments show that with rising normal stress levels (from 207 to 562 kPa, i.e. approximately 8–21 m rock overburden), fracturing along rock-ice interfaces is replaced by creep deformation of the ice (Günzel, 2008; Krautblatter et al., 2013). In addition, higher normal stresses increasingly cause ice fillings to be squeezed away from "abutments" and preferentially lead to stress concentrations along rock-rock contacts (Krautblatter et al., 2013). Various inventories of rock slope failures in the Mont Blanc Massif show that virtually all of the failures displayed a plate-like shape with an area ranging from 25 m² to 33.800 m² (average of 1.570 m²) and scar depths of 1–20 m (average of 4 m) (Ravanel et al., 2010; Ravanel and Deline, 2008; Ravanel and Deline, 2011). Most of the events have been linked to the degradation of bedrock permafrost and ice-filled joints. 97 % of them had volumes ≤ 3 ∗ 10^4~~0.000~~ m³ which correspond to the relevant size of dominantly ice-fracturing-controlled rock slope failures (considering the approx. ≤ 20 m rock overburden and the average area of the reported failure planes). 94 % of the failures had volumes ≤ 2.3 ∗ 10^4~~3.000~~ m³ which also refer~~s~~ to mainly ice-fracturing-controlled rock slope failures (considering the tested 15 m rock overburden in this study and the average area of the documented failures), as will be shown in this paper. However, even larger volumes will be partially influenced by rock-ice fracturing phenomena.

Warming of permafrost in rock slopes reduces the shear resistance along rock joints in a chronological order by (i) reducing the fracture toughness of cohesive rock bridges, (ii) by lowering friction along rock-rock contacts, (iii) by altering the creep of ice infillings and (iv) finally reducing the fracture toughness of the ice itself and of rock-ice contacts (Krautblatter et al., 2013)~~.~~ . Cyclic thermal expansion or contraction in the shallow bedrock occurs due to warming or cooling as a result of daily or seasonal variations in temperature. Variations of high frequency and magnitude can cause thermal gradients in the rock which leads to alterations in the stress field. This can induce thermal fatigue which, over long timescales, reduces the shear resistance along weakened discontinuities (Draebing et al., 2017; Gischig et al., 2011; Hall and Thorn, 2014; Jia et al., 2015; Weber et al., 2017).

When ice becomes mechanically stressed, it can deform by (i) elastic or ductile creep without fracture or by (ii) brittle or ductile-brittle fracture including crack formation and propagation (Sanderson, 1988). The deformation and failure behaviour of ice changes from ductile creep to brittle fracture with strain rates > 10^{-4} and 10^{-3} s^{-1} (Arenson and Springman, 2005a; Fellin, 2013; Sanderson, 1988; Schulson and Duval, 2009). Thus, the accelerating final failure along predefined slip surfaces is increasingly likely to be governed by the brittle failure of ice (Krautblatter et al., 2013). When the ice ceases to be able to bear a certain applied load, it fails and then brittle fracture occurs. In this case, the applied load at fracture can be described as "strength" (Sanderson, 1988), an analogue to the strength at fracture in rock mechanics. In this paper, we use the term "strength" when talking about ice-mechanical behaviour as we simulate accelerating final rock slope failure conditions with strain rates that provoke ice fracturing (10^{-3} s^{-1}).

The temperature-dependence of mechanical properties of ice has been studied in numerous publications up to now (Arakawa and Maeno, 1997; Barnes et al., 1971; Fish and Zaretzky, 1997; Gagnon and Gammon, 1995; Jones and Glen, 1968; Sanderson, 1988; Schulson and Duval, 2009). The unconfined compressive strength of polycrystalline ice decreases by 82 % (from approx.

17 to approx. 3 MPa) with increasing temperature from -50 to 0 °C (at strain rates of 10^{-3} and 10^{-1} s^{-1}; (Schulson and Duval, 2009). A warming of artificommercial ice from -10 to 0 °C results in a decrease in the unconfined compressive strength by 50 % (from ca. 4 to ca. 2 MPa) and in tensile strength by 13.3 % (from 1.5 to 1.3 MPa) (Butkovich, 1954b in Hobbs, 1974). The fracture toughness of polycrystalline ice decreases by 27 % (from approx. 110 to approx. 80 kPa/$m^{-0.5}$) when warming from -50 to -2 °C (Schulson and Duval, 2009). The behaviour of sediment-ice mixtures has been investigated in detail by Arenson and Springman (2005a). According to them, the strain rates of frozen soil increase with rising temperature and higher volumetric ice content. The peak shear strength of ice-rich soil (ice content > 60 %) decreases with increasing temperature from -5 to -1 °C.

Laboratory tests on the shear strength of ice-filled rock joints reveal a decreasing shear stress at failure with decreasing normal stress and increasing temperature towards 0 °C (Davies et al., 2000; Davies et al., 2001; Günzel, 2008; Krautblatter et al., 2013). These studies rely on approx. 40 constant stress and 50 constant strain shear experiments at temperatures from -5 to 0 °C, where the joints were composed of concrete and ice (Davies et al., 2000; Günzel, 2008). However, the applied strain rates in constant strain tests were too low to enforce fracturing of ice. Constant stress tests delivered significantly higher strain rates (Günzel, 2008; Krautblatter et al., 2013), but they are difficult to interpret in terms of fracturing initiation due to the rapidly changing strain rate conditions. In these tests, the shear strength of laboratory ice-filled rock joints consisting of concrete and ice decreases by 144 kPa $°C^{-1}$ between -0.5 and -5 °C (Krautblatter et al., 2013). could be approximated as

$$\tau_f = 144 \times T_c + \tau_0 \quad (1)$$

$$\tau_0 = 0.42 \times \sigma' + 41.3 \quad (2)$$

where σ' is the effective normal stress, T_C (°C) is the temperature of the ice at failure, τ_f is the shear stress at failure and τ_0 is the shear strength at 0 °C (Krautblatter et al., 2013). Equation (1) exhibits a shear strength decrease of 144 kPa/°C between -0.5 and -5 °C. Experiments by Davies et al. (2000) demonstrate a reduction in shear strength by 16 or 18 % $°C^{-1}$/°C (i.e. 124 or 69 kPa /°C^{-1} respectively depending on the normal stress level) due to warming from -5 to -0.5 °C. A similar relation is shown for sandwich samples composed of ice and polished steel plates whose shear strength decreases by 10 %/°C (i.e. 113 kPa $°C^{-1}$/°C) with increasing temperature from -10 to -2 °C (Jellinek, 1959).

We measured acoustic emission (AE) in this study to monitor the strength reduction due to creep or brittle failure of ice and rock-ice contacts and to document the progressive evolution of damage. AE refers to the generation of transient elastic waves generated by a sudden release of energy in a material (Hardy, 2003). AE events can indicate damage increase, i.e. microcrack generation and coalescence, initiation and propagation of fractures or shearing and failure along fractures or the shearing of existing fractures (Cox and Meredith, 1993; Scholz, 1968;). AE technology has been used extensively on the laboratory rock samples in the laboratoryscale (Lockner, 1993; Nechad et al., 2005; Yamamoto and Springman, 2014). Scaling properties of fracturing dynamics in the domains of size, space and time have usually been observed during mechanical loading (Alava et al., 2006). In the time domain, the seismic events induced by damage processes display a power-law distribution

$$N(s) \sim s^{-b} \quad (13)$$

where N is the probability distribution function of the event size estimation s (e.g. the maximum amplitude of the AE signal or its energy) and b is a constant (Amitrano et al., 2012). The exponent b, originally defined in seismology, describes the slope of the magnitude distribution and provides information on the states of fractures (Scholz, 1968). Larger b exponents indicate the more predominant occurrence of microscopic fractures, while smaller b exponents indicate the occurrence of macro-fractures. An improved b exponent approach, defining the number of AE either by accumulation from the starting data or per time unit, enables the application in the acoustic (Shiotani et al., 1994) with an appropriate number of AE data between 50 and 100 (Shiotani et al., 2001).

In this study, we performed 141 shear tests, using limestone-ice-limestone samples with realistic ISRM (International Society for Rock Mechanics and Rock Engineering) rock surface roughness and predefined strain rates provoking fracturing. The onset of fracturing was controlled using the AE technique. To simulate the real-world fracturing of ice and rock-ice-contacts along discontinuities in alpine permafrost rock slopes, our tests were performed in a temperature-controlled, cooled laboratory shear box with samples collected in the field. Our experiments focus on the impact of temperature and normal stress on the fracturing behaviour ~~of ice-filled rock joints~~. Temperatures between -10 and -0.5 °C were tested to represent recently observed daily and annual mean temperatures of mountain bedrock permafrost (Böckli et al., 2011; Delaloye et al., 2016). Normal stresses of 100, 200 and 400 kPa (corresponding to rock overburdens of approx. 4, 8 and 15 m or more) were chosen to reconstruct relevant stress conditions for ice- and rock-ice-fracturing processes in permafrost rock joints mostly below the annual maximum thaw ~~active layer thaw~~depth. Additional tests at 800 kPa (i.e. 30 m rock overburden) were performed to study a potential stress-dependent transition from brittle fracture to creep at stress levels above 400 kPa ~~(Krautblatter et al., 2013; Sanderson, 1988)~~.

~~So far the failure of ice-filled permafrost rock joints has been studied using concrete as a rock analogue (Davies et al., 2000; Günzel, 2008). For the first time, we use rock to closely reproduce real conditions along rock joints. Synthetic materials possibly deviate from shear strength values representative for rock joints in the field. For instance, ice sliding on granite shows a friction coefficient μ approx. 0.5 higher than ice sliding on glass or metals, all having a similar surface asperity roughness. The higher friction of the granite-ice interfaces is due to a higher effective adhesion (Barnes et al., 1971). To use rock instead of other materials probably has a greater effect on the shear strength than different rock types.We assume that the shear strength of rock-ice interfaces is mostly affected by temperature, normal stress and joint surface roughness while the rock type is less important. Further, the standardised preparation of a uniform joint surface roughness for all rock samples in this study prohibits any potential effect of differing rock types. Consequently, we use limestone as a representation for all rock types. The thermal conductivity of rocks varies in a small range of 0.5–7 W m^{-1} K^{-1} (Clauser and Huenges, 1993). As such, we do not expect any effect of the thermal conductivity on the shear strength which may arise due to facilitated melting along surfaces of heat-insulating solids causing a decrease in friction (Barnes et al., 1971). Consequently, we use limestone as a representation for all rock types. Further, the standardised preparation of a uniform joint surface roughness for all rock samples in this study prohibits~~

~~any potential effect of differing rock types. To use rock instead of other materials probably has a greater effect on the shear strength than different rock types.~~

This paper addresses the following questions:

1) How does the shear strength of ice-filled rock joints respond to permafrost warming (-10° C to -0.5° C) and sudden changes in rock/ice overburden (i.e. normal stress)?
2) Can acoustic emission be applied to decipher precursors of breaking ice and rock-ice interfaces within fractures?
3) Can we derive a comprehensive stress- and temperature-dependent failure criterion for ice-filled rock joints?
~~4)~~ ~~Which real-world conditions of permafrost rock slope destabilisation can be simulated by the new failure criterion?~~
~~5)~~4)

2 Methodology

2.1 Real-world setting to constrain laboratory tests

The design of the presented laboratory test setup is inspired by a benchmark example of shallow, ice-supported rock instability prior to failure exemplified by an approx. 10^4 m^3 large rockslide at the summit crestline (2885 m a.s.l.) of Germany´s highest peak, the Zugspitze (2962 m a.s.l.; Fig. 1a and Fig. 1b). Since 2007, the rock mass creeps slowly at an average of 3.75 mm/year. From July to October it moves ~~with~~ more than five times faster than ~~higher deformation rates in July to October~~ in ~~comparison to~~ the remaining months.

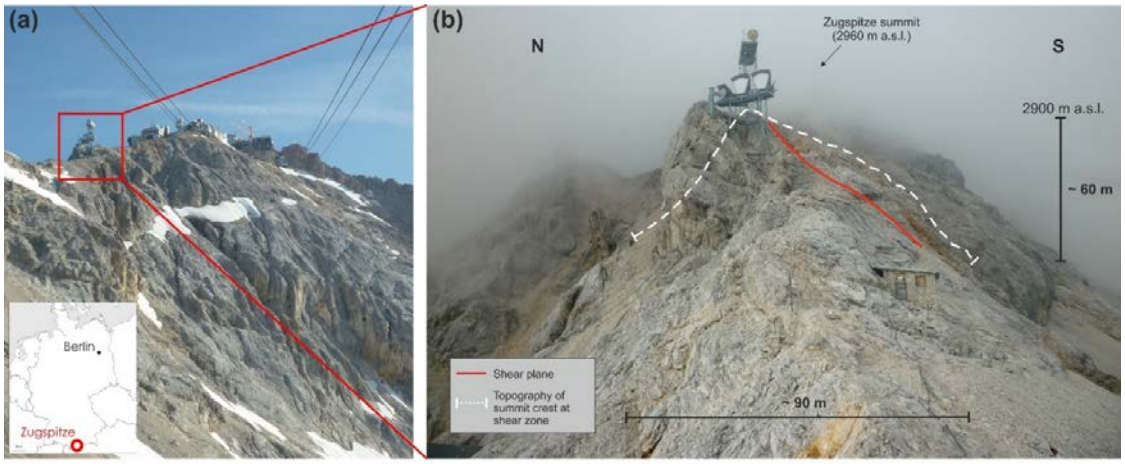
(a)
Berlin
Zugspitze
(b)
N
S
Zugspitze summit
(2960 m a.s.l.)
2900 m a.s.l.
~ 60 m
Shear plane
Topography of summit crest at shear zone
~ 90 m

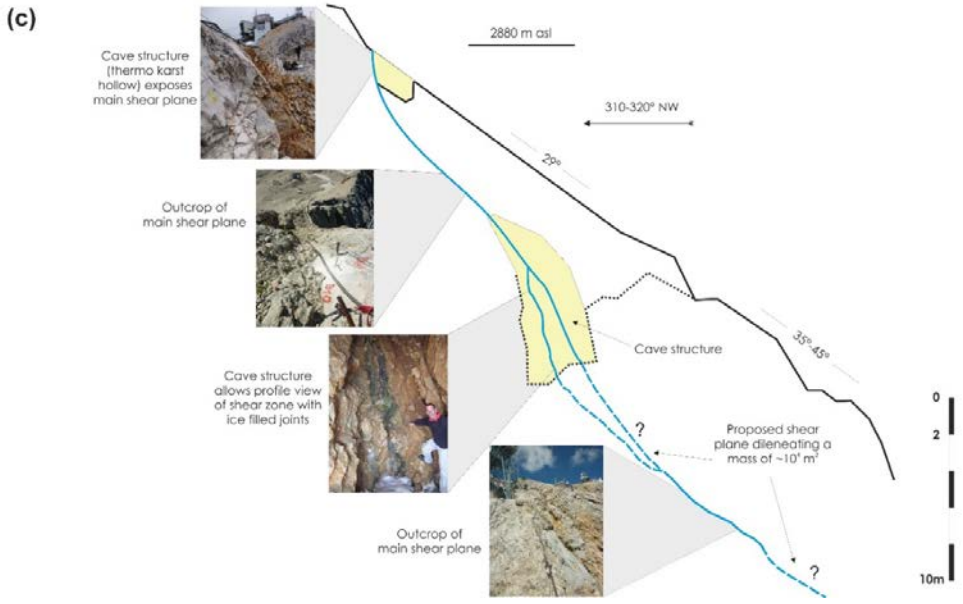
(c)
2880 m asl
Cave structure (thermo karst hollow) exposes main shear plane
310-320° NW
29°
Outcrop of main shear plane
Cave structure
35°-45°
Cave structure allows profile view of shear zone with ice filled joints
Proposed shear plane dileneating a mass of ~10⁶ m³
Outcrop of main shear plane
0
2
10m

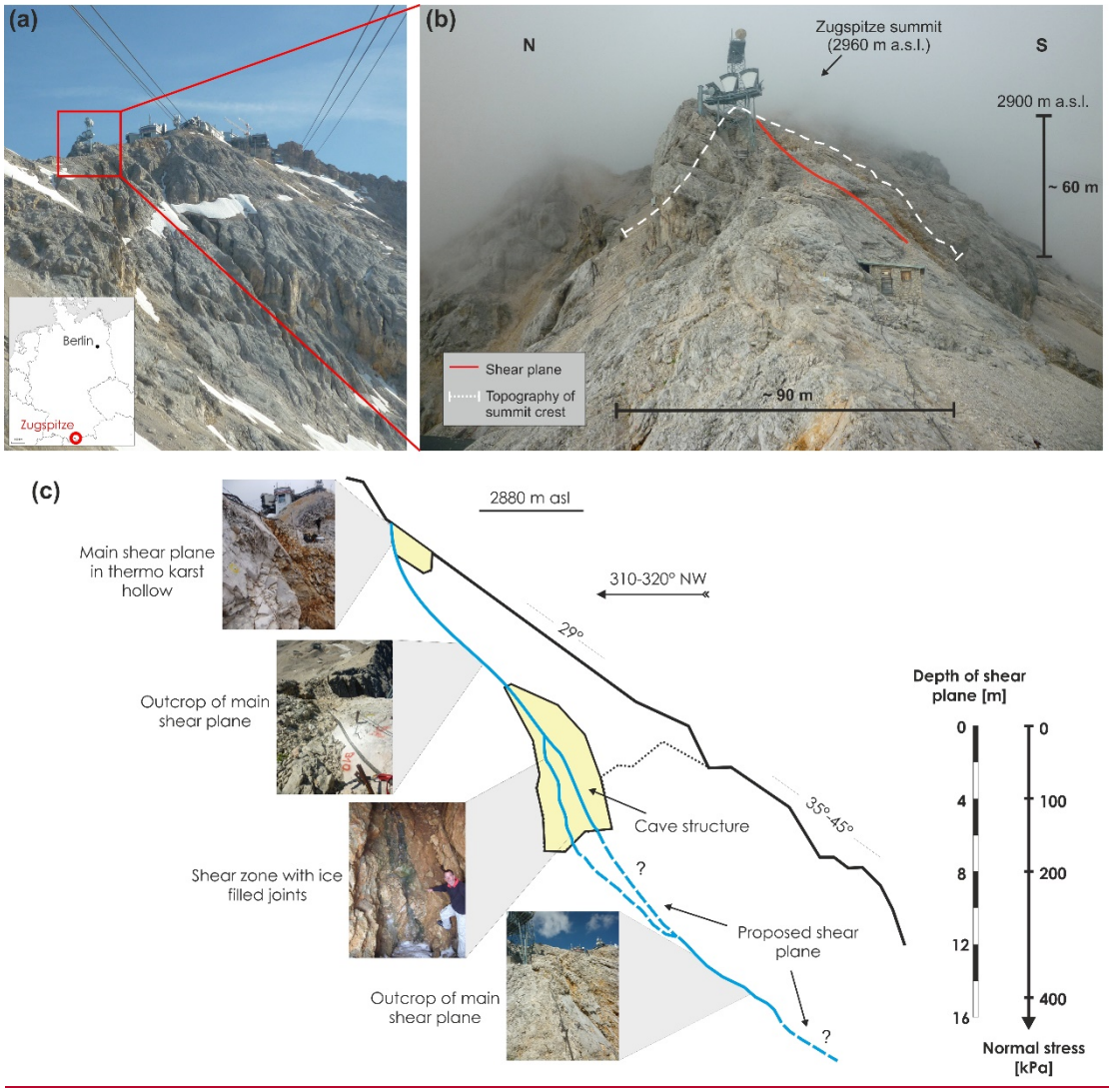

Figure 1: (a) The Zugspitze summit area with Germany's highest peak (2962 m a.s.l.). (b) Profile view of the Zugspitze summit crest with dimensions of the rockslide. The supposed shear plane is indicated by the red line. (c) Mechanical situation and geometry of the ice-supported rockslide that is used as a real-world exemplification of the simulated temperature and stress-controlled fracturing along rock-ice interfaces in the laboratory.

The ice-supported rockslide acts as a real-world exemplification of the simulated temperature and stress-controlled fracturing along rock-ice interfaces in our laboratory, and as such, it is a benchmark analogue to constrain temperature and stress conditions for the performed tests:

(i) ~~(i)~~ The depth of the main shear plane is assessed to a maximum of 10–15 m due to field mapping ~~(Fig. 1c)~~. The corresponding normal stresses on this shear plane (mostly ≤ 400 kPa) lie within the range of the tested stress levels (Fig. 1c).

(ii) The occurrence of permafrost is confirmed by permanent ice-filled caves and fractures along the main shear zone (Fig. 1c).

(iii) The Zugspitze summit area is located at the lower permafrost extension limit. Current borehole temperatures at the peak of the Zugspitze average -1.3 °C within the permafrost core area (approx. 24 m away from the south face and 21 m away from the north face) and approach minima of -6 °C at the margins (ca. 5 m away from the north face) (Böckli et al., 2011; Gallemann et al., 2017; Krautblatter et al., 2010; Noetzli et al., 2010). These temperatures lie well within the range of the tested temperature levels in this study.

(iv) A climatic warming in the last century and an even stronger temperature increase since the late 19~~8~~90s can be observed at the Zugspitze, i.e. the mean annual air temperature (MAAT) in 1991–2007 was 0.8–1.1 °C warmer than in the three prior 30 year~~20th century~~ reference periods between 1901 and 1990 (Gallemann et al., 2017; Krautblatter et al., 2010). An ongoing warming may potentially cause the degradation of permafrost in the summit crest leading to an accelerated movement in the future and thus to the fracturing of ice and rock-ice contacts, among other processes.

2.2 Sample preparation

The tested rock samples were collected at the Zugspitze summit crest (Fig. 1a)~~, the same site which acts as a real-world exemplification of our laboratory tests~~. The rock samples consist of Triassic Wetterstein limestone, which builds up the upper part of the Zugspitze (Jerz and Poschinger, 1995). The limestone is fine-grained, dolomised, has a porosity of approximately 4.4 % and shows little heterogeneity in terms of its lithological properties (Krautblatter et al., 2010). Seven pairs of rock cylinders with a diameter of 148±1 mm and a height of 82±3 mm were prepared. Following the ~~the ISRM (International Society for Rock Mechanics and Rock Engineering) recommendations~~ ISRM recommendations for standardised tests (Ulusay, 2015) and Coulson (1979, in Cruden and Hu, 1988)~~for standardised tests, ,~~ the roughness of the specimen's surfaces was produced using abrasive grinding powder with a grit of 80 grains per inch (FEPA, Federation of European Producers of Abrasives Standard) leading to a roughness amplitude equivalent to the mean diameter of the abrasive grains of 0.185 mm. Consequently, the rock surfaces are reproducible and close to the conditions of fractures in the field. The uniform joint surface roughness prohibits any potential effect ~~of differing rock types~~ on the shear strength results. Rock cylinders were saturated in a water bath~~sin~~ under atmospheric pressure for at least 72 h.

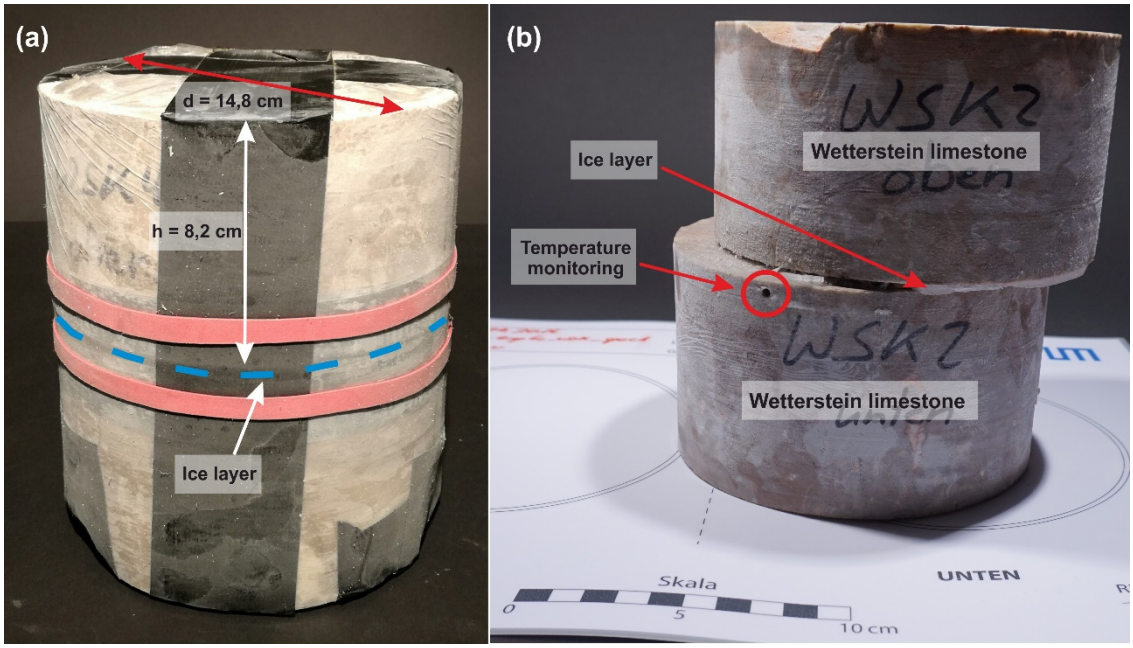

Figure 2: Sandwich sample before (a) and after (b) shearing.

The rock-ice-rock sandwich samples were produced by freezing two cylinders of Wetterstein limestone with a gap filled with tap water, using matchsticks as spacers. The samples were subjected to a number of pre-tests to guarantee uniform conditions. Pre-tests showed that simultaneous freezing of the interlocking rock surface and the ice surface is necessary to generate a firm contact. The gap was wrapped with tape and transparent film to prevent water draining~~flowing out~~ (Fig. 2a). The 3±1 mm-thin ice layer resembles the thin nature of most encountered infillings and provokes fracturing, as thicker ice infill produces more creep camouflaging the fracturing behaviour. Our experiments (including the pre-tests) have shown that unavoidable thickness variations of ±1 mm yield no significant differences in fracture toughness (Fig. S1a). In other shear tests with constant stress~~experiments~~, the shear strength of sandwich samples with a 1 mm thick ice layer did also not differ significantly from the results of concrete-ice specimens representing a 25 mm thick ice infilling (Günzel, 2008). All samples were frozen for at least 14 h at -14 °C to ensure that the ice layer was entirely frozen and firmly attached to the rock surfaces. During the freezing process, the shear planes and the gap for the ice layer were oriented vertically to make sure that no air bubbles could form in the ice. A hole was drilled into the lower rock cylinder (Fig. 2b) to monitor the rock temperature during the shear test with a 0.03 °C precision Pt100 sensor (Greisinger GMH 3750).

2.3 Experimental setup

After freezing, the sandwich specimens were fixed within the upper and lower ring of the RDS-100 direct rock shear machine from GCTS (Geotechnical Consulting & Testing Systems; Fig. 3a). The ice layer position then corresponded to the open gap between the upper and the lower shear ring (Fig. 3b). Consequently, failure within the ice layer or along the ice-rock-interface is provoked. During the whole test series, we did not change the constellation of specimen pairs and always placed them identically oriented into the shear frame to prevent effects of variations in the surfaces of the shear planes.

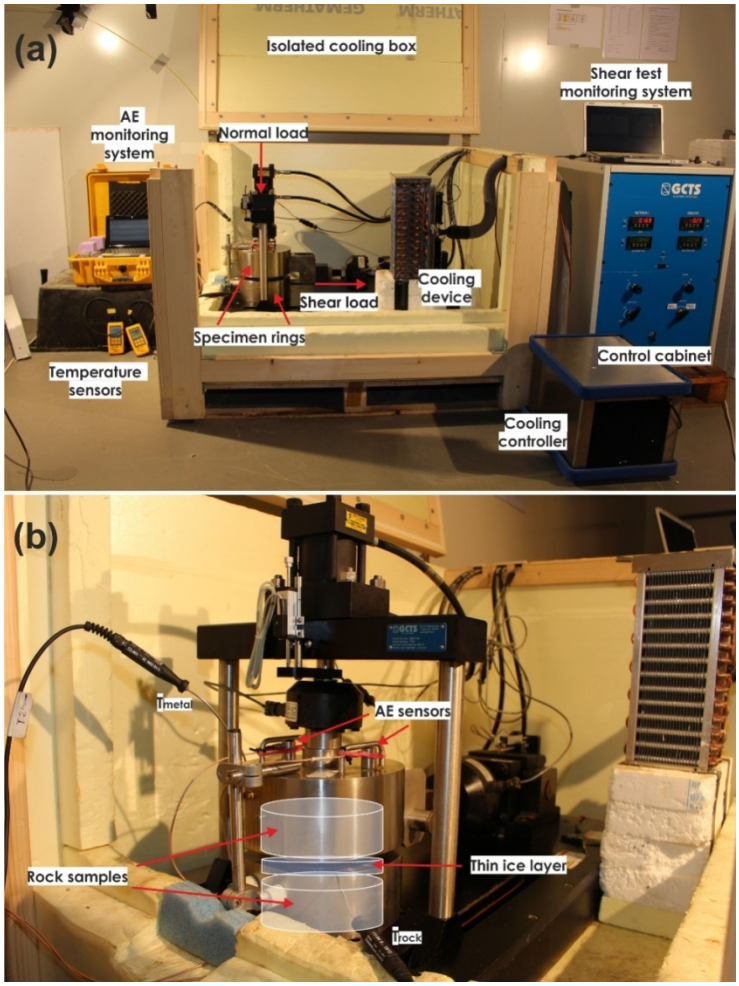

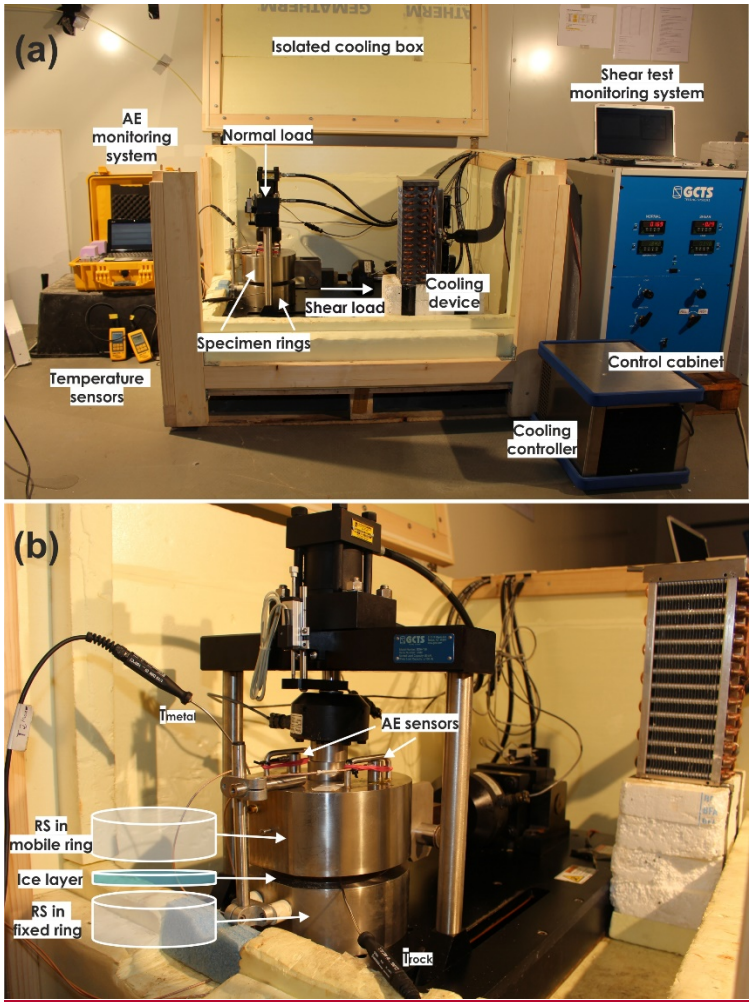

Figure 3: Experimental setup showing the laboratory shear machine, acoustic emission monitoring system, the cooling device and the cooling box. RS = rock sample. T = Rock temperature sensor.

~~During the whole test campaign, we did not change the constellation of specimen pairs and always placed them identically oriented into the shear frame to prevent effects of variations in the surfaces of the shear planes.~~ The machine is embedded in an isolated box in which temperature can be hold constantly at a specified level between -10 °C and -0.5 °C by a custom-designed FRYKA cooling device. The cooling operation is controlled by a Pt 100 sensor placed inside the rock sample with 0.1 °C accuracy (Fig. 3b). The experiments were performed at temperatures -0.5, -1, -2, -3, -4, -5, -6, -8 and -10 °C. Ventilation prevents thermal layering inside the cooling box. An AE monitoring system with two sensors is fixed at the top of the upper specimen ring (Fig. 3b) to record the elastic waves generated during fracturing events. Due to the external hydraulic control, AE can be better recorded than in servo-controlled devices.

The hydraulically driven normal load and shear velocity are adjusted by the rock shear machine and were held at constant levels during the shear tests. Normal stress levels of 100, 200 and 400 kPa were applied for the whole temperature range. Tests at 800 kPa were performed to study a potential gradual stress-dependent transition from brittle fracture to creep. This transition is observed with increasing confining pressure in triaxial tests (Sanderson, 1988) and with increasing normal stress in uniaxial shear tests (Günzel, 2008) and is expected under the similarly tested normal stress conditions above 400 kPa. High rock overburden (i.e. 800 kPa) was simulated for temperatures from -4 to -0.5 °C, representing most of the recently measured annual mean temperatures of alpine and Arctic bedrock permafrost (Delaloye et al., 2016; Gallemann et al., 2017; Harris et al., 2003). ~~Normal stress levels of 100, 200, 400 and 800 kPa were applied. Tests at 800 kPa were performed to study a potential gradual stress-dependent transition from brittle fracture to creep at stress levels above 400 kPa. This transition is observed with increasing confining pressure in triaxial tests (Sanderson, 1988) and with increasing normal stress in uniaxial shear tests (Günzel, 2008) and is expected under the similarly tested normal stress conditions above 400 kPa.~~ In steep rock faces shear planes are rather inclined than horizontal. With increasing inclination of a shear plane at a certain depth, the normal stress acting on it will decrease and downhill forces will increase. Correspondingly, a shear plane with a normal stress of 200 kPa but a dip > 0 ° will also exist in depths greater than 4 m. The mean horizontal displacement rate was 0.7 ± 0.1 mm/min, corresponding to a mean strain rate of 4.8~~0.7~~ ± 1~~0~~.4~~2~~ $*$ 10^{-3} s^{-1}. The minimum test strain rate was 1.58 $*$ 10^{-3} s^{-1}, which combines the minimum accounted deformation speed (0.005 mm/s) and the maximum ice layer thickness of 4 mm. The shear rate was hereby calculated as the shear velocity (mm/s) divided by the height of the ice layer (mm). This strain rate guaranteed the dominant deformation mode to be ice fracturing instead of creep, as 10^{-3} s^{-1} is the strain rate threshold for ice fracturing~~provokes brittle failure inside the ice or along rock-ice contacts and corresponds to predefined sliding planes at the accelerating failure stage of rockslides~~ (Arenson and Springman, 2005a~~; Krautblatter et al., 2013~~; Sanderson, 1988). As the shear and compressive strength of pure and dirty ice increase with the strain rate (Arenson et al., 2007; Sanderson, 1988; Schulson and Duval, 2009; Yasufuku et al., 2003), variations in the shear rate were kept as low as possible (with ± 0.1 mm/min) and had no measureable influence on the shear strength at failure (Fig. S1b). These conditions were applied to all tested stress and temperature conditions.

During the shear tests, normal load, shear load, normal deformation and shear deformation were recorded and used to calculate normal and shear stress considering the changing area of contact $A_{contact}$ (Fig. S2):

$$A_{contact} = 2\left(r^2\cos^{-1}\left(\frac{\varepsilon}{2r}\right) - \frac{\varepsilon}{4}(4r^2 - \varepsilon^2)^{1/2}\right) \quad (24)$$

with specimen radius r (mm) and shear strain ε (mm).

Between one and six experiments were performed for each test condition characterised by a specific temperature and normal stress level (Table S1). The total number of tests was 141, significantly more than the cumulative number of the tests in all previously published studies on rock-ice failure.

290

~~Normal stress levels of 100, 200 and 400 kPa were applied for the whole temperature range whereas 800 kPa was tested for temperatures from -4 to -0.5 °C.~~

2.4 AE monitoring

For measuring the acoustic activity, a two-channel high-frequency acquisition system composed of two USB Acoustic Emission Nodes (Mistras, Physical Acoustics) employing a single channel AE digital signal processor with 16-bit resolution and 10 V maximum amplitude, was used. The AE sensors were coupled to the specimen holder using silicone-free lubricating grease (Glisseal HV, Borer Chemie). The AE piezo-electrical sensors (PK6I) provided an operating frequency range of 40–70 kHz with a resonant frequency of 55 kHz. They included a pre-amplifier of 26 dB and were connected to the USB AE node with coaxial cables. The system was controlled by AEwin (Mistras, Physical Acoustics), a real-time data acquisition software. The system sampled continuously with 1 MSPS (mega samples per second), while events over a fix threshold of 70 dB were recorded. The signal characteristics (timestamp, rise time, amplitude, pulse count, energy and length) was parameterised according to (Girard et al., 2012, Fig. 1).

2.5 Uncertainty analysis of shear strength at failure, cohesion and friction

The linear fitting is estimated by a linear regression model using the LinearModel class of MATLAB (Version R2017a (9.2.0.556344)). The predictor and response variable are arithmetic means, while only the predictor variable is weighted with the reciprocal value of its variance. Beside the correlation coefficient (r) and the coefficient of determination (R^2), the MATLAB function returns the regression parameters “intercept” and “slope” with its standard error (MathWorks, 2017).

3 Results

3.1 Typical behaviour of shear stress, shear deformation and acoustic signals

A representative time series for shear stress, shear deformation and AE activity is shown in Fig. 4. A selection of additional time series is displayed in Fig. S3.

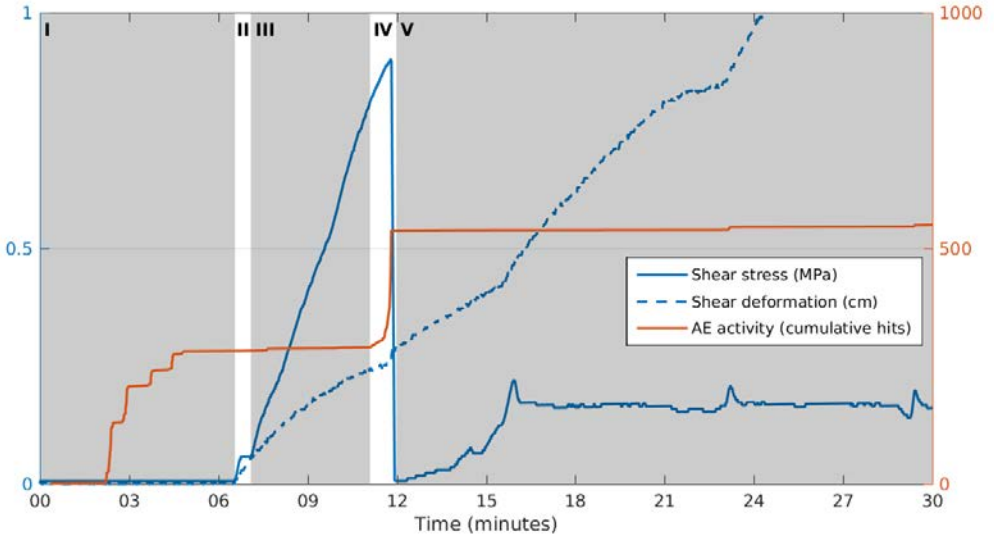

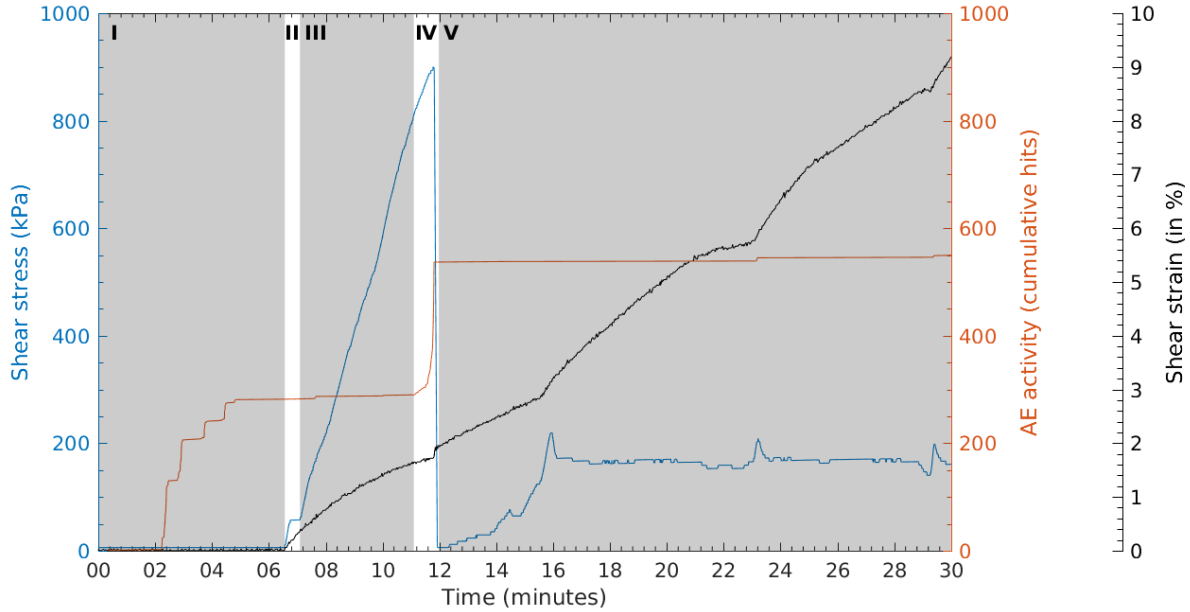

Figure 4: Typical curves of shear stress ~~at failure~~, shear strain~~deformation~~ and acoustic activity for a shear test at T = -3 °C and σ = 200 kPa. I-V represent the typical stages of each experiment: Consolidation (I), sample fitting to shear rings (II), pre-peak shear deformation (III), shear failure (IV) and post-peak shear strength. Rupture is clearly detectable by the strong decrease in shear stress. An increase in the evolution of the cumulative AE hits can be observed before rupture.

In Stage I, the experiment starts with a consolidation of approximately 5–6~~five~~ minutes applying the specified normal load. After initial AE activity during initial consolidation (starting after 2–3 minutes, Fig. 4), the AE hit rate decreases again to

almost zero (after five minutes, Fig. 4) before entering Stage II. Shearing starts, the shear rings gain tight fit to the sample and then start to apply the stress. In Stage III, shear stress increases without significant changes in AE hit rate corresponding to elastic and ductile ice deformation. In Stage IV, a pronounced peak shear stress is observed in all experiments after a few minutes coinciding to a pronounced rise in the AE hit rate that indicates brittle failure~~deformation~~. Correspondingly, the ice infill between the rock cylinders fails and shear deformation reaches one of its maximum values. The moment of failure can also be identified by a clearly audible cracking. In Stage V, just after failure, the shear stress suddenly drops to a minimum, then rises again and quickly reaches a plateau of residual shear stress. In a few experiments (such as in Fig. 4), the post-failure shear stress exhibits several small peaks, which are often accompanied by a minor~~n~~ increase in AE hits, ~~and~~ audible cracking and a pronounced rise in shear strain. The peaks in shear stress may refer to healed ice that breaks when stresses exceed a certain threshold. Further, more than 90 % of the samples with observed post-failure-peaks also failed within the ice or both in the ice and along the rock-ice interface. Hence, these peaks may also be caused by ice-ice interlocking leading to the observed decrease in shear strain (Fig. 4). Subsequent failure occurs when the shear stresses overcome the ice strength. ~~(ice healing).~~

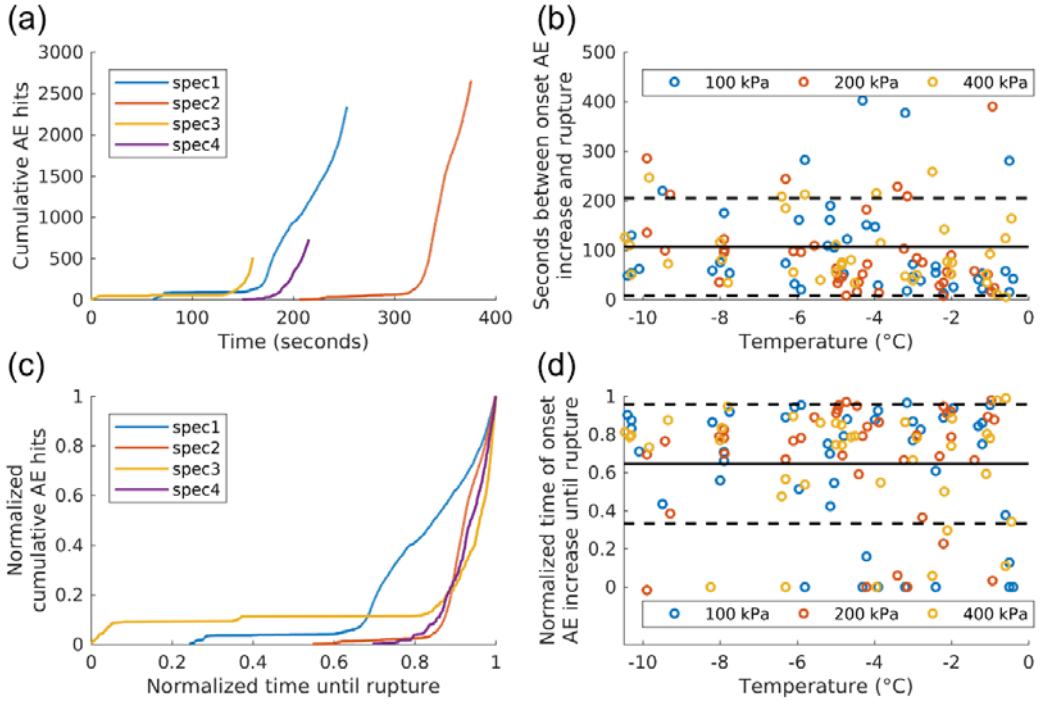

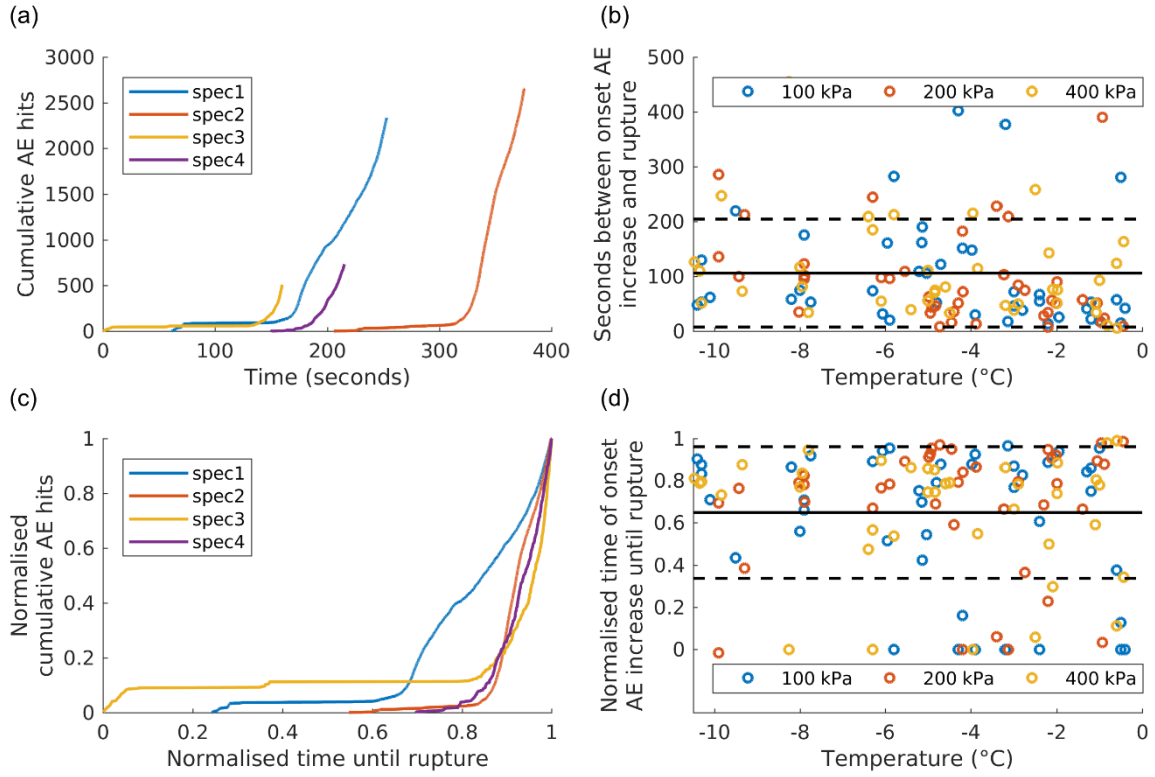

Figure 5: Time series of (a) cumulative AE hits and (c) normalised cumulative AE hits with 400 kPa normal stress and at -4° C. Time zero corresponds to the shear start of the experiments (spec1-4). Curves starting at x > 0 represent tests where first AE signals were recorded a certain time after shear start. T~~Further, t~~he temperature-dependent time between onset of AE increase and rupture is displayed in seconds (b) and normalised (d). The black lines indicate the overall mean while the dashed lines indicate the standard deviation range. Tests at 800 kPa were not considered in (b) and (d) because they were only conducted at temperatures between -0.5 and -4 °C.

The number of AE hits usually increases very suddenly and sharply just before ~~rupture~~ failure (Fig. 5a and Fig. 5c). The average offset between the onset of AE hit increase and fracturing (i.e. Stage IV) is 107 ± 98 sec (Fig. 5b). In all the experiments, the onset of AE hit increase occurs when 65 ± 31 % (mean value with standard deviation) of the time between shear start and failure has passed (Fig. 5d). However, in some experiments at temperatures between -4 and -0.5 °C, the AE hit increase starts even earlier than within the standard deviation of 31 % (outliers < 34 %). The lag in absolute and relative time shows a weak correlation to temperature, though it is not dependent on normal stress.

To analyse the scaling properties of the AE energy, we calculated the distribution for each experiment condition, combining the data of all experiments with the same condition to enlarge the number of events. The probability density functions (PDFs) of event energy show a power-law behaviour spanning 3–5 orders of magnitude (Fig. S4). The exponent b is between 1.6 and 1.9 for the different conditions, but it does not show any relation to temperature or normal load. As a result, it does not indicate any stress- or temperature dependence of the size of fracturing events.

3.2 F~~Observed f~~ailure type and its ~~temperature~~ dependence on temperature and normal stress

Three types of failure could be observed during the shearing tests: i) Fracture along the rock-ice interfaces (Fig. S5a), ii) fracture within the ice layer and iii) a composite fracture type of i) and ii) (Fig. S5b). In the first type, the entire ice infill stuck to either the upper or the lower rock cylinder, whereas in the second case the rock surfaces were unaffected by failure. The last fracture type refers to specimens whose ice layer broke transversely and was separated so that the rear portion remained at the lower cylinder and the front part stuck to the upper one.

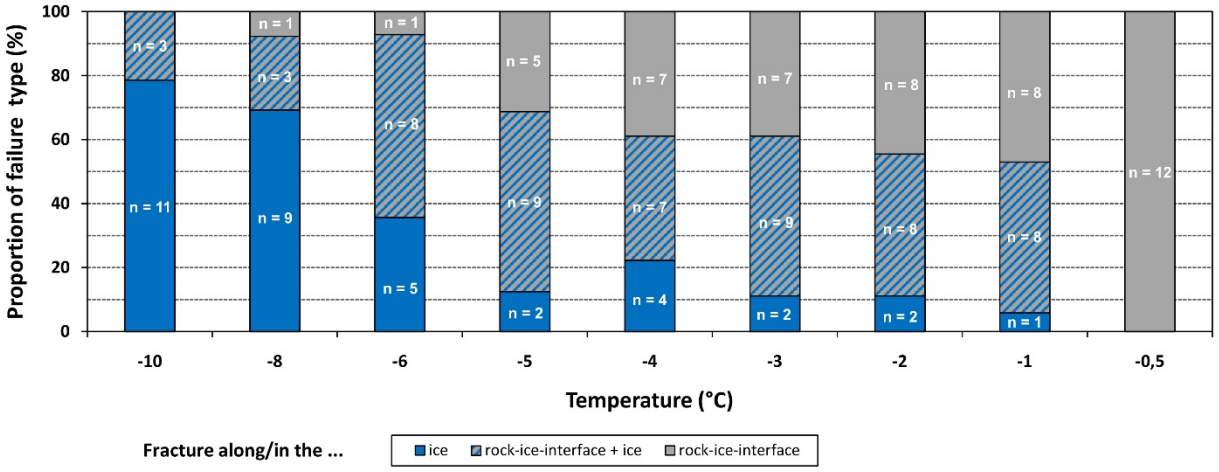

Figure 6: Proportions and absolute numbers of fracture types plotted at temperatures from -10 °C to -0.5 °C (for tests at 100–800 kPa). Failures inside the ice dominate at low temperatures whereas failure along rock-ice interfaces become more important close to 0 °C.

With temperatures rising from -8 to -0.5 °C, the percentage of tests with fracture along the rock-ice interface increase from 8 to 100 % (Fig. 6). At -0.5 °C it constitutes the only failure type. However, the lower number of tests at this temperature level has to be considered. Vice versa, the proportion of fracturing within the ice infillings increases with decreasing temperature from 6 % at -1 °C to 79 % at -10 °C. At ~~-9~~ -8 and -10 °C, it is the dominating failure type. The composite failure type shows no clear trend, either with decreasing or with increasing temperature. A clear relationship between failure type and normal stress could not be identified (Fig. S6).

3.3 Shear stress at failure and its temperature-dependence

The shear stress at failure decreases with increasing temperature a~~A~~t all tested ~~classes of~~ normal stress levels ~~(100–800 kPa) the shear stress at failure decreases with increasing temperature~~ (Fig. S~~7~~6). Table 1 shows t~~T~~he decrease of shear stress at failure with increasing temperature~~hen warming is shown in Table 1~~ for each tested normal stress condition. The calculated

total decrease at stresses 100–400 kPa ranges between 63.5 and 78.1 % and refers to a warming from -10 to -0.5 °C. The maximum decrease at 800 kPa measures 60.1 % and refers to temperatures from -4 to -0.5 °C. ~~The coefficients of determination R^2 range from 0.44 to 0.75.~~

Table 1

3.4 Developing a temperature-controlled brittle failure criterion for ice-filled permafrost rock joints

Shear stress at failure versus normal stress was plotted for all temperature levels ~~s from -10 to -0.5 °C~~ and normal stresses from 100 to 400 kPa (blue regression lines) ~~(Fig. 7a)~~ and additionally for temperatures from -4 to -0.5 °C and normal stresses from 100 to 800 kPa (orange regression lines; ~~(~~Fig. 7~~b~~). Here, the peak shear stresses generally increase with increasing normal stresses at all tested temperatures.

~~Tests at 800 kPa were performed to study a potential stress-dependent transition from brittle fracture to creep at stress levels above 400 kPa. For this purpose, a smaller temperature range from -4 to -0.5 °C was tested representing most of the recently measured annual mean temperatures of Alpine and Arctic bedrock permafrost (Delaloye et al., 2016; Gallemann et al., 2017; Harris et al., 2003). In Fig. 7, the peak shear stresses generally increase with increasing normal stresses at all tested temperatures. The low values of R^2 are partially an effect of the tests clustering around the four predefined stress levels.~~

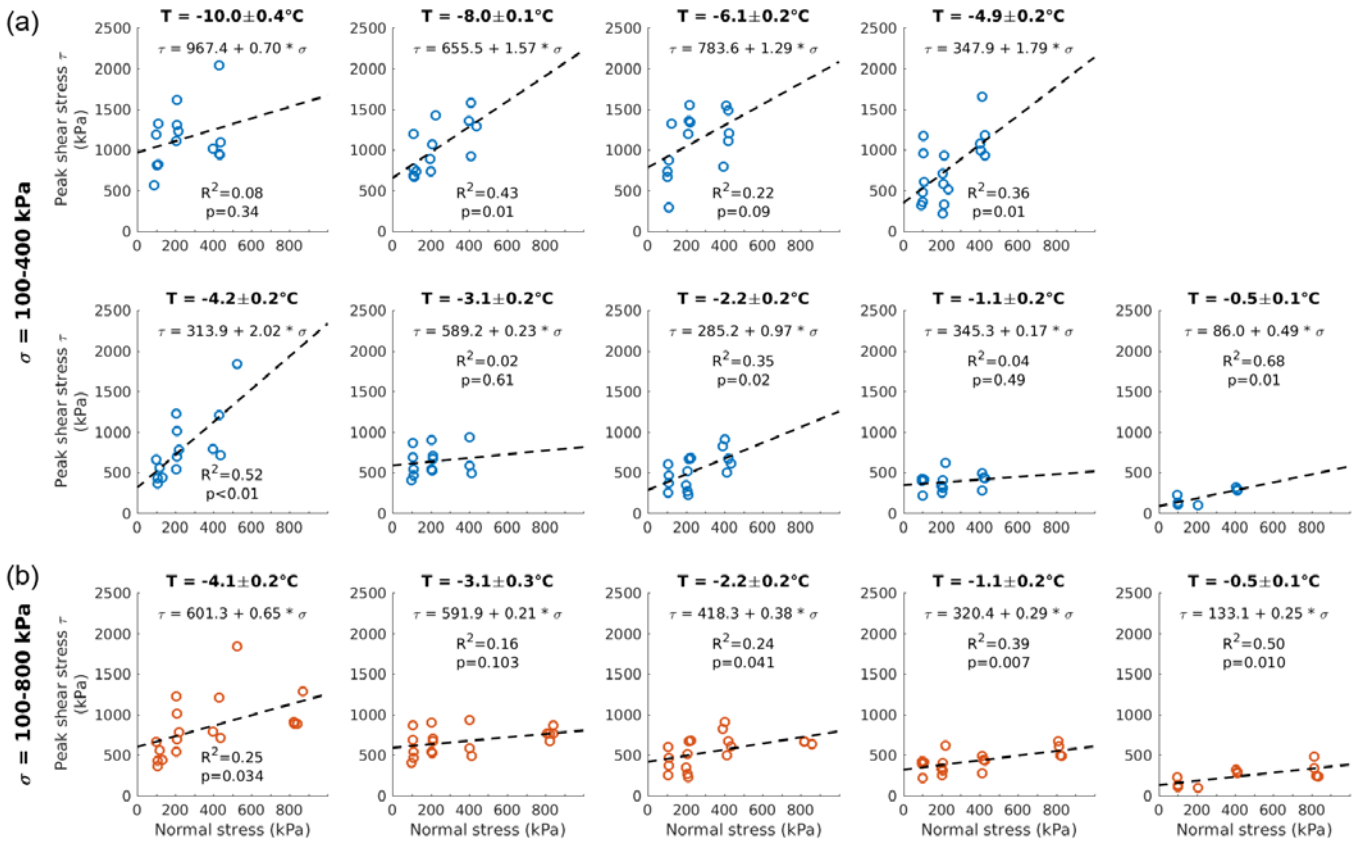
(a)
σ = 100-400 kPa
T = -10.0±0.4°C
τ = 967.4 + 0.70 * σ
R²=0.08
p=0.34
T = -8.0±0.1°C
τ = 655.5 + 1.57 * σ
R²=0.43
p=0.01
T = -6.1±0.2°C
τ = 783.6 + 1.29 * σ
R²=0.22
p=0.09
T = -4.9±0.2°C
τ = 347.9 + 1.79 * σ
R²=0.36
p=0.01
T = -4.2±0.2°C
τ = 313.9 + 2.02 * σ
R²=0.52
p<0.01
T = -3.1±0.2°C
τ = 589.2 + 0.23 * σ
R²=0.02
p=0.61
T = -2.2±0.2°C
τ = 285.2 + 0.97 * σ
R²=0.35
p=0.02
T = -1.1±0.2°C
τ = 345.3 + 0.17 * σ
R²=0.04
p=0.49
T = -0.5±0.1°C
τ = 86.0 + 0.49 * σ
R²=0.68
p=0.01
(b)
σ = 100-800 kPa
T = -4.1±0.2°C
τ = 601.3 + 0.65 * σ
R²=0.25
p=0.034
T = -3.1±0.3°C
τ = 591.9 + 0.21 * σ
R²=0.16
p=0.103
T = -2.2±0.2°C
τ = 418.3 + 0.38 * σ
R²=0.24
p=0.041
T = -1.1±0.2°C
τ = 320.4 + 0.29 * σ
R²=0.39
p=0.007
T = -0.5±0.1°C
τ = 133.1 + 0.25 * σ
R²=0.50
p=0.010
Peak shear stress τ (kPa)
Normal stress (kPa)

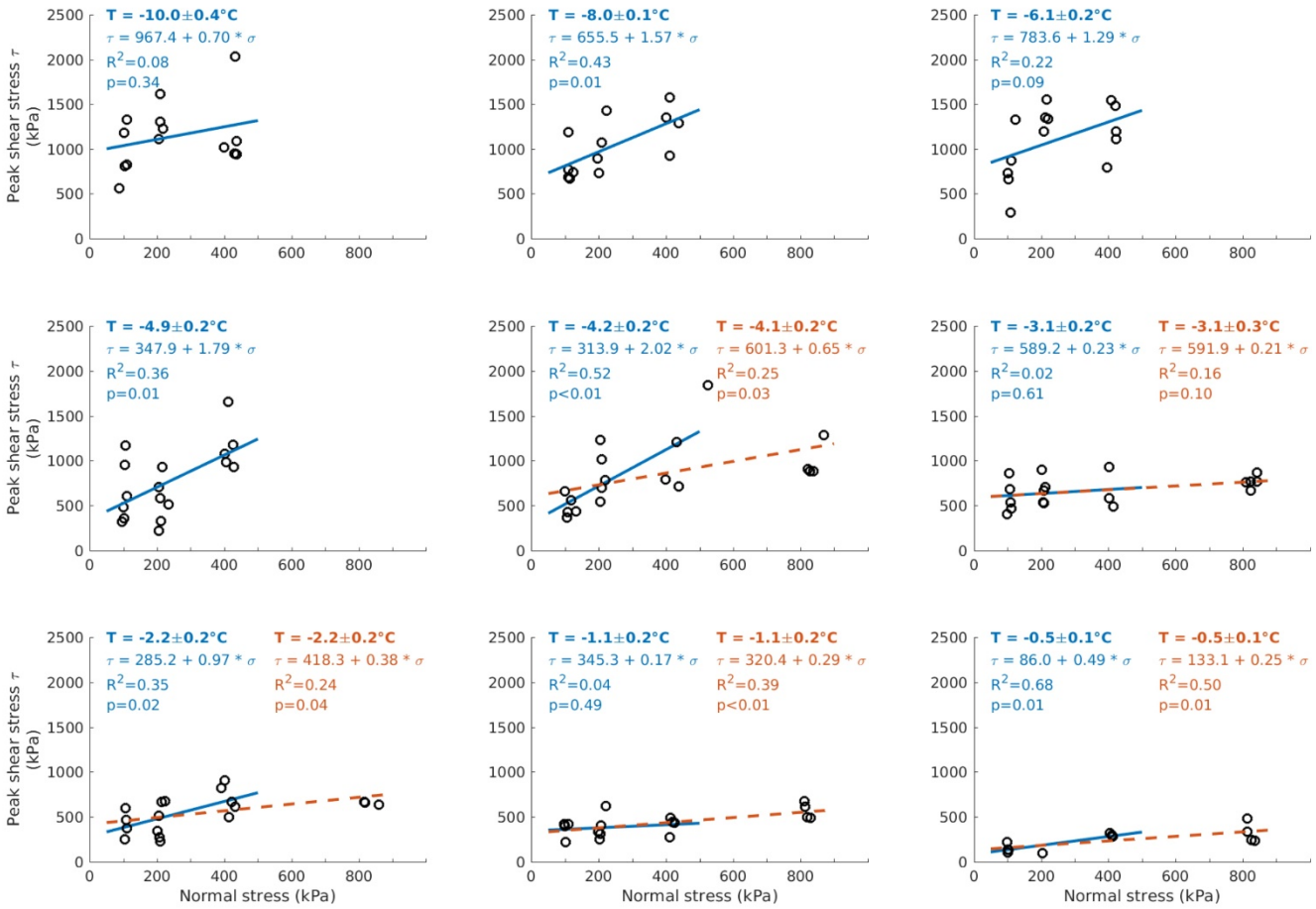

Figure 7: Measured ~~peak~~ shear stress at failure as a function of normal stress for temperatures between -10 and -0.5 °C. The temperature values are ~~corrected by~~ the means (including standard deviation) of the measured rock sample temperatures (close to the moment of failure) of all experiments belonging to a specific ~~the respective~~ temperature level. ~~(a)~~ Normal stress levels of 100, 200 and 400 kPa were applied for the whole temperature range ~~(blue circles)~~. ~~(b)~~ 800 kPa was additionally tested between -4 and -0.5 °C ~~(orange circles)~~. Blue solid lines = ~~The~~ calculated regression lines for normal stresses 100-400 kPa. Orange dashed lines = calculated regression lines for 100-800 kPa. ~~were used to derive temperature-specific cohesion and friction values.~~ p = Probability of rejecting the null hypothesis (H_0) although it is true.

To develop a shear strength description of ice-filled permafrost rock joints we used the linear and stress-dependent Mohr-Coulomb failure criterion (a combination of Coulomb (1773) and Mohr (1900); a discussion of its limitations is given in Jaeger et al. (2007))

$$\tau = \sigma' * \tan(\varphi) + c \quad (35)$$

which represents the shear stress at failure τ as a function of the ~~effective~~ normal stress σ', the cohesion c and the friction angle φ. For the cohesion, we utilised Fig. 7 to derive the shear stress values at the intercepts of the regression lines with the abscissas for each temperature level. To determine the friction, we took the slope values from the linear regression functions which correspond to the coefficient of friction μ. Values for the friction angle were derived by calculating the respective arctangents of μ.

A temperature-dependent cohesion and friction for all test temperatures is displayed in Fig. S8~~7~~. Here, R^2-values range between 0.61–0.92 for the cohesion and between 0.12–0.40 for the coefficient of friction. P-values measure 0–12 % for the cohesion and 7–57 % for the coefficient of friction. The ranges depend on the included stress levels and the temperature range tested. Due to these high uncertainties, we used only specific temperature levels with a statistical significance level of $p \leq 5$ % for the elaboration of the Mohr-Coulomb failure criterion. The p-values had been calculated earlier for the relation between peak shear stress and normal stress at the tested temperature levels (Fig. 7). The temperature levels with p-values > 5 % were excluded from further steps of the model development, as the corresponding peak shear stresses are considered to be not significantly dependent on the normal stress. Further, only the shear experiments from 100 to 400 kPa were utilised for the development of the failure criterion, as they cover the whole range of tested temperatures. This leads to a greater valid temperature range for the model and to a more robust correlation between cohesion or friction and temperature.

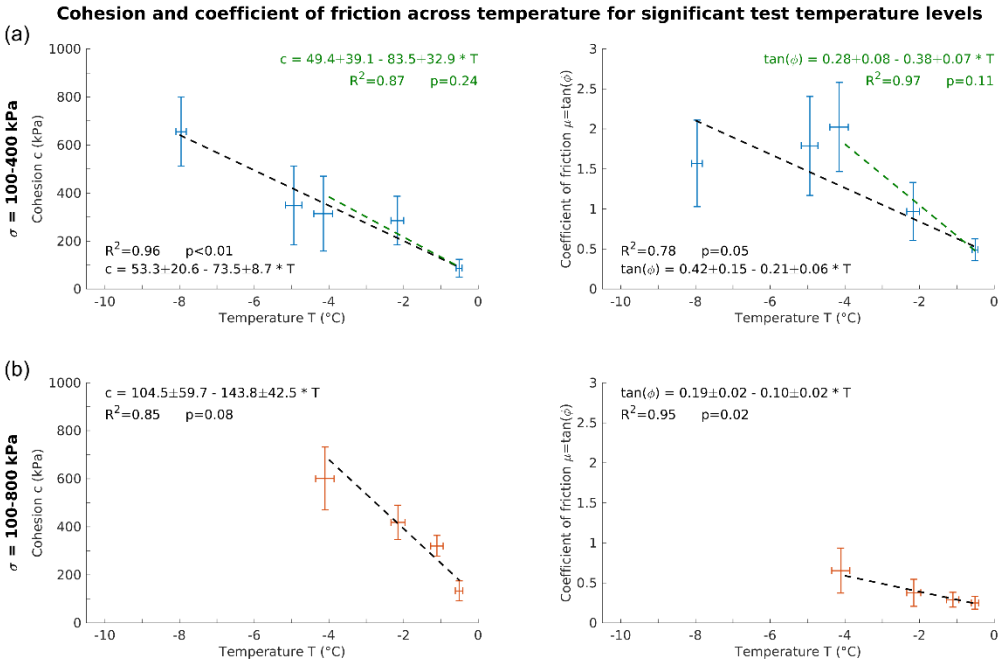

Cohesion and coefficient of friction across temperature for significant test temperature levels
(a)
σ = 100-400 kPa
Cohesion c (kPa)
c = 49.4±39.1 - 83.5±32.9 * T
R²=0.87 p=0.24
R²=0.96 p<0.01
c = 53.3±20.6 - 73.5±8.7 * T
Temperature T (°C)
Coefficient of friction μ=tan(ϕ)
tan(ϕ) = 0.28±0.08 - 0.38±0.07 * T
R²=0.97 p=0.11
R²=0.78 p=0.05
tan(ϕ) = 0.42±0.15 - 0.21±0.06 * T
(b)
σ = 100-800 kPa
c = 104.5±59.7 - 143.8±42.5 * T
R²=0.85 p=0.08
tan(ϕ) = 0.19±0.02 - 0.10±0.02 * T
R²=0.95 p=0.02

Figure 8: Cohesion and friction of ice-filled rock joints as a function of temperature for significant temperature levels with a statistical significance level of p ≤ 5 %. The crosses display the means and standard deviations of rock temperature and cohesion or friction, grouped by the tested temperature classes. (a) Tests at normal stresses 100–400 kPa and temperatures -8 to -0.5 °C (blue crosses). (b) Tests at normal stresses 100–800 kPa and temperatures -4 to -0.5 °C (orange crosses). The dashed lines represent the linear regression functions, which were inversely weighted with the squared standard errors. The green regression lines in (a) refer to a temperature range from -4 to -0.5 °C. The grey areas represent the valid temperature range for the respective parameter.

Fig. 8 shows the temperature-dependent cohesion and friction of ice-filled rock joints for temperature levels with p ≤ 5 % (Fig. 7). Here, the temperature-dependent loss of cohesion of ice-filled rock joints is described by

$$c\,[\mathrm{kPa}] = 53.3 - 73.5 * T \quad (46)$$

where T (°C) is the temperature of the ice-filled joint at failure, valid for temperatures from -8±0.1 °C to -0.5±0.1 °C and normal stresses from 100 to 400 kPa (Fig. 8a).

Table 2

When approaching the melting point, the cohesion decreases by 86 % from -8 °C to -0.5 °C (Table 2). Equation (6) exhibits a decrease in cohesion of 74 kPa /°C^{-1} due to warming, which refers to a reduction by 12 % °C^{-1}/°C. The temperature-dependent friction coefficient can be expressed by

$$\mu = 0.42 - 0.21 * T \quad (57)$$

where T (°C) is the temperature of the ice-filled fracture at failure, valid for temperatures between -8±0.1 °C to -0.5±0.1 °C and normal stresses from 100 to 400 kPa (Fig. 8a). The coefficient of friction falls by 75 % with increasing temperature from -8 °C to -0.5 °C (Table 2). The corresponding friction angle decreases by 60 % (64.5–27.7°). This equation shows a warming-dependent loss of friction of 0.21 /°C^{-1} corresponding to a reduction by 10 % /°C^{-1}.

We did not perform tests at temperatures warmer than -0.5 °C because we assume the ice to melt or be squeezed out of the rock cylinders which leads to shearing along rock-rock contacts. Cohesion will be absent at the melting point and shear strength values will rise. This is shown by the tests of Davies et al. (2001) where the shear strengths of ice-concrete samples closely approach the concrete-concrete sample line.

Combining Eq. (46) and (67) in a Mohr-Coulomb failure criterion (Eq. (35)), we can describe a temperature- and normal stress-dependent shear stress at failure τ (kPa) for ice-filled rock joints

$$\tau\,[\mathrm{kPa}] = \sigma' * (0.42 \pm 0.15 - 0.21 \pm 0.06 * \mathrm{T}) + (53.3 \pm 20.6 - 73.5 \pm 8.8 * \mathrm{T}) \quad (6)$$

where the friction angle is the arctangent of μ while both friction ~~(0.42 − 0.21 ∗ T)~~ and cohesion ~~(53.3 − 73.5 ∗ T)~~ respond to a temperature increase. This formula is valid for normal stresses between 100 to 400 kPa and temperatures between -8±0.1 °C to -0.5±0.1 °C.

3.5 Cohesion and friction for normal stresses between 100 and 800 kPa

When comparing the loss of friction and cohesion for normal stresses 100–400 kPa with the loss for 100–800 kPa, both in the same temperature range of -4 and -0.5 °C, the following can be observed (Fig. 8, Table 2): (i) The absolute reduction in cohesion is more pronounced for tests including all normal stress levels. (ii) The absolute decrease in friction is stronger for tests excluding 800 kPa. (iii) Percentage decreases are nearly the same for both groups of tests.

4 Discussion

Our experimental results generally show decreasing shear strength of ice-filled rock joints with increasing temperature and decreasing normal stress. We use these data to develop a new brittle failure criterion for ice-filled permafrost rock joints which is based on Mohr-Coulomb and shows that both, the cohesion and the friction ~~angle~~, are temperature-dependent and decrease with increasing temperature (R^2 = 0.96 for the cohesion and R^2 = 0.78 for the friction). Similar tendencies have been indicated by previous studies of the shear strength of ice-filled rock joints (Davies et al., 2000; Davies et al., 2001; Günzel, 2008; Krautblatter et al., 2013). However, all of these studies were performed with a much smaller number of experiments and with concrete as rock analogue; further, their results have not yet been combined to a comprehensive failure criterion.

4.1 Real-world conditions of permafrost rock slope destabilisation simulated by the new failure criterion

The experiments presented apply to real-world rock-ice fracturing in rock slope failures (i) with ice-filled failure planes in a depth of 4 to 15 m, i.e. mainly below the active layer and shallower than the ice fracturing suppression in favour of creep deformation of ice, (ii) with virtually all realistic a~~A~~lpine and Arctic permafrost bedrock temperatures between -0.5 °C and -10 °C and (iii) with fast displacements (0.7±0.1 mm/min) coinciding with the final accelerating failure stage. Rock-ice fracturing certainly dominates rock failure volumes of ≤ 2.3 ∗ 10~~.000~~^{4} m^3 where all ice-filled failure planes are ≤ 15 m deep (Sect. 1), but it might also play an important role for larger failures, where just a certain proportion of ice-filled failure planes is ≤ 15 m deep.

If we leave the range of considered boundary conditions in terms of (i) higher normal stresses, (ii) lower temperatures or (iii) lower strain rates, fracturing along ice-filled permafrost rock joints will presumably not occur: (i) A potential gradual stress-dependent transition from brittle fracture to creep is expected at the tested normal stresses above 400 kPa. In our experiments, all sandwich shear samples, including those at 800 kPa normal stress, only failed by fracturing, presumably due to the elevated strain rate of 10^{-3} s^{-1} leading to fracture. It appears that the transition from shear fracturing to creep is not only stress-dependent but also strain-rate-dependent within a certain transition level of normal stress (Sanderson, 1988). Other reasons for the unexceptional fracture-dominated failures are that the simulated rock overburden of 30 m may be still within the transition depth and seems to favour fracturing at elevated strain rates. (ii) Tests at temperatures below -10 °C were not performed because measured daily and annual mean temperatures at various alpine and Arctic permafrost bedrock sites do not drop below -10 °C at depth (Böckli et al., 2011; Delaloye et al., 2016; Harris et al., 2003). (iii) The samples were sheared with high strain rates of 10^{-3} s^{-1} to provoke brittle failure of ice and rock-ice contacts. At lower strain rates, stress concentrations along the shear zone can be relaxed and the mechanical behaviour changes to ductile creep deformation without fracturing (Arenson and Springman, 2005a; Arenson et al., 2007; Krautblatter et al., 2013; Renshaw and Schulson, 2001; Sanderson, 1988;).

~~As we assume that the shear strength along ice-filled rock joints is independent of the rock type, the tests presented simulate rock-ice fracturing along joints of all rock types. Anyhow, a potential shear strength dependence on different rock types has to be tested in additional experiments.~~

Our experiments simulate the final accelerating stage of rock slope failure where the structure of the ice infillings is deformed by intense shear displacement. The ice infill at the start of the shear tests reproduces an ice-filled joint that has already been loaded and deformed by uniaxial compression. This is somehow similar to polycrystalline ice in natural fractures as ice has a high capacity to perform self-healing and thus deletes previous deformation-induced imperfections. At strain relaxation, the ice-bonding heals itself within hours and days due to refreezing and causes a strengthening of the sample (Arenson and Springman, 2005a; Sanderson, 1988); thus a sample with a pre-set normal stress is similar to an ice-filled fracture under similar conditions irrespective of the deformation history. In this study, the bonding of the rock-ice interface is mostly established by adhesion whereas rock-ice interlocking is less important due to the small surface roughness of the rock samples.

So far the failure of ice-filled permafrost rock joints has been studied using concrete as a rock analogue (Davies et al., 2000; Günzel, 2008). For the first time, we use rock to closely reproduce real conditions along rock joints. Synthetic materials possibly deviate from shear strength values representative for rock joints in the field. For instance, ice sliding on granite shows a friction coefficient μ approx. 0.5 higher than ice sliding on glass or metals, all having a similar surface asperity roughness. The higher friction of the granite-ice interfaces is due to a higher effective adhesion (Barnes et al., 1971). We assume that the shear strength of rock-ice interfaces is mostly affected by temperature, normal stress, strain rate and joint surface roughness. However, the applied constant strain rate as well as the standardised preparation of a uniform joint surface roughness prohibit any potential effects on the shear strength. We postulate that the influence of the rock type on the shear strength is less important:

(i) The thermal conductivity of the rock may affect the shear strength by facilitated melting along heat-insulating surfaces causing a decrease in friction (Barnes et al., 1971). The thermal conductivity of rocks varies in a range of 0.3–5.4 W m^{-1} K^{-1} (Clauser and Huenges, 1993; Schön, 2015). A metal like brass, with a much higher thermal conductivity of 100 W m^{-1} K^{-1}, would lead to a warming at the interface 14.5 °C lower than granite (Barnes et al., 1971). Due to the relatively small range of thermal conductivities for different rock types we do not expect a rock type-dependent effect on the shear strength.

(ii) The porosity of the rock and the type of constitutive minerals may play a role for the growth of ice crystals along the rock-ice interface which in turn affects the shear strength. The strain rate and the compressive strength of ice crystals are significantly higher for those oriented parallel to the applied stress than for those oriented randomly (Hobbs, 1974; Paterson, 1994). However, we assume any potential rock type-dependent orientations of ice crystals to be deleted before shearing starts due to the applied uniaxial compression during initial consolidation.

(iii) The strength of the constitutive minerals of the rock surfaces may control the friction of the rock-ice contact. However, we assume the strength of minerals to play a minor role for the shear strength, because at the rock-ice interface the ice will fail before the rock material and ice strength will control the failure process. In our tests we could not observe particles breaking off the rock surfaces. Elastic moduli of most rock minerals (bulk modulus k: 17–176 GPa; shear modulus μ: 9–95 GPa) are 2–20 times higher than of ice (k: 8.9 GPa; μ: 3.5 GPa) (Schulson and Duval, 2009; Schön, 2015). The small applied roughness of the shear surfaces additionally prevented any relevant impact of differing mineral strengths.

(iv) Rock minerals heat up differently and can generate thermal stresses (Gómez-Heras et al., 2006) in the intact rock and along discontinuities causing thermal fatigue and a reduction in the shear resistance (Dräbing et al., 2017). However, we do not expect an impact on the shear strength as repetitive temperature cycles with high magnitude and frequency are required for thermal stress fatigue (Hall and Thorn, 2014). During our tests, temperatures were kept constant.

Thus, the tests using limestone represent rock-ice fracturing along joints of all rock types. To use rock instead of other materials probably has a greater effect on the shear strength than different rock types. Still, a potential shear strength dependence on different rock types has to be proven in additional experiments. Further, i

~~If we leave the range of considered boundary conditions in terms of (i) lower temperatures, (ii) lower strain rates or (iii) higher normal stresses, fracturing along ice-filled permafrost rock joints will presumably not occur: (i) Tests at temperatures below -10 °C were not performed because measured daily and annual mean temperatures at various Alpine and Arctic permafrost bedrock sites do not drop below -10 °C at depth (Böckli et al., 2011; Delaloye et al., 2016; Harris et al., 2003). (ii) The samples were sheared with high strain rates of 10^{-3} s^{-1} to provoke brittle failure of ice and rock-ice contacts. At lower strain rates, stress concentrations along the shear zone can be relaxed and the mechanical behaviour changes to ductile creep deformation without fracturing (Arenson and Springman, 2005a; Arenson et al., 2007; Krautblatter et al., 2013; Renshaw and Schulson, 2001; Sanderson, 1988;). (iii) A potential gradual stress-dependent transition from brittle fracture to creep, which is observed with increasing confining pressure in triaxial tests (Sanderson, 1988) and with increasing normal stress in uniaxial shear tests (Günzel, 2008), is expected under the similarly tested normal stress conditions above 400 kPa. In our experiments, all sandwich shear samples, including those at 800 kPa normal stress, only failed by fracturing, presumably due to the elevated strain rate~~

~~of 10^{-3} s^{-1} leading to fracture. It appears that the transition from shear fracturing to creep is not only stress-dependent but also strain-rate dependent within a certain transition level of normal stress (Sanderson, 1988). Other reasons for the unexceptional fracture-dominated failures are that the simulated rock overburden of 30 m may be still within the transition depth and seems to favour fracturing at elevated strain rates. I~~t is certainly interesting to systematically analyse in other studies the strain-rate dependent brittle fracture-creep transition beyond 800 kPa normal stress or the influence of the joint surface roughness on the shear strength and the failure behaviour~~in detail in an additional study,~~ but this is beyond the scope of this study.

~~The joint surface roughness and ice layer thickness may be varied in further studies to assess their influence on the shear strength of ice-filled rock joints and the failure behaviour.~~

4.2 Validation of the new failure criterion ~~for temperature- and stress-dependent fracturing along ice-filled rock joints~~

The new derived failure criterion (Eq. (6~~8~~)) describes the shear strength of ice-filled fractures in all types of rock and combines a temperature-dependent cohesion and friction angle. A temperature-dependence of both, the cohesion and friction angle, has not been demonstrated yet, but for pure ice (Fish and Zaretzky, 1997). However, other publications have either postulated a temperature-dependence of the cohesion of ice-rich soils (Arenson and Springman, 2005b; Arenson et al., 2007) or a temperature-dependence of the friction coefficient of granite-ice interfaces (Barnes et al., 1971). Here, we develop a failure criterion for rock-ice interfaces that contains both a temperature-dependent coefficient of friction and an even stronger temperature-dependent cohesion.

~~Figure 9 depicts the new Mohr-Coulomb failure criterion (Eq. (8)) with the range of uncertainty for the different temperature levels tested and corrected by their true means (including standard deviation). The means of the measured peak shear stress values, represented by the intersections of the error bars of normal stress and peak shear stress, mostly correlate well with the calculated failure criterion and the respective error ranges. Statistical dispersion measures of the measured peak shear stress values around the failure criterion are shown in Table S2. Best accordance is achieved for the shear stress means used for model calibration (correspond to significant temperature levels with p-values ≤ 5 %). The mean absolute deviation (MAD) and coefficient of variation (CV) range between 40–146 kPa and 8.8–24.6 % respectively. The experiments at temperatures –1, –3, –6 and –10 °C (with p-values > 5 %), which had been excluded from the elaboration of the failure criterion, were used for validation. Their shear stress means show higher deviations from the failure criterion, i.e. the MAD and the CV range from 98 to 252 kPa and from 15 to 43.5 % respectively. For normal stresses 100–400 kPa, the model seems to show a robust fit even with values not included in the initial model development data set. The means of peak shear stress at 800 kPa mostly lie within the calculated error margins, but at their lower boundaries. This demonstrates the mechanical parameters controlling the failure behaviour start to change at higher normal stresses (800 kPa) and temperatures close to the melting point.~~

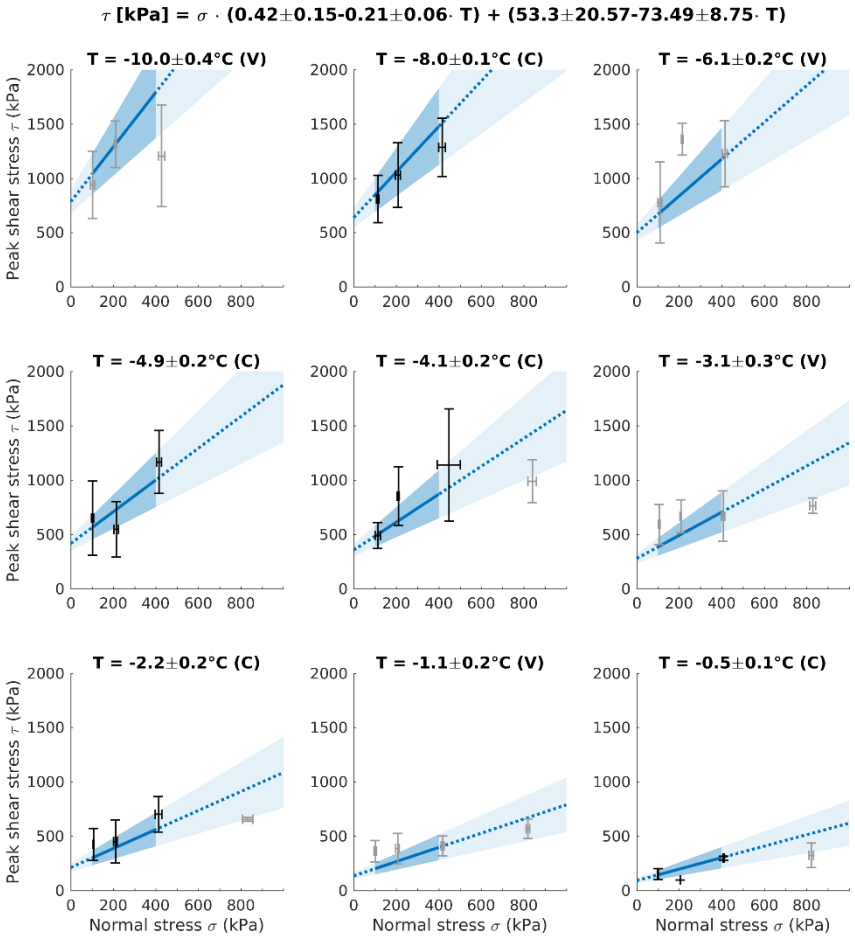

595

Figure 9: Validation test for the new Mohr-Coulomb failure criterion for ice-filled rock joints (Eq. (6~~8~~)). The black and grey crosses represent means and standard deviations of normal stress and peak shear stress, grouped by the tested normal stress classes 100, 200, 400 and 800 kPa. C = Calibration temperature level that was used for the model as p ≤ 5 % (black crosses). V = Validation temperature level that was excluded from the elaboration of the failure criterion because p > 5 % (grey crosses). As tests at 800 kPa
600 **were excluded from the development of the failure criterion, they also serve as validation (grey crosses). Solid blue lines and dark blue areas represent the calculated failure criterion and respective error ranges within the valid normal stress range. Dotted blue lines and light blue areas are extrapolations of the failure criterion and error margins beyond the valid normal stress range.**

605 Figure 9 depicts the new Mohr-Coulomb failure criterion (Eq. (6)) with the range of uncertainty for the different temperature levels tested and corrected by their true means (including standard deviation). The means of the measured peak shear stress values, represented by the intersections of the error bars of normal stress and peak shear stress, mostly correlate well with the calculated failure criterion and the respective error ranges. Statistical dispersion measures of the measured peak shear stress values around the failure criterion are shown in Table S2. Best accordance is achieved for the shear stress means used for

model calibration (correspond to significant temperature levels with p-values ≤ 5 %). The mean absolute deviation (MAD) and coefficient of variation (CV) range between 40–146 kPa and 8.8–24.6 % respectively. The experiments at temperatures -1, -3, -6 and -10 °C (with p-values > 5 %), which had been excluded from the elaboration of the failure criterion, were used for validation. Their shear stress means show higher deviations from the failure criterion, i.e. the MAD and the CV range from 98 to 252 kPa and from 15 to 43.5 % respectively. For normal stresses 100–400 kPa, the model seems to show a robust fit even with values not included in the initial model development data set. The means of peak shear stress at 800 kPa mostly lie within the calculated error margins, but at their lower boundaries. This demonstrates the mechanical parameters controlling the failure behaviour start to change at higher normal stresses (800 kPa) and temperatures close to the melting point.

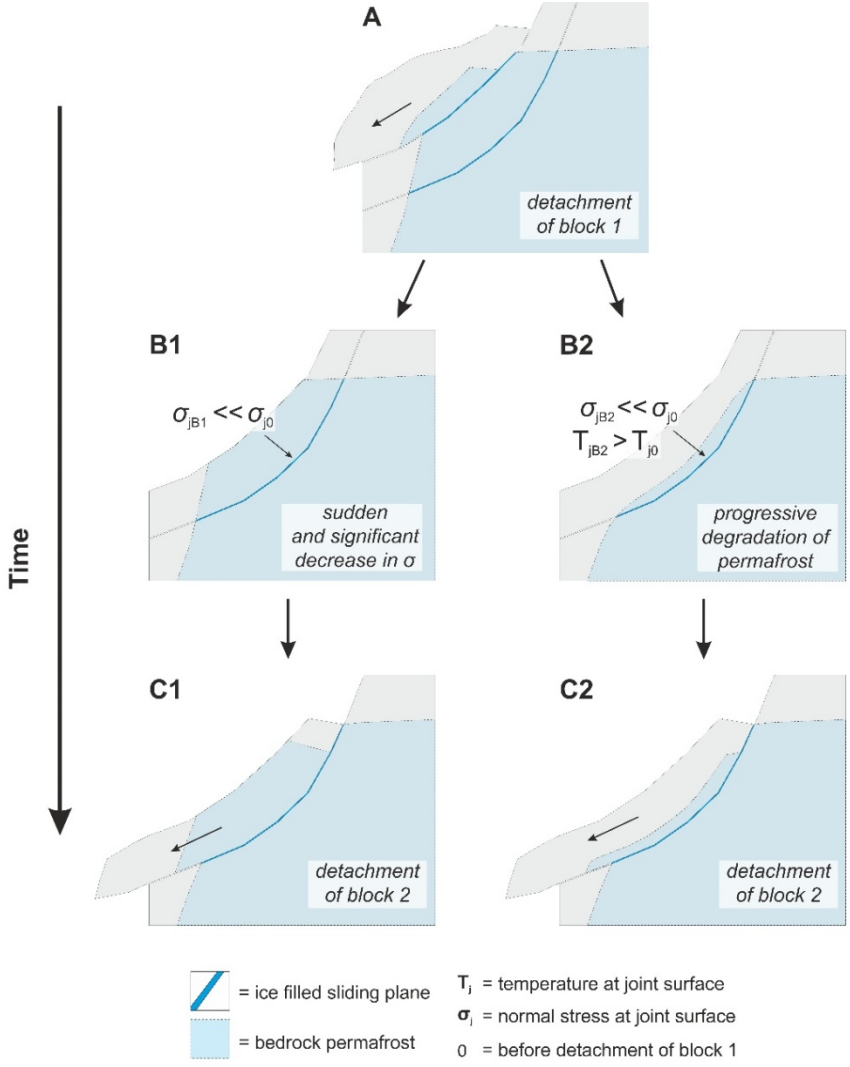

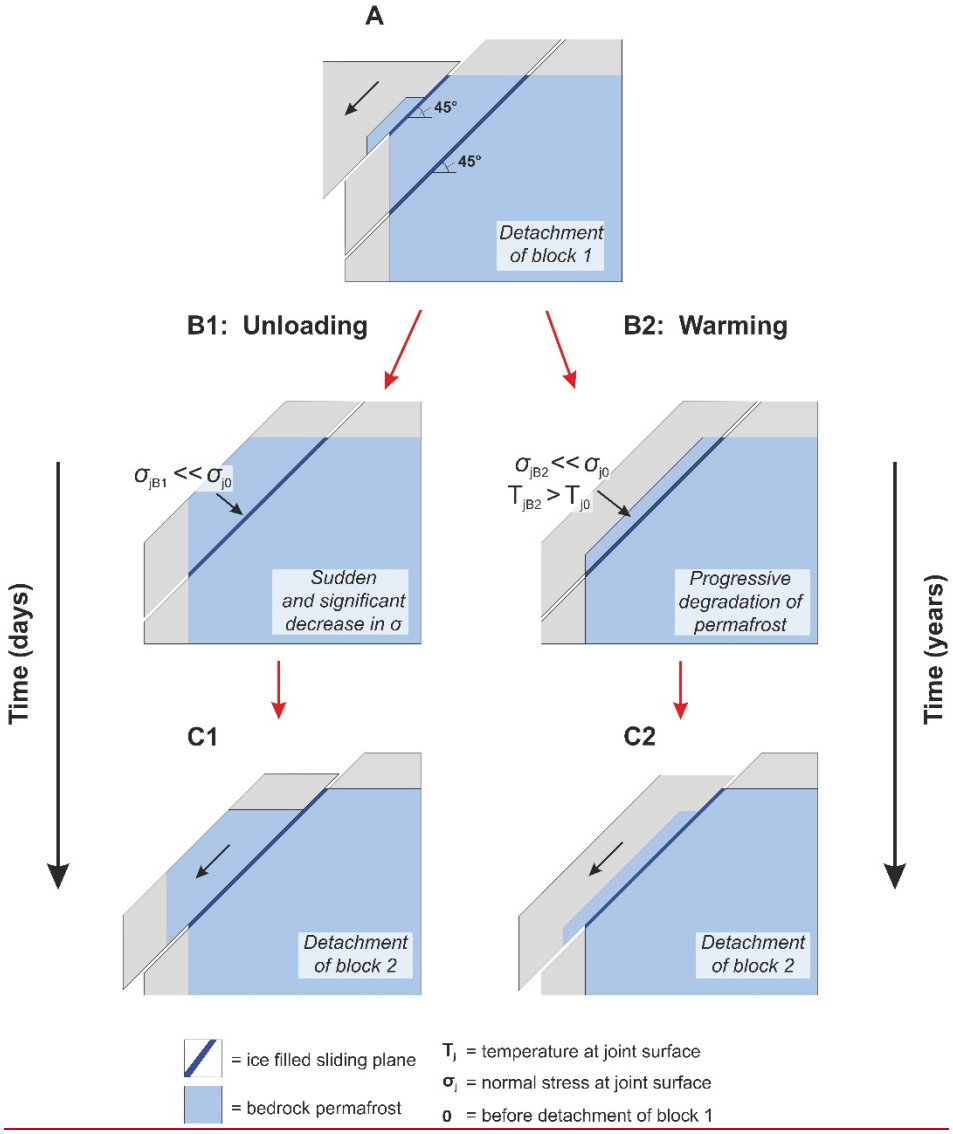

Figure 10: Progressive failure in a warming permafrost rock slope displaying thermal and normal stress conditions before and after detachment of a first slab. Both (B2) progressive thermal warming (i.e. permafrost degradation), but even faster (B1) sudden unloading can initiate failure.

This study shows that both warming and unloading of ice-filled rock joints, lead to a significant drop in shear resistance, which may cause a self-enforced rock slope failure propagation. The progressive degradation of bedrock permafrost and ice in rock joints may control the cohesion and friction angle of the joints. However, as soon as a first slab has detached from the rock slope (A in Fig. 10), further slabs below can become unstable and finally detach as the shear strength along the ice-filled failure

plane is affected by progressive warming (i.e. permafrost degradation, B2 in Fig. 10), but even faster by sudden unloading (B1 in Fig. 10). The latter is represented by a significant drop in normal stress in the Mohr-Coulomb failure criterion (Fig. 11).

Temperature class [°C]	Coefficient of friction [μ]	Cohesion [kPa]	Normal stress-dependent friction at σ_1 =			
			100 kPa	200 kPa	400 kPa	800 kPa
$\lvert\tau\rvert = \sigma * (0.42 - 0.21 * T) + (53.3 - 73.5 * T)$						
			Unloading reduces stability of underlying frozen rock mass		Critical stability loss of underlying frozen rock mass	
-10	2.52	788	252	504	1008	2016
-8	2.10	641	210	420	840	1680
-6	1.68	494	168	336	672	1344
-5	1.47	421	147	294	588	1176
-4	1.26	347	126	252	504	1008
-3	1.05	274	105	210	420	840
			Unloading increases stability of underlying frozen rock mass			
-2	0.84	200	84	168	336	672
-1	0.63	127	63	126	252	504
-0.5	0.53	90	53	105	210	420

Figure 11: Three scenarios of rock slope stability after the sudden unloading of an underlying frozen rock mass with 45 ° fractures. Green boxes: Increasing stability of underlying frozen rock mass. Unloading increases shear resistance relative to shear forces in 45 ° fractures. Orange boxes: Reducing stability. Unloading reduces shear resistance (friction) relative to shear stress in 45 ° fractures. Red boxes: Critical stability loss. Friction loss along underlying 45 ° fractures even exceeds ice cohesion.

We consider three scenarios of rock slope stability depending on the reduction in normal stress and its relationship to cohesion along a specific shear plane with an inclination of 45 °. Correspondingly, all changes in shear forces equal the changes in the shear resistance $\Delta\tau = \Delta\sigma$. However, instability may increase when the loss in friction surpasses the loss of applied shear forces: $\Delta\sigma * tan\,\varphi > \Delta\tau$. This may happen in an underlying frozen rock mass upon unloading when μ or $(0.42 - 0.21 * T) > 1$. The cohesion may possibly compensate the decrease in friction when $c > \Delta\sigma * tan\,\varphi$. In this case the shear plane could become more unstable without complete failure. This is valid for temperatures between -10 and -3 °C and normal stresses 100–200 kPa (orange boxes in Fig. 11). When the loss of friction in an underlying frozen rock mass upon unloading is much bigger than the reduction in the shear forces $\Delta\sigma * tan\,\varphi \gg \Delta\tau$ and even exceeds the ice cohesion $c < \Delta\sigma * tan\,\varphi$, then failure along the shear plane is strongly promoted. This is valid for temperatures between -10 and -0.5 °C and normal stresses 400–800 kPa (red boxes in Fig. 11). Rock slope stability in an underlying frozen rock mass upon unloading is only weakly affected if the reduction in friction is smaller than the reduction in the shear force: $\Delta\sigma * tan\,\varphi + c < \Delta\tau$. This is valid for temperatures

between -2 and -0.5 °C and normal stresses 100–200 kPa (green boxes in Fig. 11). In summary, the red scenario in Fig. 11 indicates a high likelihood of subsequent failures by unloading the underlying frozen rock mass, the orange scenario exposes a moderate likelihood and the green scenario shows a small likelihood. Unloading may lead to instability or even failure when the shear planes (i) are affected by a high reduction in normal stress exceeding the ice cohesion and/or (ii) are below -2 °C due to a friction coefficient higher than 1.~~This study shows that both warming and unloading of ice-filled rock joints, lead to a significant drop in shear resistance, which may cause a self-enforced rock slope failure propagation. The progressive degradation of bedrock permafrost and ice in rock joints may control the cohesion and friction angle of the joints. However, as soon as a first slab has detached from the rock slope (A in Fig. 10), further slabs below can become unstable and finally detach as the shear strength along the ice-filled failure plane is affected by (B2 in Fig. 10) progressive thermal warming (i.e. permafrost degradation), but even faster by (B1 in Fig. 10) sudden unloading. The latter is represented by a significant drop in normal stress in the Mohr-Coulomb failure criterion.~~

~~A-C1, A-C2 or a combination of both may also be possible scenarios for the observed rockslide at the Zugspitze summit crest, once the movement of the unstable rock mass accelerates.~~

4.3 Failure types

Three types of failure were identified: Fracture along the rock-ice interfaces, fracture within the ice layer and a composite type. From a practical point of view, Eq. (6~~8~~) has to include all types of failure due to five main reasons:

(i) ~~(i)~~ We cannot observe what types occur in natural systems.

(ii) A specific stress, strain or temperature condition could not be assigned explicitly to one of the failure types.

(iii) Along spatially extensive rock joints, all these failure types coexist and coincide.

(iv) All three types together fit in a failure criterion, showing that they converge to a range of values under given temperature and stress conditions.

(v) It is physically impossible to constrain the exact fracturing plane in a sub-millimetre range away from the rock-ice interface.

In this study we observe a tendency of temperature-dependence of the distinct failure types: when comparing fractures in the ice with fractures along the rock-ice contact, tests with the first failure type rather dominate at cold temperatures between -10 to -6 °C, while the proportion of tests with fracture along the rock-ice-interface dominate at higher temperatures between -5 to -0.5 °C. This behaviour is similar to the pattern observed by Jellinek (1959), albeit at lower temperatures, showing “cohesive breaks” (comparable with fracture within the ice infilling) of ice-steel interfaces at temperatures colder than -13 °C and “adhesive breaks” (equal to fracture of rock-ice interfaces) at temperatures warmer than -13 °C. Previous publications highlight three potential reasons for this pattern that explains the formation of liquids, which may support the failure of rock-ice-contacts at warmer conditions:

(i) ~~(i)~~ Above -3 °C the deformation of ice is increasingly influenced by pressure melting (Hobbs, 1974), which can be pronounced in regions of stress concentration along the shear plane (Arenson and Springman, 2005a; Arenson et al., 2007).

(ii) In porous media, curvature-induced and interfacial pre-melting (caused by long-range intermolecular forces between different materials and phases) leads to a depressed equilibrium freezing temperature. An unfrozen liquid melt film, several nanometres thick, forms at the ice-solid-interface at -1 °C, increasing its thickness when approaching 0 °C (Rempel et al., 2004).

(iii) Grain boundary sliding occurs at temperatures above approximately -10 °C, which generates heat by friction (Hobbs, 1974) and may additionally support the formation of this liquid like layer along the rock-ice interface.

4.4 Cohesion and friction for normal stresses including 800 kPa

~~Due to the fact that at higher stresses significantly exceeding 400 kPa brittle fracturing can be suppressed in favour of creep behavior, we also conducted experiments at 800 kPa.~~ Combining the 100–400 kPa with the 800 kPa tests results in a higher (absolute) reduction of cohesion and a lower (absolute) loss in friction with increasing temperature (Fig. 8). The relatively low peak shear stress values at 800 kPa normal stress flatten the linear regression curves and raise their intercepts with the abscissas (Fig. 7~~b~~). This behaviour can presumably be explained due to an enhanced pressure melting effect at higher normal stresses and temperatures close to 0 °C leading to liquid formation along the rock-ice interface and decreasing the friction (see also Sect. 4.3; Arenson and Springman, 2005a; Barnes and Tabor, 1966; Hobbs, 1974). This hypothesis is supported by two findings: (i) Failures along the rock-ice contact dominate at higher temperatures between -0.5 and -5 °C (Fig. 6). (ii) The proportion of rock-ice failures to all failure types is 42 % for normal stresses 100–400 kPa and temperatures from -0.5 to -4 °C. The corresponding proportion for the same temperature range and normal stresses 100–800 kPa is 51 %. When tests at 800 kPa are added, particularly the rock-ice failures increase in numbers whereas failures within the ice are not affected. At normal stresses of 800 kPa and temperatures below -4 °C, the enhanced pressure melting effect may reduce and shear stresses are expected to rise significantly.

4.5 AE activity as an indication for correlated damage, potentially preconditioning failure

AE is generally well capable to anticipate rock-ice failure as (i) all failures are predated by an AE hit increase, (ii) the hit rate increases well before brittle failure starts and (iii) ~~it~~ AE hits peak~~s~~ immediately prior to failure. This AE pattern coincides with observations in triaxial constant strain rate tests on frozen soil (Yamamoto and Springman, 2014). The experiments conducted ~~is manuscript~~ clearly show~~s~~ that precursors before failure can be observed by the AE technique providing complementary information to the displacement measurements. To exceed the AE trigger level, AE events have to be emitted from significantly large evolving microcracks and thus document microcrack generation and coalescence. It is interesting to consider that in ice, even secondary and tertiary creep are constituted by the generation and healing rate of microfractures (Paterson, 1994; Sanderson, 1988). The measured pre-failure increase in AE activity (Fig. S3) is, thus, an indication for damage increase, i.e. microcrack generation and coalescence ~~(which can also be observed in the presented tests, Fig. S3)~~ typical for cryospheric damage propagation (Murton et al., 2016; Yamamoto and Springman, 2014). The culmination of progressive damage involves complex interaction between multiple defects and growing microcracks (Eberhardt et al., 1999; Senfaute et al., 2009; Sornette,

2006). An increase in the AE hit rate prior to failure accompanies the evolution of the internal damage and can therefore be used as a precursor signal.

The power-law distribution of the AE event energy, which shows only small variations for all different temperature and loading conditions, indicates that strength heterogeneity, a main factor influencing this parameter (Amitrano et al., 2012), is similar for all tests at different conditions. Hence, neither a stress nor a temperature dependence of the size of fracturing events is expected in the tested conditions. A main challenge with AE monitoring is the absolute comparison of the event number and energy. The measured signal is strongly influenced by the coupling of the sensor with the medium. Additionally, the event triggering depends on the selection of an amplitude threshold. However, relative comparison (e.g. evolution of the hit rate) and statistical means (e.g. exponent b) are not very sensitive to above-mentioned challenges, as long as enough events are detected.

At temperatures above -4 °C, a higher number of samples displayed an earlier start in fracturing before failure occurred. This trend is visible in the higher number of outliers below the standard deviation range and at temperatures above -4 °C (Fig. 5d). It may be explained by the lower shear strength of samples at warmer temperatures. Accordingly, at colder temperatures failure is increasingly characterised by a later onset of AE events because of higher shear strengths. Challenges remaining for field application of the recorded offset between the onset of AE hit increase and shear failure are the positioning of the sensors and their density, the strength of the signal and the missing signal emission history prior to instrumentation.~~Challenges remaining for field application of the recorded offset between the onset of AE hit increase and shear failure are (i) the positioning of the sensors and their density, (ii) the strength of the signal and (iii) the missing signal emission history prior to instrumentation.~~

5 Conclusions

Most of the documented~~observed~~ failures in permafrost~~-affected~~ rock walls are likely triggered by the mechanical destabilisation of warming bedrock, discontinuities with rock bridges as well as joints with or without ice fillings. ~~permafrost including effects in ice-filled joints, which~~ The latter may ~~evolve~~ evolve into~~into~~ ~~potential~~ shear ~~shear~~ planes~~-~~ supporting~~ing~~ destabilisation on a larger spatial scale and leading to failure. To anticipate failure in a warming climate, we need to better understand how rock-ice mechanical processes affect rock slope destabilisation ~~and failure~~ with temperatures increasing close to 0 °C.

This paper presents a systematic series of constant strain-rate shear tests on sandwich-like limestone-ice-limestone samples (i) to simulate the brittle failure of ice infillings and rock-ice interfaces along ice-filled shear planes of rockslides, ii) to study its dependence on temperature and normal stress and (iii) to develop a new brittle failure criterion for ice-filled permafrost rock joints. The setup and boundary conditions of our experiments are inspired by a 10^4 m³, ice-supported rockslide at the Zugspitze summit crest~~. which potentially accelerates its movement in the future due to climate-induced permafrost degradation causing fracturing of ice-and-rock-ice-contacts, among other processes.~~ Our tests apply to ~~simulate the fracture of ice-and-rock-ice~~

~~contacts that may occur during~~ failures of permafrost rock slopes (i) with volumes of ≤ 2.3~~3.000~~ ∗ 10^{4} m³, (ii) with ice-filled shear planes in a depth of 4–15 m, (iii) with bedrock temperatures between -0.5 °C and -10 °C and (iv) with high~~fast~~ strain rates (4.8~~0.7~~ ± 1.4~~0.2~~ ∗ 10^{-3} s^{-1}) coinciding with the accelerating final failure stage. Tests at a rock overburden of 30 m and temperatures from -4 to -0.5 °C were performed to study a potential stress-dependent transition from brittle fracture to creep. Of all the previous laboratory studies on the shear strength of ice-filled joints, the data set presented is the most extensive, containing 141 tests at nine temperature and four normal stress levels. For the first time, pre-conditioned rock from a permafrost-affected rock slope was used.

Monitoring of AE activity during the shear tests was successfully used to describe the fracturing behaviour of rock-ice contacts focusing on the precursors of failure. The onset of ~~an~~ AE hit increase occurred when 65 % of the time between shear start and failure had passed (107 ± 98 sec before failure). ~~A strong increase in the AE hit rate was measured shortly before failure (107 ± 98 sec in advance). The onset of an AE hit increase occurred when 65 % of the time between shear start and failure had passed.~~

~~The experimental results clearly show a decline in~~ The shear strength clearly declines with decreasing normal stress and increasing temperature. At rock overburdens of 4 to 15 m, warming from -10 to -0.5 °C causes a decrease in shear strength by 64 to 78 %. At a rock overburden of 30 m and warming from -4 to -0.5 °C, shear strength decreases by 60 %. Warming drastically reduces the shear resistance of ice-filled rock joints and is thus a key process contributing to permafrost rock slope failure. P~~We have developed a conceptual model for p~~rogressive failure ~~that~~ is initiated ~~as soon as~~when a first slab has detached from a rock slope. The underlying frozen rock mass is~~; further slabs below are~~ subsequently destabilised by progressive thermal warming and even more quickly by sudden unloading~~.~~. The latter may lead to instability or even failure when the shear planes (i) are affected by a high reduction in normal stress exceeding the ice cohesion and/or (ii) are below -2 °C due to a friction coefficient higher than 1.

For the first time, we have introduced a failure criterion for ice-filled permafrost rock joints that includes the fracturing of ice infillings, rock-ice interfaces and a combination of both. It is based on ~~-~~ a Mohr-Coulomb failure criterion, it refers to joint surfaces which we assume similar for all rock types and it is valid for normal stresses 100–400 kPa and temperatures from -8 to -0.5 °C. The failure criterion contains a temperature-dependent cohesion and coefficient of friction ~~which~~ decreasinge by 12 % °C^{-1} and by 10 % °C^{-1} respectively with increasing sub-zero temperatures. ~~with increasing sub-zero temperatures. Per increase of one °C the cohesion reduces by 12 % and the coefficient of friction by 10 %.~~ The model fits well to the measured calibration means and even to the values excluded from the model development which mostly lie within or close to the calculated error margin. Further, we show that the failure type depends on the temperature and is also affected by higher normal stresses (i.e. 800 kPa) above -4 °C which can presumably be explained by an enhanced pressure melting effect along the rock-ice interface.

The new failure criterion can be applied in numerical modelling and enables scientists and engineers to anticipate more accurately the destabilisation of degrading permafrost rock slopes, as it reproduces better real shear strength conditions along

sliding planes. ~~In this way, it may also be used for the assessment of Mohr-Coulomb shear parameters integrated into rock wall stability modelling of the permafrost-affected Zugspitze summit crest.~~

6 Data availability

All data concerning the tested samples, test conditions, time series of the shear experiments, acoustic emission and mechanical properties are available in the supplementary material as *.xlsx or *.pdf files.

7 Supplement link

8 Author contribution

Philipp Mamot, Samuel Weber and Michael Krautblatter designed the laboratory experiment. Philipp Mamot and Samuel Weber prepared the experimental setup as well as the rock samples. The experiment execution was supervised by Philipp Mamot, Samuel Weber and Michael Krautblatter. The tests were mainly carried out by Tanja Schröder. Philipp Mamot and Samuel Weber performed the data analysis and prepared the manuscript, both with a substantial contribution from Michael Krautblatter.

9 Competing interests

The authors declare that they have no conflict of interest.

10 Acknowledgments

The work was funded by the Technical University of Munich and Nano-Tera.ch (ref. no. 530659). We acknowledge Maximilian Marcus Rau, who supported the experiment execution in the context of his Bachelor's Thesis, and we thank Christina Utz for her support in performing experiments in the course of her student research project.

11 References

Alava, M. J., Nukala, P. K. V. V. and Zapperi, S.: Statistical model of fracture, Adv. Phys., 55, 349–476, doi: 10.1080/00018730300741518, 2006.

Amitrano, D., Gruber, S. and Girard, L.: Evidence of frost-cracking inferred from acoustic emissions in a high-alpine rock-wall, Earth Planet. Sc. Lett., 341-344, 86–93, doi: 10.1016/j.epsl.2012.06.014, 2012.

Arakawa, M. and Maeno, N.: Mechanical strength of polycrystalline ice under uniaxial compression, Cold Reg. Sci. Technol., 26, 215–229, 1997.

Arenson, L. U. and Springman, S. M.: Triaxial constant stress and constant strain rate tests on ice-rich permafrost samples, Can. Geotech. J., 42, 412–430, doi: 10.1139/t04-111, 2005a.

Arenson, L. U. and Springman, S. M.: Mathematical descriptions for the behaviour of ice-rich frozen soils at temperatures close to 0 °C, Can. Geotech. J., 42, 431–442, doi: 10.1139/t04-109, 2005b.

Arenson, L. U., Springman, S. M. and Sego, D. C.: The rheology of frozen soils, Appl. Rheol., 17, 12147, 1–14, doi: 10.3933/ApplRheol-17-12147, 2007.

Baer, P., Huggel, C., McArdell, B. W. and Frank, F.: Changing debris flow activity after sudden sediment input: a case study from the Swiss Alps, Geology Today, 33, 216–223, doi: 10.1111/gto.12211, 2017.

Barnes, P. and Tabor, D.: Plastic flow and pressure melting in the deformation of ice I, Nature, 210, 878-&, doi:10.1038/210878a0, 1966.

Barnes, P., Tabor, D. and Walker, J. C. F.: The friction and creep of polycrystalline ice, P. R. Soc. London. Series A, 127–155, 1971.

Beniston, M., Farinotti, D., Stoffel, M., Andreassen, L. M., Coppola, E., Eckert, N., Fantini, A., Giacona, F., Hauck, C., Huss, M., Huwald, H., Lehning, M., López-Moreno, J.-I., Magnusson, J., Marty, C., Morán-Tejéda, E., Morin, S., Naaim, M., Provenzale, A., Rabatel, A., Six, D., Stötter, J., Strasser, U., Terzago, S. and Vincent, C.: The European mountain cryosphere. A review of its current state, trends, and future challenges, Cryosphere, 12, 759–794, doi: 10.5194/tc-12-759-2018, 2018.

Böckli, L., Nötzli, J. and Gruber, S.: PermaNET-BY: Untersuchung des Permafrosts in den Bayerischen Alpen. Teilprojekt PermaNET (EU Alpine Space Interreg IVb), Zürich, 60 pp., 2011.

Clauser, C. and Huenges, E.: Thermal conductivity of rocks and minerals, in: Rock Physics & Phase Relations: A Handbook of Physical Constants, Ahrens, T. J. (Eds.), American Geophysical Union, Washington, D. C., 105–126, 1995.

Coulomb, C. A.: Essai sur une application des regles de maximis et minimis a quelques problemes de statique, relatifs a l'architecture, Memoires de Mathematique & de Physique, 7, 343–382, 1773.

Cox, S. J. D. and Meredith, P. G.: Microcrack formation and material softening in rock measured by monitoring acoustic emissions, Int. J. Rock Mech. Min., 30, 11–24, doi: 10.1016/0148-9062(93)90172-A, 1993.

Cruden, D. M. and Hu, X. Q.: Basic friction angles of carbonate rocks from Kananaskis country, Canada, Bulletin of the International Association of Engineering Geology, 38, 55–59, doi: 10.1007/BF02590448, 1988.

Davies, M. C.R., Hamza, O., Lumsden, B. W. and Harris, C.: Laboratory measurement of the shear strength of ice-filled rock joints, Ann. Glaciol., 31, 463–467, doi: 10.3189/172756400781819897, 2000.

Davies, M. C.R., Hamza, O. and Harris, C.: The effect of rise in mean annual temperature on the stability of rock slopes containing ice-filled discontinuities, Permafrost Periglac., 12, 137–144, doi: 10.1002/ppp.378, 2001.

Delaloye, R., Hilbich, C., Lüthi, R., Nötzli, J., Phillips, M. and Staub, B.: Permafrost in Switzerland 2010/2011 to 2013/2014, Glaciological Report (Permafrost) No. 12–15, PERMOS, Cryospheric Commission of the Swiss Academy of Sciences, Fribourg, 85 pp., 2016.

Deline, P., Gruber, S., Delaloye, R., Fischer, L., Geertsema, M., Giardino, M., Hasler, A., Kirkbride, M., Krautblatter, M., Magnin, F., McColl, S., Ravanel, L. and Schoeneich, P.: Ice Loss and Slope Stability in High-Mountain Regions, in: Snow and Ice-Related Hazards, Risks and Disasters, Shroder, J. F., Haeberli, W., Whiteman, C. (Eds.), Academic Press, Boston, 521–561, 2015.

Draebing, D., Haberkorn, A., Krautblatter, M., Kenner, R. and Phillips, M.: Thermal and Mechanical Responses Resulting From Spatial and Temporal Snow Cover Variability in Permafrost Rock Slopes, Steintaelli, Swiss Alps, Permafrost Periglac., 28, 140–157, doi: 10.1002/ppp.1921, 2017.

Dramis, F., Govi, M., Guglielmin, M. and Mortara, G.: Mountain permafrost and slope instability in the Italian Alps: The Val Pola Landslide, Permafrost Periglac., 6, 73–81, doi: 10.1002/ppp.3430060108, 1995.

Dwivedi, R. D., Soni, A. K., Goel, R. K. and Dube, A. K.: Fracture toughness of rocks under sub-zero temperature conditions, Int. J. Rock Mech. Min., 37, 1267–1275, 2000.

Eberhardt, E., Stead, D. and Stimpson, B.: Quantifying progressive pre-peak brittle fracture damage in rock during uniaxial compression, Int. J. Rock Mech. Min., 36, 361–380, 1999.

Fellin, W.: Einführung in die Eis-, Schnee- und Lawinenmechanik, Springer Vieweg, Berlin, Heidelberg, 2013.

Fischer, L., Kääb, A., Huggel, C. and Noetzli, J.: Geology, glacier retreat and permafrost degradation as controlling factors of slope instabilities in a high-mountain rock wall. The Monte Rosa east face, Nat. Hazard. Earth Sys., 6, 761–772, 2006.

Fish, A. M. and Zaretzky, Y. K.: Ice strength as a function of hydrostatic pressure and temperature, in: CRREL Report, 97, 1–13, 1997.

Gagnon, R. E. and Gammon, P. H.: Triaxial experiments on iceberg and glacier ice, J. Glaciol., 41, 528–540, 1995.

Gallemann, T., Haas, U., Teipel, U., Poschinger, A. von, Wagner, B., Mahr, M. and Bäse, F.: Permafrost-Messstation am Zugspitzgipfel: Ergebnisse und Modellberechnungen, Geologica Bavarica, 115, 1–77, 2017.

Girard, L., Beutel, J., Gruber, S., Hunziker, J., Lim, R. and Weber, S.: A custom acoustic emission monitoring system for harsh environments. Application to freezing-induced damage in alpine rock walls, Geosci. Instrum. Meth., 1, 155–167, doi: 10.5194/gi-1-155-2012, 2012.

Gischig, V. S., Moore, J. R., Keith, F. E., Amann, F. and Loew, S.: Thermomechanical forcing of deep rock slope deformation: 2. The Randa rock slope instability, J. Geophys. Res., 116, F04011, doi: 10.1029/2011JF002007, 2011.

Glamheden, R. and Lindblom, U.: Thermal and mechanical behaviour or refrigerated caverns in hard rock, Tunn. Undergr. Sp. Tech., 17, 341–353, 2002.

Gobiet, A., Kotlarski, S., Beniston, M., Heinrich, G., Rajczak, J. and Stoffel, M.: 21st century climate change in the European Alps-A review, Sci. Total Environ., 493, 1138–1151, doi: 10.1016/j.scitotenv.2013.07.050, 2014.

Gómez-Heras, M., Smith, B. J. and Fort, R.: Surface temperature differences between minerals in crystalline rocks. Implications for granular disaggregation of granites through thermal fatigue, Geomorphology, 78, 236–249, doi: 10.1016/j.geomorph.2005.12.013, 2006.

Gruber, S., Hoelzle, M. and Haeberli, W.: Permafrost thaw and destabilization of Alpine rock walls in the hot summer of 2003, Geophys. Res. Lett., 31, L13504, doi: 10.1029/2004GL020051, 2004.

Gruber, S. and Haeberli, W.: Permafrost in steep bedrock slopes and its temperature-related destabilization following climate change, J. Geophys. Res., 112, 1–10, doi: 10.1029/2006JF000547, 2007.

Günzel, F. K.: Shear strength of ice-filled rock joints, in: Proceedings of the 9th International Conference on Permafrost, Fairbanks, Alaska, 28 June–3 July 2008, 581–586, 2008.

Hall, K. and Thorn, C. E.: Thermal fatigue and thermal shock in bedrock: An attempt to unravel the geomorphic processes and products, Geomorphology, 206, 1–13, doi: 10.1016/j.geomorph.2013.09.022, 2014.

Hardy, H. R.: Acoustic Emission/Microseismic Activity - Volume 1. Principles, Techniques and Geotechnical Applications, A.A. Balkema Publisher, a member of Swets & Zeitlinger Publishers, 2003.

Harris, C., Vonder Mühll, D., Isaksen, K., Haeberli, W., Sollid, J. L., King, L., Holmlund, P., Dramis, F., Guglielmin, M. and Palacios, D.: Warming permafrost in European mountains, Global Planet. Change, 39, 215–225, doi: 10.1016/j.gloplacha.2003.04.001, 2003.

Harris, S. A., French, H. M., Heginbottom, J. A., Johnston, G. H., Ladanyi, B., Sego, D. C. and van Erdingen, R. O.: Glossary of Permafrost and Related Ground-Ice Terms, Technical Memorandum No. 142, Permafrost-Subcommittee, Associate Committee on Geotechnical Research, National Research Council Canada, Ottawa, 159 pp., doi: 10.4224/20386561, 1988.

Hobbs, P. V.: Ice Physics, Oxford University Press, Oxford, New York, 837 pp., 1974.

Jaeger, J. C., Cook, N. G. and Zimmerman, R. W.: Fundamentals of rock mechanics, 4th Edition, Blackwell Publishing Ltd, 475 pp., 2007.

Jellinek, H. H. G.: Adhesive properties of ice, J. Coll. Sci. Imp. U. Tok., 14, 268-280, 1959

Jerz, H. and Poschinger, A. von: Neuere Ergebnisse zum Bergsturz Eibsee-Grainau, Geologica Bavarica, 99, 383–398, 1995.

Jia, H., Xiang, W. and Krautblatter, M.: Quantifying rock fatigue and decreasing compressive and tensile strength after repeated freeze-thaw cycles, Permafrost Periglac., 26, 368–377, doi: 10.1002/ppp.1857, 2015.

Jones, S. J. and Glen, J. W.: The mechanical properties of single crystals of ice at low temperatures, International Association of Hydrological Sciences Publ., 79, 326–340, 1968.

Kodama, J., Goto, T., Fujii, Y. and Hagan P.: The effects of water content, temperature and loading rate on strength and failure process of frozen rocks, Int. J. Rock Mech. Min., 62, 1–13, 2013.

Krautblatter, M., Verleysdonk, S., Flores-Orozco, A. and Kemna, A.: Temperature-calibrated imaging of seasonal changes in permafrost rock walls by quantitative electrical resistivity tomography (Zugspitze, German/Austrian Alps), J. Geophys. Res., 115, 1–15, 2010.

Krautblatter, M., Funk, D. and Günzel, F. K.: Why permafrost rocks become unstable: a rock-ice-mechanical model in time and space, Earth Surf. Proc. Land., 38, 876–887, 2013.

Lockner, D.: The role of acoustic emission in the study of rock, Int. J. Rock Mech. Min., 30(7), 883–899, 1993.

MathWorks: Statistics and machine learning toolbox, regression, model building and assessment, coefficient standard errors and confidence intervals (R2017a): https://ch.mathworks.com/help/stats/coefficient-standard-errors-and-confidence-intervals.html?searchHighlight=standard%20error%20estimate%20linearmodel&s_tid=doc_srchtitle

Mellor, M.: Mechanical properties of rocks at low temperatures, in: Proceedings of the 2nd International Conference on Permafrost, Yakutsk, Siberia, 13-28 July 1973, 334–344, 1973.

Mohr, O.: Welche Umstände bedingen die Elastizitätsgrenze und den Bruch eines Materials? Zeitschrift des Vereins Deutscher Ingenieure, 44, 1524–1530, 1900.

Murton, J., Kuras, O., Krautblatter, M., Cane, T., Tschofen, D., Uhlemann, S., Schober, S. and Watson, P.: Monitoring rock freezing and thawing by novel geoelectrical and acoustic techniques, J. Geophys. Res., 121, 2309–2332, doi: 10.1002/2016JF003948, 2016.

Nechad, H., Helmstetter, A., Guerjouma, R. El and Sornette, D.: Creep rupture in heterogeneous materials, Phys. Rev. Lett., 94, 45501, doi: 10.1103/PhysRevLett.94.045501, 2005.

Noetzli, J., Gruber, S. and Poschinger, A. von: Modellierung und Messung von Permafrosttemperaturen im Gipfelgrat der Zugspitze, Deutschland, Geographica Helvetica, 65, 113–123, 2010.

Paterson, W. S. B.: The physics of glaciers, 3rd edition, Butterworth Heinemann, Oxford, 496 pp., 1994.

Ravanel, L. and Deline, P.: La face ouest des Drus (massif du Mont-Blanc): évolution de l'instabilité d'une paroi rocheuse dans la haute montagne alpine depuis la fin du petit age glaciaire, Geomorphologie, 4, 261–272, 2008.

Ravanel, L., Allignol, F., Deline, P., Gruber, S. and Ravello, M.: Rock falls in the Mont Blanc Massif in 2007 and 2008, Landslides, 7, 493–501, 2010.

Ravanel, L. and Deline, P.: Climate influence on rockfalls in high-Alpine steep rockwalls. The north side of the Aiguilles de Chamonix (Mont Blanc massif) since the end of the 'Little Ice Age', Holocene, 21, 357–365, doi: 10.1177/0959683610374887, 2011.

Ravanel, L. and Deline, P.: Rockfall Hazard in the Mont Blanc Massif Increased by the Current Atmospheric Warming, in: Engineering Geology for Society and Territory - Volume 1: Climate Change and Engineering Geology, Springer International Publishing, Cham, 425–428, 2015.

Rempel, A. W., Wettlaufer, J. S. and Worster, M. G.: Premelting dynamics in a continuum model of frost heave, J. Fluid Mech., 498, 227–244, 2004.

Renshaw, C. E. and Schulson, E. M.: Universal behaviour in compressive failure of brittle materials, Nature, 412, 897–900, doi: 10.1038/35091045, 2001.

Sanderson, T. J. O.: Ice Mechanics. Risks to offshore structures, Graham & Trotman, 253 pp., 1988.

Scholz, C. H.: Microfracturing and the inelastic deformation of rock in compression, J. Geophys. Res., 73, 1417–1432, doi: 10.1029/JB073i004p01417, 1968.

Schön, J. H.: Physical properties of rocks. Fundamentals and principles of petrophysics, 2nd Edition, Developments on Petroleum Science, 65, Cubitt, J. and Wales, H. (Eds.), Elsevier, Amsterdam, Oxford, 512 pp., 2015.

Schulson, E. M. and Duval, P.: Creep and Fracture of Ice, Cambridge University Press, 401 pp., 2009.

Senfaute, G., Duperret, A. and Lawrence, J. A.: Micro-seismic precursory cracks prior to rock-fall on coastal chalk cliffs. A case study at Mesnil-Val, Normandie, NW France, Nat. Hazard. Earth Sys., 9, 1625–1641, 2009.

Shiotani, T., Fujii, K., Aoki, T. and Amou, K.: Evaluation of progressive failure using AE sources and improved b-value on slope model tests, Progress in AE VII, 529–534, 1994.

Shiotani, T., Li, Z., Yuyama, S. and Ohtsu, M.: Application of the AE improved b-value to quantitative evaluation of fracture proces in concrete materials, Journal of AE, 19, 118–133, 2001.

Sornette, D.: Critical Phenomena in Natural Sciences, Springer Verlag, Berlin, 2006.

Ulusay, R.: The ISRM Suggested Methods for Rock Characterization, Testing and Monitoring: 2007-2014, Springer International Publishing, 2015.

Weber, S., Beutel, J., Faillettaz, J., Hasler, A., Krautblatter, M. and Vieli, A.: Quantifying irreversible movement in steep, fractured bedrock permafrost on Matterhorn (CH), Cryosphere, 11, 567–583, doi: 10.5194/tc-11-567-2017, 2017.

Yamamoto, Y. and Springman, S. M.: Axial compression stress path tests on artificial frozen soil samples in a triaxial device at temperatures just below 0 °C, Can. Geotech. J., 51, 1178–1195, doi: 10.1139/cgj-2013-0257, 2014.

Yasufuku, N., Springman, S. M., Arenson, L. U. and Ramholt, T.: Stress-dilatancy behaviour of frozen sand in direct shear, in: Proceedings of the 8th International Conference on Permafrost, Zurich, Switzerland, 21-25 July 2003, 1253–1258, 2003.

Tables

Table 1: Calculated decrease in shear stress at failure with increasing temperature.

Normal stress class [kPa]	Temperature range used for calculation [°C]	Calculated percentage decrease due to warming [%]		R^2	p-value
		Total	Per increase of 1 °C		
100	-10 to -0.5	70.2	7.4	0.47	< 0.01
200	-10 to -0.5	78.1	8.2	0.58	< 0.01
400	-10 to -0.5	63.5	6.7	0.44	< 0.01
800	-4 to -0.5	60.1	17.2	0.75	< 0.01

Table 2: Calculated absolute and percentage decrease of cohesion and friction due to warming for various normal stress- and temperature ranges.

Valid normal stress range [kPa]	Valid temperature range [°C]	Mechanical parameter	Decrease due to warming				R^2	p-value
			total		per increase of 1 °C			
			absolute	%	absolute	%		
100 to 400	-8 to -0.5	c [kPa]	551.3	86.0	73.5	11.5	0.96	0.00
		μ	1.58	75.0	0.21	10.0	0.78	0.05
	-4 to -0.5	c [kPa]	257.3	74.1	83.5	21.2	0.87	0.24
		μ	0.74	58.3	0.38	16.7	0.97	0.11
100 to 800	-4 to -0.5	c [kPa]	503.3	74.1	143.8	21.2	0.85	0.08
		μ	0.35	59.3	0.10	17.0	0.95	0.02

Supplement of

A temperature- and stress-controlled failure criterion for ice-filled permafrost rock joints

Philipp Mamot[1], Samuel Weber[2], Tanja Schröder[2], Michael Krautblatter[2]

[1]Chair of Landslide Research, Technical University of Munich, 80333 Munich, Germany
[2]Department of Geography, University of Zurich, 8057 Zurich, Switzerland

Correspondence to: Philipp Mamot (philipp.mamot@tum.de)

The supplementary material gives additional information to:

(i) potential error sources, i.e. variations in the ice layer thickness of the samples and the shear rate during the tests (Fig. S1),

(ii) the decreased area of contact between the upper and the lower rock cylinder developing due to shear deformation and considered for the calculation of the peak shear stress (Fig. S2),

(iii) the specific number of performed tests per stress-temperature condition (Table S1),

(iv) the character of time series for shear stress, shear deformation and AE activity at various temperatures (Fig. S3),

(v) the results of AE monitoring (Fig. S4),

(vi) the characteristics of the various failure types (Fig. S5),

~~(vi)~~(vii) the relationship between failure type and normal stress level (Fig. S6),

~~(vii)~~(viii) the results of shear stress at failure as a function of temperature (Fig. S7~~6~~),

~~(viii)~~(ix) the cohesion and coefficient of friction as a function of temperature (Fig. S8~~7~~) and

~~(ix)~~(x) the statistical dispersion measures of the measured peak shear stress values around the calculated failure criterion (Table S2).

Following data (as *.xlsx files) is provided in the zipped folder “Suppl. material”:

- data_acoustic_pdf_Fig. S4
- data_experiments
- data_frictioncoeff_cohesion_Fig. 8
- data_timeseries_acoustic_exp1b_spec4_Fig. S3
- data_timeseries_acoustic_exp2b_spec3_Fig. S3
- data_timeseries_acoustic_exp3b_spec3_Fig. S3

- data_timeseries_acoustic_exp5b_spec2_Fig. S3
- data_timeseries_acoustic_exp5c_spec1_Fig. 5
- data_timeseries_acoustic_exp5c_spec2_Fig. 5
- data_timeseries_acoustic_exp5c_spec3_Fig. 5
- data_timeseries_acoustic_exp5c_spec4_Fig. 5
- data_timeseries_acoustic_exp6b_Fig. 4
- data_timeseries_acoustic_exp6b_spec1_Fig. S3
- data_timeseries_acoustic_exp7b_spec2_Fig. S3
- data_ timeseries_shearmachine_exp1b_spec4_Fig. S3
- data_ timeseries_shearmachine_exp2b_spec3_Fig. S3
- data_ timeseries_shearmachine_exp3b_spec3_Fig. S3
- data_ timeseries_shearmachine_exp5b_spec2_Fig. S3
- data_timeseries_shearmachine_exp6b_Fig. 4
- data_ timeseries_shearmachine_exp6b_spec1_Fig. S3
- data_ timeseries_shearmachine_exp7b_spec2_Fig. S3
- the Supplement text (as *.pdf file) including figures and tables

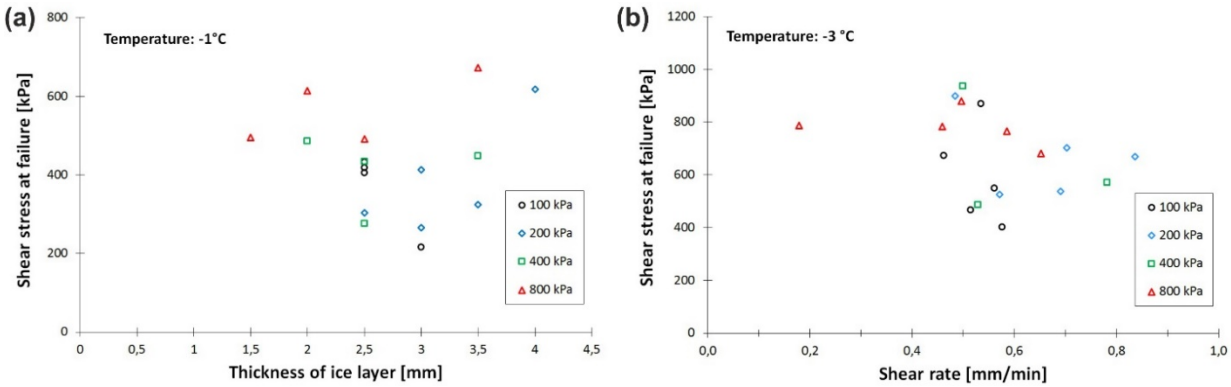

Figure S1: Typical variations in (a) ice layer thickness and (b) shear rate at certain temperatures, both plotted against shear stress at failure and for normal stress levels of 100, 200, 400 and 800 kPa.

Variations in the shear rate (0.3–1.0 mm/min) and in the ice layer´s thickness (1.5–4 mm) were kept low and have no influence on the shear stress at failure (Fig. S1). This is valid for all tested stress and temperature conditions.

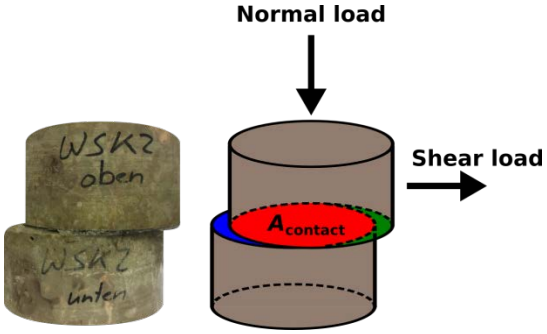

Figure S2: Schematic visualisation of decreasing area of contact $A_{contact}$ between upper and lower rock cylinder during shear experiments.

Normal and shear load as well as normal and shear deformation were recorded during the shear tests and used to calculate normal stress and shear stress considering the changing area of contact $A_{contact}$ which is schematically shown in Fig. S2.

Table S1: Number of experiments per temperature and normal stress condition.

Normal stress class [kPa]	Temperature level [°C]								
	-10	-8	-6	-5	-4	-3	-2	-1	-0.5
100	5	5	5	6	5	5	4	4	4
200	4	4	4	6	5	5	6	5	1
400	5	4	5	5	4	3	5	4	3
800	-	-	-	-	4	5	3	4	4

65

The number of experiments for each test condition (characterised by a specific temperature and normal stress level) ranged between 1 and 6 (Table S1). The total number of tests was 141. ~~For test conditions without a number we did not perform any experiment.~~

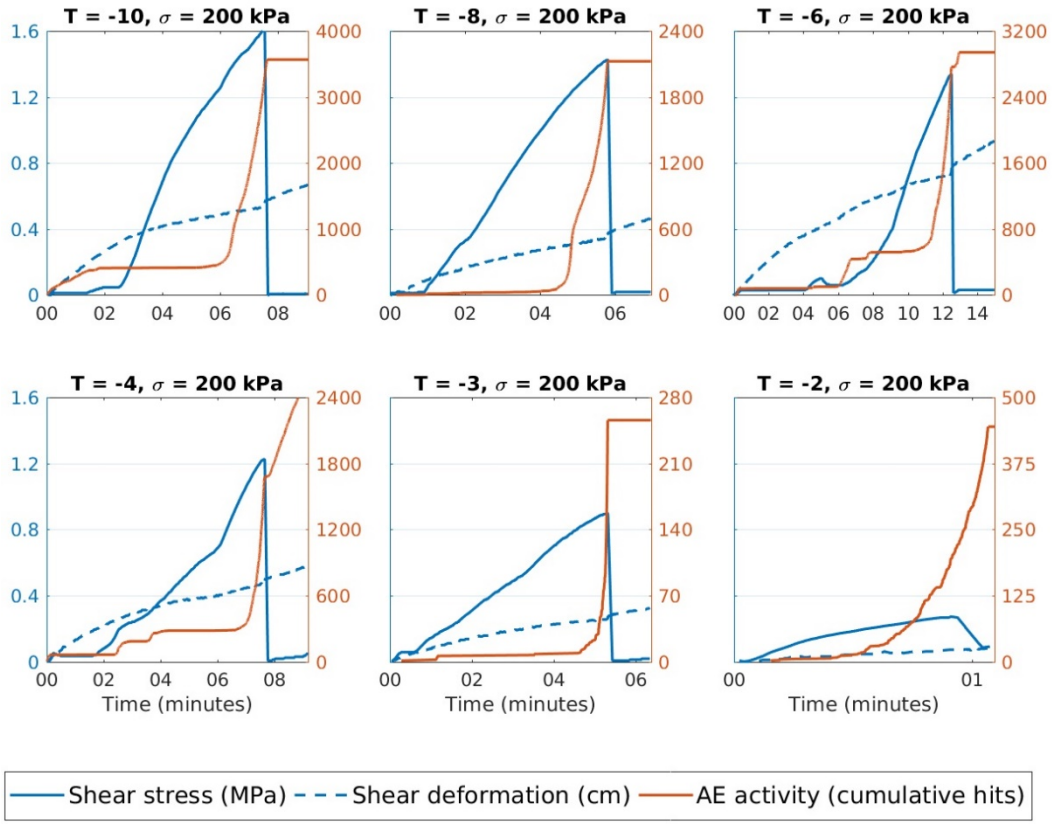
T = -10, σ = 200 kPa
T = -8, σ = 200 kPa
T = -6, σ = 200 kPa
T = -4, σ = 200 kPa
T = -3, σ = 200 kPa
T = -2, σ = 200 kPa
Time (minutes)
Time (minutes)
Time (minutes)
Shear stress (MPa)
Shear deformation (cm)
AE activity (cumulative hits)

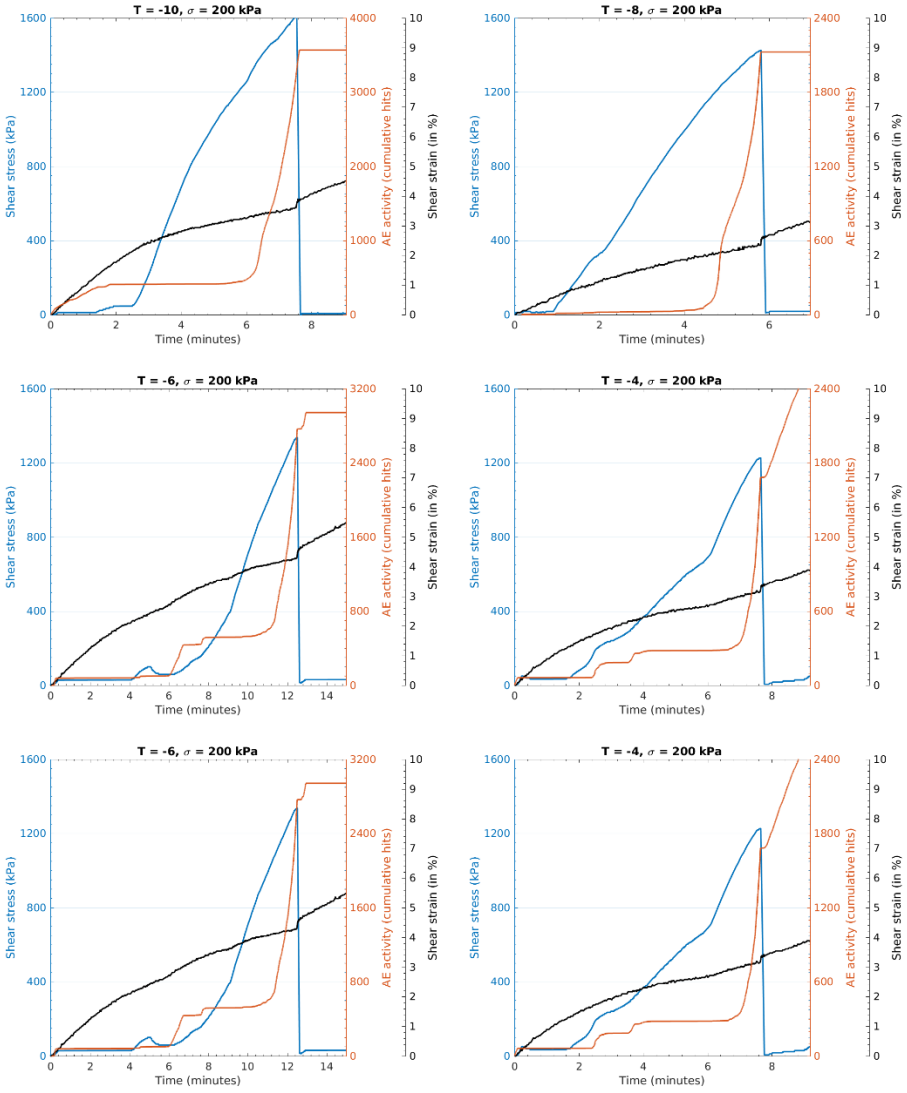

Figure S3: Typical curves of shear stress, shear deformation and acoustic activity for tests applying a normal stress of 200 kPa and various temperatures. All stages of the shearing process (Fig. 4) are depicted including the first part ~~early phase~~ of stage V (~~the~~ post-failure ~~stage~~).

Figure S3 displays a selection of representative time series of shear stress, shear deformation and AE activity. Failure is clearly detectable at all presented temperature levels by the peaks in shear stress and their following strong decrease. Furthermore, an increase in cumulative AE hits can be observed just before rupture, pointing to growing microcracks that coalesce and lead to progressive damage. In most of the experiments, the shear deformation reaches one of its maxima~~um value~~ at failure. The character of the presented curves corresponds to the demonstrated stages in Fig. 4.

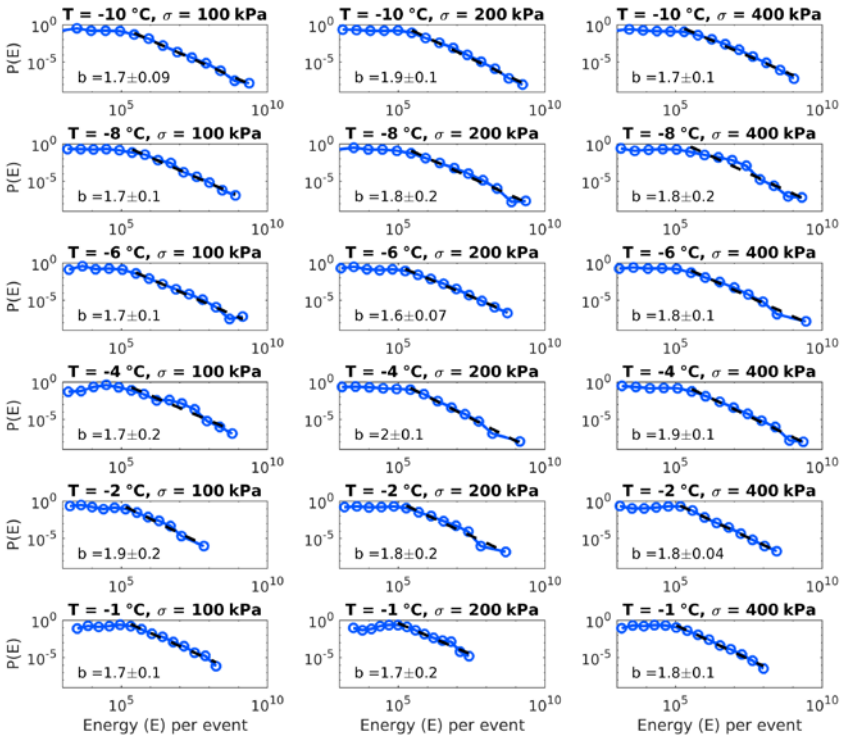

Figure S4: Probability distribution of the event energy for different conditions (temperature and stress level). The power-law function is marked with a dashed black line and its exponent b is given with an error estimation.

85

The probability density functions (PDFs) of event energy show a power-law behavior spanning 3–5 orders of magnitudes (Fig. S4). The exponent b ranges between 1.6 and 1.9 for the different conditions, but it does not show a relation to temperature or normal load.

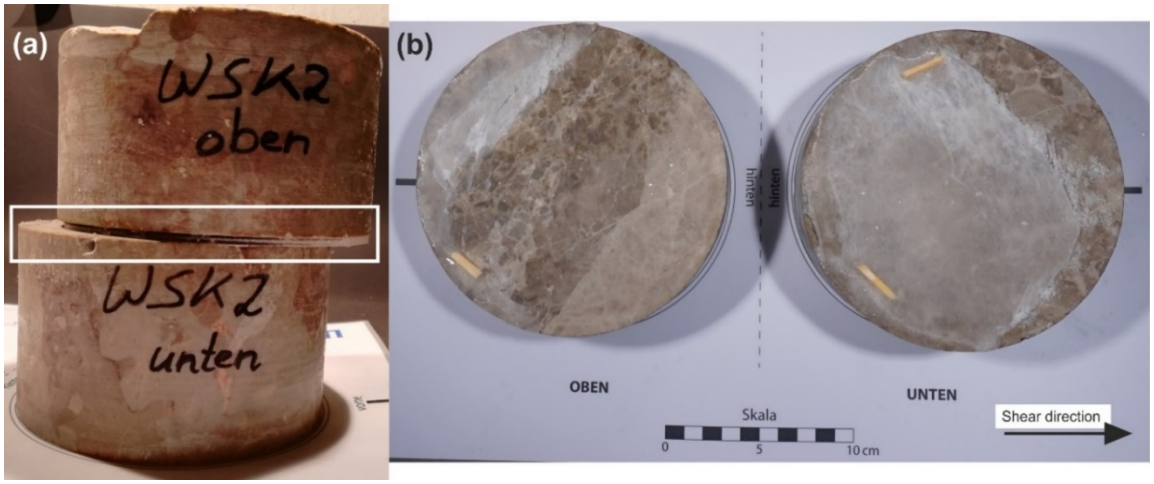

Figure S5: (a) Sheared sandwich sample with fracture along the rock-ice contact. (b) Shear plane after testing with the composite failure type.

Three different types of failure could be identified:

(i) ~~(i)~~ Fracture along the rock-ice interface, where the entire ice infill sticks to the upper rock cylinder (Fig. S5a)

(ii) ~~,~~ F~~(ii) f~~racture within the ice layer ~~and~~

(iii) A~~a~~ composite fracture type of (i) and (ii), ~~. The first failure type is shown in Fig. S5a, where the entire ice infill sticks to the upper rock cylinder. The third fracture type is shown in Fig. S5b~~ where the ice layer broke transversely and was separated so that the rear portion remains at the lower cylinder and the front part sticks to the upper one ~~.~~(Fig. S5b).

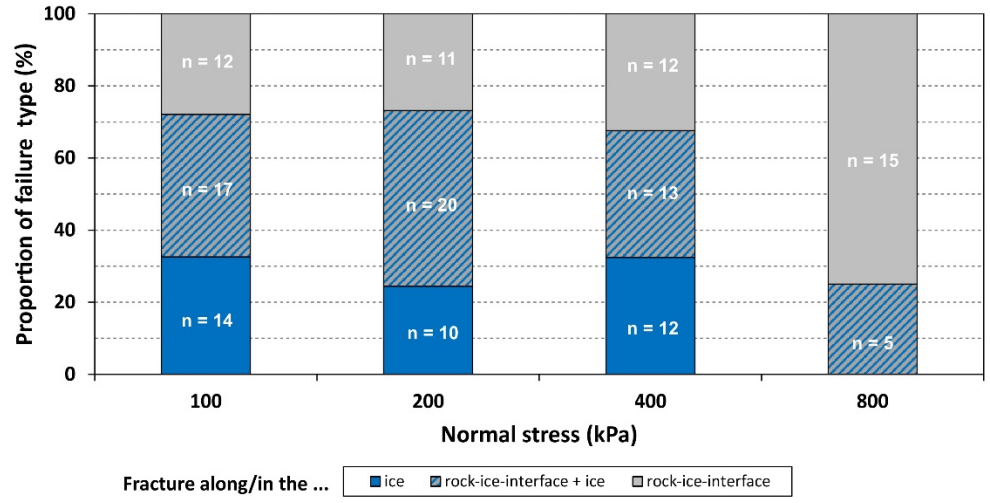

Figure S6: Proportions and absolute numbers of failure types for normal stresses 100–800 kPa and temperatures from -10 to -0.5 °C.

A relationship between failure type and normal stress could not be identified for stress levels 100–400 kPa (Fig. S6). However, at normal stresses of 800 kPa fracturing in the ice did not occur whereas fracturing of rock-ice contacts dominated with 75 %. This overrepresentation of failures along the rock-ice interface may be caused due to the absence of tests at temperatures below -4 °C, where much higher proportions of failures in the ice were observed for tests at ≤ 400 kPa (Fig. 6).

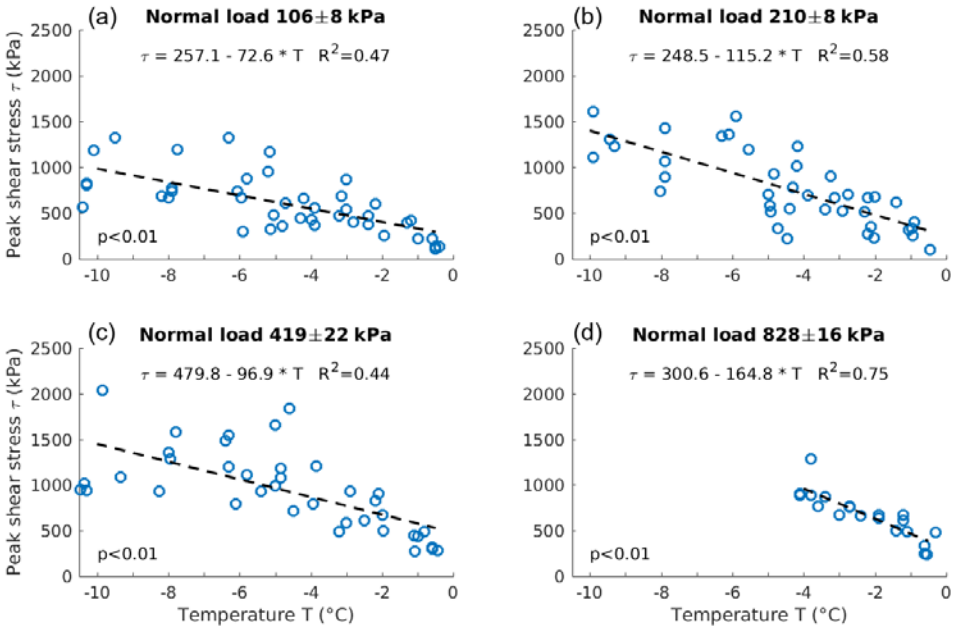

Figure S7~~6~~: Shear stress at failure as a function of temperature for normal stress levels of 100, 200, 400 and 800 kPa.

At all tested normal stress levels (100, 200, 400 and 800 kPa) the shear stress at failure decreases with increasing temperature (Fig. S7~~6~~). The calculated total decrease at stresses 100–400 kPa ranges between 63.5 and 78.1 % and refers to a warming from -10 to -0.5 °C. The maximum decrease at 800 kPa measures 60.1 % and refers to temperatures from -4 to -0.5 °C. The measured~~true~~ normal stress means and errors of the tests assigned to a certain normal stress class differ little from the respective class values (maximum 28 ± 16 kPa).

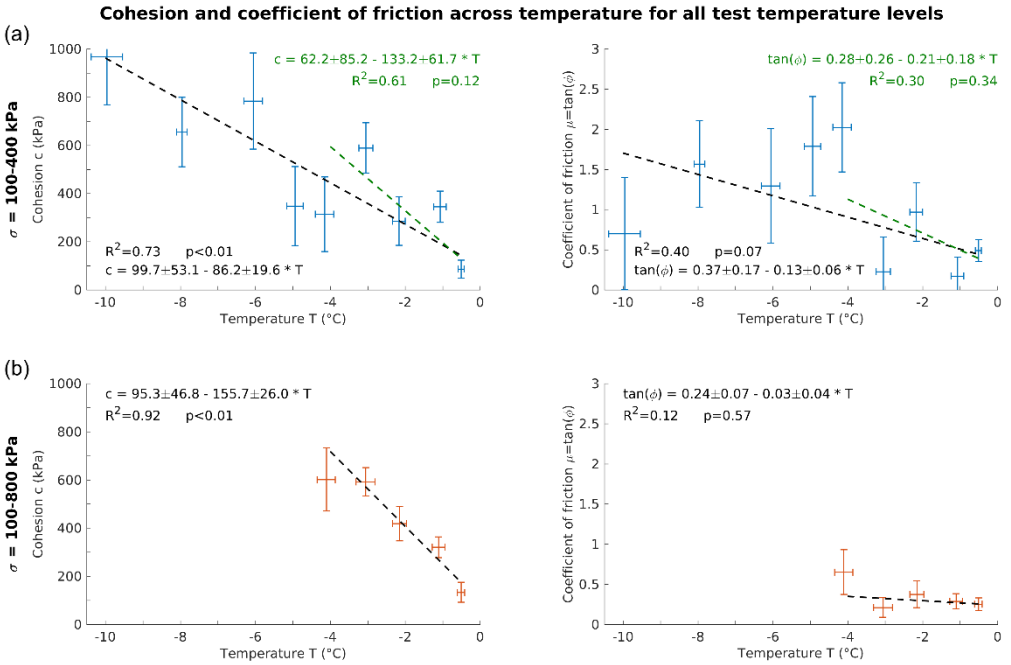

Figure S8~~7~~: Cohesion and coefficient of friction of ice-filled rock joints as a function of temperature for all tested temperature levels. The crosses display the means and standard deviations of rock temperature and cohesion or friction for the different test temperature classes. (a) Tests at normal stresses 100–400 kPa and temperatures -10 to -0.5 °C (blue crosses). (b) Tests at normal stresses 100–800 kPa and temperatures -4 to -0.5 °C (orange crosses). The dashed lines represent the linear regression functions, which were inversely weighted with the squared standard errors. The green regression lines in (a) refer to a temperature range from -4 to -0.5 °C.

Figure S8~~7~~ displays the development of formulas for a temperature-dependent cohesion and friction at all tested temperatures. The values of the regression lines correspond roughly to the ones taken for the Mohr-Coulomb failure criterion, which only considers temperature levels with a statistical significance level of $p \leq 5$ % (see Sect. 3.4; Fig. 8). In Fig. S8~~7~~, R^2-values range between 0.61–0.92 for the cohesion and between 0.12–0.40 for the coefficient of friction. P-values measure 0–12 % for the cohesion and 7–57 % for the coefficient of friction. The ranges depend on the included stress levels and the temperature range tested. The uncertainties presented are higher than the errors of the functions used for the failure criterion (Fig. 8). This justifies the exclusion of tests at certain temperature levels for the development of a robust model.

Table S2: Statistical dispersion measures of the measured peak shear stress values around the new derived failure criterion (Fig. 10). Errors calculated for normal stresses 100–400 kPa refer to the valid stress range of the failure criterion. Validation data (V) correspond to temperatures not utilised for the elaboration of the failure criterion. CV = Coefficient of variation. MAD = Mean absolute deviation.

Mean temperature [°C]	σ = 100-400 kPa		Used for model development [C]	Used as validation data for error measurement [V]
	MAD [kPa]	CV [%]		
-0.5 ± 0.1	40.0	19.9	x	
-1.1 ± 0.2	97.5	43.5		x
-2.2 ± 0.2	99.3	24.6	x	
-3.1 ± 0.2	137.8	30.5		x
-4.2 ± 0.2	145.7	19.8	x	
-4.9 ± 0.2	136.4	17.9	x	
-6.1 ± 0.2	206.6	24.6		x
-8.0 ± 0.1	110.4	8.8	x	
-10.0 ± 0.4	252.3	15.0		x

Statistical dispersion measures of the measured peak shear stress values around the failure criterion (Fig. 10) are shown in Table S2. Best accordance is achieved for the shear stress means used for model calibration (correspond to significant temperature levels with p-values ≤ 5 %). The mean absolute deviation (MAD) and coefficient of variation (CV) range between 40–146 kPa and 8.8–24.6 % respectively. The experiments at temperatures -1, -3, -6 and -10 °C (with p-values > 5 %), which had been excluded from the elaboration of the failure criterion, were used for validation. Their shear stress means show higher deviations from the failure criterion, i.e. the MAD and the CV range from 98 to 252 kPa and from 15 to 43.5 % respectively.